SOLAR DRYING OF TROPICAL FISH IN INDONESIA

by

BARSONG

Grad.Dip.Sc.

Submitted in fulfilment of the requirements

for the degree of

MASTER OF SCIENCE

in

Department of Physics

UNIVERSITY OF TASMANIA

AUSTRALIA

OCTOBER 1992

CONTENTS page

I hereby declare that this thesis contains no material which has been accepted for the award of any other degree or diploma in any university, and that, to the best of condidate's knowledge and belief, the thesis contains no copy or paraphrase of material previously published or written by another person, except where due reference is made in the text of this thesis.

Barsong

ACNOWLEDGEMENT

The author would like to express his appreciation and gratitude to his supervisor Dr P.E.Doe (Mechanical Engineering) and joint supervisor Dr.J.Greenhill (Department of Physics) for their assistance and encouragement and also to Mr.Idam Arif (Ph.D Student, Department of Physics) for his guidance during writing the computer program. Special appreciation is due to my wife, Pranulida and daughter, Nurkhalimah.B, for enduring so patiently the division of living during the study.

ABSTRACT

Mathematical models were developed to simulate performance of an indirect solar fish drier. A computer simulation was carried out to predict a drying rate including moisture content and water activity of dried fish. Based on the simulation, a new design of a solar fish drier was constructed and tested in Indonesia.

Salted fish Gulamah (Pseudociena amoyensis) and Pari Kelapa (Trygon sepheu) were dried over a four day period. Meteorological data and data relating to the fish were measured. The results were compared with prediction from the computer model to assess its validity and limitations. The mathematical model predicted a slightly lower drying rate, final moisture contents and water acitvity of the dried fish than those measured.

NOMENCLATURE

Symbol	Meaning	Units	Equation first used
α	– Absorption coefficient		(2.36)
	– Thermal diffusivity of air	m^2/sec	(3.11)
	– Inverse of diffusivity of non-fatty fish	sec/m^2	(4.28)
β	– The slope of a surface	rad	(2.14)
	– The slope of a linear line	--	(4.28)
δ	Declination angle	rad	(2.2)
Δt	Increment of time	sec	(4.4)
ε	– Emission coefficient	--	(3.5)
	– Evaporation rate	kg/sec	(4.30)
ε_c	Emission coefficient of the cover	--	(3.15)
ε_p	Emission coefficient of absorbing plate	--	(3.15)
ρ_c	Reflection coefficient of the cover	--	(3.15)
ρ_p	Reflection coefficient of absorbing plate	--	(3.15)
γ	Azimuth angle	rad	(2.14)
η	Efficiency	%	(4.34)
λ	Latent heat of evaporation of water	J/kg	(4.10)
ν	– Kinematic viscosity	m^2/sec	(3.11)
	– Specific Volume	m^3/kg	(4.35)
ν_a	Specific volume of air	m^3/kg	(4.37)
$\nu_{(mix)}$	Specific volume of (air-water vapour)	m^3/kg	(4.37)
ν_v	Specific volume of water vapour	m^3/kg	(4.36)
$(\nu_v)_s$	Specific volume of water vapour at saturation pressure	m^3/kg	(4.36)
θ	Incident angle of bean radiation	rad	(2.14)
θ_θ	Effective angle of solar radiation	rad	(2.38)
θ_z	Zenith angle	rad	(2.3)
ρ	– Reflectance of surroundings	--	(2.19)
	– Density of the mixture of air and vapour	kg/m^3	(4.39)
σ	Stefan-Boltzmann constant	W/m^2K	(3.4)
τ	– Transmittance coefficient	--	(2.29)
	– Time constant	sec^{-1}	(4.31)
τ_a	Transmittance coefficient of absorbing material	--	(2.33)
τ_b	Atmospheric transmittance for clear sky	--	(2.6)
τ_c	Transmission coefficient of the cover	--	(3.16)

τ_d	Transmission coefficient of diffuse radiation	--	(2.9)
τ_N, ρ_N, α_N	Transmission, reflection and absorption coefficients for perpendicular components of the polarization		(2.34a–c)
$(\tau\alpha)$	Transmittance-absorptance product	--	(2.40)
φ	Latitude	rad	(2.3)
ω	Hour angle	rad	(2.1)
A	– Altitude	km	(2.7)
	– Cross-section of inlet air	m^2	(4.41)
	– Surface area	m^2	(3.1)
A_c	Surface area of collector	m^2	(3.4)
A_{fs}	Saturated surface area of fish	m^2	(4.2)
A_w	Water activity	--	(4.33)
a	Half thickness of fish	m	(4.30)
C	– Extinction coefficient	m^{-1}	(2.31)
	– Circumference of the collector	m	(3.4)
	– Discharge coefficient	--	(4.41)
Ce	Equilibrium moisture concentration	kg/m^3	(4.23)
Co	Equilibrium moisture content	kg/m^3	(4.25)
C_{pa}	Specific heat of air	J/kg K	(3.39)
C_{pf}	Specific heat of fish	J/kg K	(3.16)
C_{pv}	Specific heat of water vapour	J/kg K	(4.12)
D_e	Diffusivity of fish	m^2/sec	(4.27)
d	Thickness of material	m	(3.22)
E	Energy of activation for diffusion	J/kg Mol	(4.27)
E_b	Total emissive power for ideal blackbody	W/m^2	(3.4)
E_{nb}	Radiation energy per unit area for non-blackbody	W/m^2	(3.5)
E_i, E_r, E_t	Tangential components for incident, reflected and transmitted electric waves	N/C	(2.21)
$(E_r/E_i)_P$	Reflected amplitude coefficient where incident electric wave E_i parallel to the plane of incident	--	(2.22a)
$(E_t/E_i)_P$	Transmitted amplitude coefficient where incident electric wave E_i parallel to the plane of incident	--	(2.22b)
$(E_r/E_i)_N$	Reflected amplitude coefficient where incident electric wave E_i perpendicular to the plane of incident	--	(2.24a)
$(E_t/E_i)_N$	Transmitted amplitude coefficient where incident electric wave E_i perpendicular to the plane of incident	--	(2.24b)
F_{1-2}	Shape factor	--	(3.6)
F'	Efficiency factor of collector	--	(3.24)

F''	Flow factor	--	(3.46)
F_R	Heat removal factor	--	(3.43)
Gc	Solar constant	W/m^2	(2.4)
Go	Extra-terrestrial solar radiation	W/m^2	(2.4)
g	Acceleration of gravity	m/sec^2	(3.11)
H	Solar radiation intensity	W/m^2	(3.23)
H_i, H_r, H_i	Tangential components for incident, reflected and transmitted magnetic waves	A/m	(2.21)
h	Convective heat transfer coefficient	W/m^2K	(3.3)
h_i, h_o	Enthalpies of air at inlet and outlet	J/kg	(4.5)
h_m	Surface mass transfer coefficient	W/m^2K	(4.2)
h_{p-c}	Convective heat transfer coefficient between absorbing plate and cover	W/m^2K	(3.11)
H_{1p-c}	Convective heat transfer coefficient from absorbing plate to enclosed air	W/m^2K	(3.36)
h_{2p-c}	Convective heat transfer coefficient from enclosed air to cover of collector	W/m^2K	(3.37)
h_r	Radiative heat transfer coefficient between two surfaces	W/m^2K	(3.8)
h_{rc-s}	Radiative heat transfer coefficient between the cover of collector and the sky	W/m^2K	(3.19)
h_{rp-c}	Radiative heat transfer coefficient between the absorbing plate of collector and cover	W/m^2K	(3.15)
h_{rp-s}	Radiative heat transfer coefficient between the absorbing plate of collector and the sky	W/m^2K	(3.17)
h_t	Surface heat transfer coefficient	W/m^2K	(4.9)
h_v	Moisture enthalpy	J/kg	(4.5)
h_w	Forced convective heat transfer coefficient	W/m^2K	(3.13)
I	Measured global radiation intensity	W/m^2	(2.12)
$I_{(t)}$	The same as I	W/m^2	(6.1)
I_b	Hourly beam sky radiation	J/m^2	(2.13)
I_c	Hourly clear sky total radiation	J/m^2	(2.11)
I_{cb}	Clear sky hour's beam radiation	J/m^2	(2.8)
I_{cd}	Clear sky hour's diffuse radiation	J/m^2	(2.10)
I_d	Hourly sky diffuse radiation	J/m^2	(2.12)
I_o	Hourly radiation intensity above the atmospheric air	J/m^2	(2.5)
I_t	Transmitted radiation intensity	J/m^2	(2.29)
I_T	Hourly total radiation on tilted surface	J/m^2	(2.19)
i, t	Incident and transmitted angle	rad	(2.20)
k	– Wave number	rad/m	(2.21)

	– Thermal conductivity	W/m K	(3.2)
k_c	Ratio of I/I_c	--	(2.12)
L	– Length of material	m	(3.2)
	- Length of collector	m	(3.39)
M	Mass of fish	kg	(4.4)
Ma	Molecular weight of air	kg/kg Mol	(4.35)
M_b, M_f	Masses of bone and fat	kg	(4.19)
M_s, M_w	Masses of salt and water	kg	(4.19)
M_e	Equilibrium mass of fish	kg	(4.26)
M_{fs}	Mass of fish	kg	(4.16)
M_o	Initial mass of fish	kg	(4.4)
M_v	Molecular weight of water vapour	kg/kg Mol	(4.38)
m	Mass flow rate	kg/sec	(3.39)
mc,sc, fc	Moisture, salt and fat contents (w.b)	%	(4.20)
md,sd,fd	Moisture, salt and fat contents (d.b)	%	(4.20)
md_e	Equilibrium moisture content (d.b)	%	(4.24)
n	The day of the year	--	(2.2)
n1, n2	Indices of refraction	--	(2.20)
Nu	Nusselt number	--	(3.11)
P	Atmospheric pressure	N/m^2	(4.35)
P_n–P_{n+1}	Pressure difference (n = 1, 2, 3,.....,8)	N/m^2	(4.41)
Pr	Prandtl number	--	(3.13)
P_s	Saturation pressure	N/m^2	(4.36)
q	Useful energy gain	W/m^2	(3.23)
q"	Actual energy gain	W/m^2	(3.42)
q_{ab}	Heat absorbed	W	(4.16)
q_{cond}	Rate of conduction heat transfer	W	(3.1)
q_{conv}	Rate of convection heat transfer	W	(3.3)
q_{LH}	Latent heat for evaporation	W	(4.17)
q_{rad}	Rate of radiation heat transfer	W	(3.6)
$q_{rp\text{-}s}$	Net radiation between absorbing plate and the sky	W	(3.16)
q_s	Heat absorbed by fish	W/m^2	(4.5)
Q_L	Heat loss	W/m^2	(4.5)
R	– Energy reflection coefficient	--	(2.25a)
	– Thermal resistance	K/W	(3.10)
	– Drying rate	kg/sec	(4.1)
	– Gas constant	J/kg Mol	(4.27)

Ra	Rayleight number	--	(3.11)
R_b	View factor for beam radiation	--	(2.16)
R_d	View factor for diffuse radiation	--	(2.17)
Re	Reynolds number	--	(3.4)
R_g	View factor for grounded-reflected radiation	--	(2.18)
R_N, T_N	Energy reflection and transmission coefficient for the case the incident electric wave E_i perpendicular to the plane of incident	--	(2.27 a–b)
R_P, T_P	Energy reflection and transmission coefficient for the case the incident electric wave E_i parallel to the plane of incident	--	(2.26 a–b)
r	Fraction of beam radiation	--	(2.29)
s	Air space of collector	m	(3.11)
T	– Energy transmission coefficient	--	(2.25b)
	– Temperature	K	(3.4)
T_a	Air temperature	°C	(3.18)
T_{av}	Average temperature	°C	(4.15)
T_c	Temperature of cover	°C	(3.19)
T_f	Temperature of fluid	°C	(3.3)
Tf_i	Temperature of air at inlet	°C	(3.21)
Tf_o	Temperature of air at outlet	°C	(3.41)
Tf_s	Temperature of fish surface	°C	(4.16)
T_p	Temperature of absorbing plate	°C	(3.21)
Ts	– True solar time	hr	(2.1)
	– Surface temperature	°C	(3.3)
Tf_{ave}	Average fluid temperature along collector	°C	(3.47)
Tp_{ave}	Average temperature of absorbing plate along collector	°C	(3.48)
T_{sky}	Temperature of the sky (surroundings)	K	(3.18)
t_c	Time at the end of constant rate period	sec	(4.30)
U_b	Bottom loss coefficient	W/m^2K	(3.22)
U_t	Top loss coefficient	W/m^2K	(3.20)
U_L	Overall loss coefficient	W/m^2K	(3.29)
U_o	Total heat transfer coefficient from enclosed air to ambient air	W/m^2K	(3.38)
V''	Volumetric coefficient expansion	K^{-1}	(3.11)
v	Wind speed	m/sec	(3.13)
x	Thickness of material	m	(2.31)
Y	Absolute humidity	kg H^2O/kg dry air	(4.37)
Y_i, Y_o	Absolute humidities at inlet and outlet		(4.1)
y	Width of collector	m	(3.39)

CHAPTER 1

INTRODUCTION

A solar drier is a development of simple sun or natural drying used to dry agricultural products, such as fruit, corn and paddy, including fish. Several kinds of solar fish driers have been developed over the world, particularly in developing countries in tropical areas. The solar fish driers that have been built include a solar cabinet drier, a polythene tent drier and a SCD (Separate Collector Drier) solar drier. Most of the driers were built without regard to optimum dimensions, fish capacity or drying rate.

Sun drying is a traditional method used to preserve fish in order to increase its storage life. This method is still practiced, particularly in the rural areas of developing tropical countries because it is very simple and low cost. Fish are spread on concrete, the ground or racks during daylight. The disadvantages of the method are loss of quality from dust, dirt, flies, and so on. Fish must be covered at night and uncovered again in the morning. Drying takes several days and may be interrupted by rain.

Due to the disadvantages of sun drying, other alternatives must be found. Problems which exist in sun drying need to be reduced. A simple and low cost drier was constructed by Doe et al (1977) in Bangladesh. The drier is called a polythene tent drier. The drier was erected on a triangular bamboo frame. The base and rear sides were covered with black sheeting and the side facing incoming solar radiation was covered with clear plastic. Fish were loaded on a bamboo lattice about 30 cm from the base inside the drier. Materials used for construction of the drier were obtained locally and were inexpensive. This method increased the drying rate and temperature inside the drier. With high air temperature, fly larvae and adult flies were killed easily.

A solar cabinet drier can also be used to dry fish. This form of drier was developed by Lawan (1966), in Trim and Curran (1983) and further developed by the Brace Research Institute (1973). It was built in a rectangular shape from plywood with a sloping transparent cover. Each side wall was constructed in two layers. The innermost surfaces were blackened to increase the absorption of solar radiation. There were several holes drilled in the bottom to let air into the cabinet. Outlet holes were located at the top front and sides of the cabinet. Fish were placed inside the drier.

At the Asian Institute of Technology (AIT) in Thailand, a SCD drier was built for drying paddy. This was developed by Exell and Kornsakoo (1978 and 1979) and Exell (1980). The construction of the drier is different from both polythene tent driers and cabinet driers. The main difference is in the design of the solar heat collector. The collectors of the polythene tent driers and the cabinet driers are located inside the driers. In the SCD drier, the collectors are placed separately from the drying chamber. Solar radiation is collected and heats air inside the collector. Warm air is passed through the chamber to heat paddy. The chamber of the SCD drier was made from wood and its bottom from a steel sheet perforated with holes. Each wall was made from wood. Clear plastic sheet was used to cover the collector and the chamber. To increase the air flow rate through the drier, a chimney from a bamboo frame covered by a black plastic sheet was attached on the top of the drier. This prototype is not only used for drying paddy but also for fish.

The three driers (polythene tent, cabinet and SCD driers) have the same fundamental basis of operation. Natural convection is created through the driers. As air temperature increases due to incoming solar radiation, its density becomes lower than ambient air. Therefore there is a pressure difference between inlet air at the bottom and outlet air on the top of the drier and the air moves out by natural convection.

Trim and Curran (1983) constructed and operated the three types of driers (polythene tent, cabinet and SCD driers) to dry fish in Ecuador. The performance of each drier was compared with that of sun drying on a rack and on rocks. Similar dimensions were used for each drier so that comparison became more accurate. Drying rates were faster in the three driers than both sun drying methods. Final moisture content was lower in solar driers than in sun drying. The polythene drier is more suitable for individual fishermen than the SCD drier because it is simple and costs less.

Other designs of solar fish driers have been developed and are described briefly in the Report of an Ad Hoc Panel of the Board on Science and Technology for International Development (1988) : for example, a solar dome drier with a capacity of around 1000 kg fish developed in Aden; an oil drum solar drier built from an oil drum and mounted on a wooden frame; a mud solar drier developed in Tanzania constructed from clay and bamboo tubes.

As mentioned earlier, most of the driers were built without regard to optimum dimensions. Thus it is likely that improvements can be made through simulation of performance and optimization of design. Simulation processes are carried out by taking into account several parameters influencing the characteristics of the drier, including meteorological data. Doe and Heruwati (1988) developed a mathematical model to simulate sun-drying which predicted microbial spoilage of the sun-dried tropical fish. During this simulation, climatic data such as temperature and humidity of air, solar radiation and wind speed were considered to be constant.

The solar fish drier discussed in this thesis was designed from simulation studies and was built in Bagan Siapi-api, Riau-Sumatra, Indonesia in 1990 by the author. The drier was similar to the SCD drier, in that it had an external heat collector (indirect solar drier). Variations of the climatic data and fish conditions

inside a drying chamber with respect to time were included. Wind speed was assumed to be constant. The thickness and surface area of fish were also assumed to be constant during the simulation.

The objective of this study is to examine the limitations of the present computer simulation (appendix G) in its ability to estimate the performance of the drier, particularly with regard to drying rate. The relationship between variations of moisture content and water activity of the dried fish and drying time are also examined. The storage life of the dried fish is predicted.

CHAPTER 2

SOLAR RADIATION

Solar radiation is the source of energy used for a solar drier. In this section there is brief information about the sun together with information about how solar radiation is absorbed by a solar collector. Also included is an explanation of the variation in extraterrestial solar radiation as measured from above the atmosphere, and a prediction of the flux of solar radiation on a horizontal or a tilted surface. Some other parameters involved in prediction of solar radiation for this purpose such as solar angles are discussed.

2.1 The sun

The source of solar energy is the sun which is a spherical body of radius (Ro) about 695,000 km with a very high temperature and with density as high as a hundred times the density of water. The temperature of the inner core of the sun with radius approximately 0.30 Ro ranges from 6.7×10^6 K to 15.5×10^6 K. This temperature is maintained constant by a continuous nuclear fusion process. The most important process in the inner core of the sun is the process of combination of Hydrogen to produce Helium. Four protons from four hydrogens build up one Helium nucleus. If we do a calculation we find that the mass of one Helium is less than the mass of the four protons. The rest of the mass is usually converted to energy which is transmitted in all directions in the form of X-rays and gamma rays with various wavelengths as well as thermal radiation.

The region from 0.3 Ro to 1.0 Ro is known as the convection zone because the convection process commences in this region. Here the temperature of the gas

drops from 130,000 to 5000 degrees Kelvin and its density decreases from 70 to 0.00001 kg/m^3.

For practical purposes the sun is considered as a blackbody radiator at fixed temperature. The effective temperature is about 5800 degrees Kelvin. Thekaekara (1974), in Thomas (1980) estimated the temperature of the sun to be 5762 degrees Kelvin. He also calculated the effective total emissive power of the sun using the Stefan-Boltzman law. The power obtained is as high as 6.25×10^7 W/m^2.

The total radiant energy emitted from the surface of the sun is proportional to the fourth power of absolute surface temperature and proportional to the surface area. Since the radiated energy is transmitted in all directions, the surface area of the sphere around the sun must be considered. By taking the radius of the sphere to be the average distance between the earth and the sun (about 1.5×10^{11} m) and the diameter of the sun to be about 1.39×10^9 m with the sun's surface temperature around 5.76×10^3 K, the rate of radiated energy per unit area on a horizontal surface at the orbit on the earth is found to be approximately 1353 W/m^2. This quantity is usually called the solar constant. The value of the solar constant varies about $\pm$ 3 % due to the variation in the distance between the earth and the sun (see section.2.3).

Solar radiation before reaching the earth's surface is attenuated by the atmosphere. For instance, gases such as nitrogen, oxygen and others absorb the components of the short wavelength gamma ray and X-ray. The ozone layer absorbs ultraviolet radiation. Solar radiation with wavelengths larger than 2.5 microns in the infrared is absorbed by water vapor and carbon dioxide. Therefore the only solar radiation that can reach the earth is electromagnetic radiation with wavelengths ranging from 0.29 to 2.5 microns. In addition to this, solar radiation is scattered and diffused by the atmosphere. Hence, only wavelengths of solar

radiation ranging from 0.29 to 2.5 microns need be considered when solar radiation is used as a source of energy for practical purposes, such as a solar heat collector.

2.2 Solar angles

The amount of solar radiation reaching the earth is only one part of the input data required for the design of a solar heat collector. To determine the intensity of radiation on a collector surface, it is necessary to know the position of the sun which depends on several angles (Benford and Bock, 1939), in Duffie and Beckman (1980). Some angles are indicated and defined in figure 2.1.

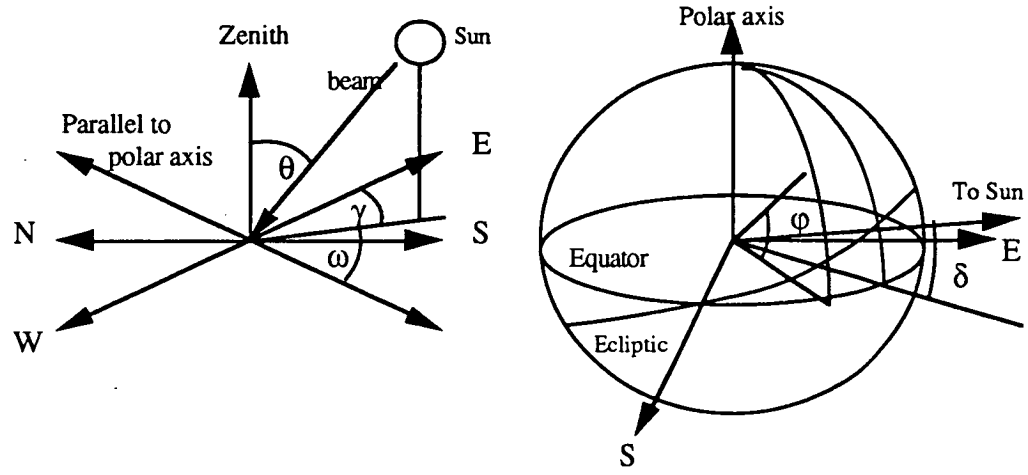

Figure 2.1. Solar angles
(After Williams, 1983)

The zenith is indicated by the vertical line which is extended from the observer. The angle between the incident ray from the sun and the zenith line is called the zenith angle θz. The projection of the incident ray on the horizontal surface forms an angle with the North-South axis. This angle is usually called the solar azimuth angle γ. The surface azimuth solar angle which is represented by γ is absolutely dependent on the orientation of the surface. For instance, γ= 0 when the surface faces South.

The hour angle ω depends on the angular displacement of the sun. Its value changes regularly with time from about -90 degrees at sunrise to about 90 degrees at sunset. The hour angle changes its value 15 degrees per hour. It will be zero when the sun is at its highest position at about 12.00 noon. The hour angle described above may be determined with the help of equation (2.1) in terms of the true solar time.

$$\omega = 15\ (12\ -\ Ts) \tag{2.1}$$

where Ts is the true solar time in hours.

Solar time is usually different from local standard time. It is not only dependent on local standard time but also on the longitude of the standard meridian for the local time zone and the local meridian. The solar time equation may be found in several books, such as Solar Engineering Technology (Jansen, 1985). Solar time in general is assumed to be the same as local time for the purposes of this work.

Table 2.1 The day of the year

Month	**n**	**Month**	**n**
January	a	July	181 + a
February	31 + a	August	212 + a
March	59 + a	September	243 + a
April	90 + a	October	273 + a
May	120 + a	November	304 + a
June	151 + a	December	334 + a

where a is the date in each month. For instance, If the day is January 7 then n = a = 7 and June 20 indicates n = 151 + 20 = 171, etc. Leap years are excluded from this table. Values of the day of the year from March onward for leap years are modified by adding 1.

The other angle is the angle between the incoming solar radiation and the plane of the earth's equator. This angle is usually called the declination angle δ. An

empirical equation to predict this angle is given by Cooper (1969), in Duffie and Beckman (1980). The angle varies in terms of a sine function of the day of the year and is given by

$$\delta = 23.45 \text{ Sin}\frac{360\ (n + 284)}{365} \tag{2.2}$$

where n is the day of the year (table 2.1).

If hour angle, declination angle and latitude of a specific place are known, the zenith angle can be calculated using equation (2.3). To obtain this relationship, the law of cosines for spherical triangles may be used (Coffari, 1977 and Jansen, 1985). The zenith angle is given as functions of ω,δ and φ by

$$\text{Cos } \theta z = \text{Cos } \varphi \text{ Cos } \delta \text{ Cos } \omega + \text{Sin } \varphi \text{ Sin } \delta \tag{2.3}$$

where φ is the latitude, that is the angular location south or north of the equator. Its value is positive in the North and negative in the South.

2.3 Extraterrestial solar radiation

The extraterrestial solar radiation is direct radiation which is measured above the atmosphere. Due to the variation of the distance between the sun and the earth depending on the time of the year, its value varies during the year by up to $\pm$ 3 % and is graphically shown in figure 2.2. A fitted empirical equation from the graph is written as

$$\text{Go} = \text{Gc}\{1 + 0.033 \text{ Cos}\frac{360\ n}{365}\} \tag{2.4}$$

where Go and Gc are the extraterrestial solar radiation and solar constant respectively and n is the day of the year (see table 2.1).

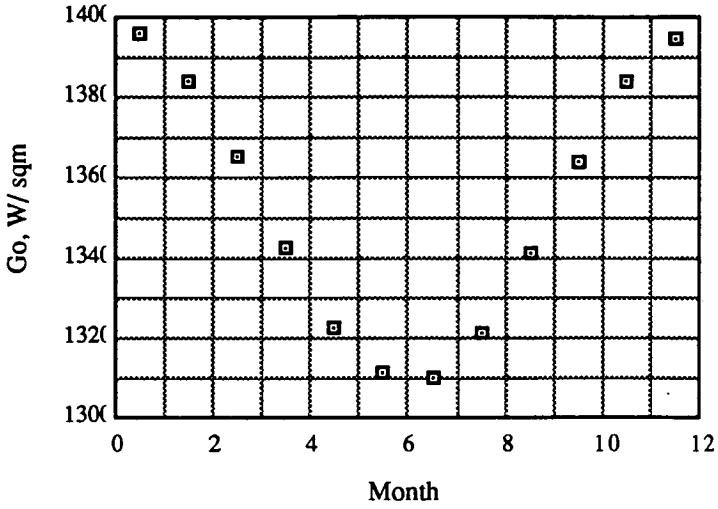

Figure 2.2 Variation of extraterrestial solar radiation
(after Duffie and Beckman, 1980)

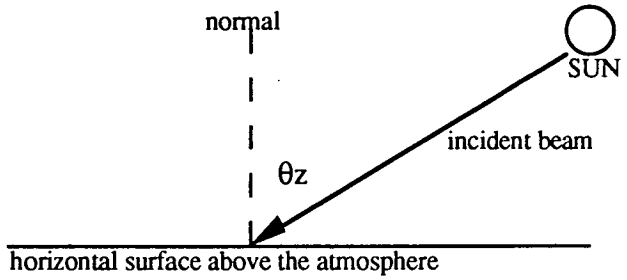

Figure 2.3 Beam radiation on a horizontal surface

It is necessary to know the solar radiation on a horizontal surface outside the earth's atmosphere I_o at any time between sunrise and sunset because it is used for calculation of a clearness index (defined in section 2.4) of the sky. The incident solar radiation and the zenith angle θ_z on the horizontal surface outside the earth's atmosphere is depicted in figure 2.3. By multiplying the extraterrestial solar radiation in equation (2.4) by the cosine of the zenith angle in equation (2.3), one obtains the relationship

$$I_o = Go \ Cos \ \theta z$$

or $$I_o = Go \ (Cos \ \varphi \ Cos \ \delta \ Cos \ \omega + Sin \ \varphi \ Sin \ \delta). \qquad (2.5)$$

2.4 Correlation between diffuse and global radiation

Solar radiation is absorbed and scattered during its propogation through the atmosphere. Therefore the intensity of the solar radiation which is measured on the ground decreases. Solar radiation reaching a horizontal surface on the earth without having been scattered is called beam or direct radiation and it is named diffuse radiation when its direction has been changed by scattering by the atmosphere. The sum of the beam and diffuse radiation is called global radiation.

Measurements of global and diffuse radiation have been carried out by several scientists to obtain empirical correlations. Orgill and Hollands (1977) used hourly diffuse and global radiation data collected in Canaada to express the relationship between (I_d/I) and k_T, where I_d is the hourly diffuse radiation, I is the hourly global radiation and k_T is the ratio between the hourly global radiation and the hourly extraterrestial radiation I_o. The hourly values of I_o are obtained from equation (2.5). Bugler (1977) and Stauter and Klein (1979), in Duffie and Beckman (1980) have developed correlations between the diffuse and global radiation from a different method. The values of the hourly diffuse fraction (I_d/I) as a function k_c were plotted to find the correlations, where k_c is the ratio between the hourly global radiation I and an estimate of hourly clear sky radiation I_c (see equation 2.12).

The hourly clear sky radiation I_c is the sum of hourly beam and diffuse clear sky radiation. To determine both kinds of radiation, one needs to know beam and diffuse atmospheric transmittance coefficients for clear sky as outlined below.

Hottel (1976) described a method to predict the beam radiation passing through the clear sky atmosphere. To do this, parameters zenith angle and altitude were considered. An empirical equation to determine the atmospheric transmittance τ_b for the clear sky atmosphere is given as

$$\tau_b = Xo + X1 \exp\left(\frac{c}{\cos \theta z}\right) \tag{2.6}$$

where θz is the zenith angle calculated from equation (2.3) and the constants Xo, X1 and c can be obtained from the equations below

$$\begin{aligned} Xo &= Xo' \,[0.4237 - 0.00821\,(6 - A)^2] \\ X1 &= X1' \,[0.5055 + 0.00595\,(6.5 - A)^2] \\ c &= c' \,[0.2711 + 0.01858\,(2.5 - A)^2] \end{aligned} \tag{2.7}$$

where A is the altitude in km.

Hottel suggested that equation (2.7) is valid for regions with altitude A less than 2.5 km from the sea level. Correction factors Xo', X1' and c' are defined for different seasons and climate. Four different climate types have been tabulated in table 2.2.

Table 2.2 Correction factors

Climate	**Xo'**	**X1'**	**c'**
Tropical	0.95	0.98	1.02
M L* Summer	0.97	0.99	1.02
Subarctic Summer	0.99	0.99	1.01
M L* Winter	1.03	1.01	1.00

* M L is abbreviated from Mid Latitude

Based on Hottel's method the clear sky beam normal radiation I_{cb} can be predicted for any zenith angle and any altitude less than 2.5 km for periods of an hour given by

$$I_{cb} = I_o \tau_b \tag{2.8}$$

where Io is calculated from equation (2.5).

Liu and Jordan (1960), in Duffie and Beckman (1980) estimated the transmission coefficient τ_d of diffuse radiation using the linear empirical relationship (2.9) as follows

$$\tau_d = 0.2710 - 0.2939\ \tau_b \qquad (2.9)$$

where τ_d is defined as the ratio of diffuse radiation to extraterrestial radiation on the horizontal surface.

Hence the clear sky hour's diffuse radiation is calculated similar to that of equation (2.8) and written as follows

$$I_{cd} = Io\ \tau_d. \qquad (2.10)$$

The hour's clear sky total radiation on the horizontal surface is now calculated by the sum of I_{cb} in equation (2.8) and I_{cd} in equation (2.10) as follows

$$I_c = I_{cb} + I_{cd}. \qquad (2.11)$$

Since the total radiation on a horizontal surface has been predicted, the effect of the clearness of the sky is now included to obtain beam and diffuse radiation passing through the earth's atmosphere. The results of (I_d/I) and the hourly clearness index of the clear sky (I/I_c) were calculated where I and I_d are the measured global and diffuse radiation respectively. Using these computed results a graph given by (I_d/I) against (I/I_c) was obtained (Stauter and Klein, 1979) in Duffie and Beckman (1980). From the graph three correlations were obtained as follows

$$\begin{aligned} I_d &= (1.00 - 0.10\ k_c)\ I && \text{for } 0 \le k_c < 0.48 \\ I_d &= (1.11 + 0.0396\ k_c - 0.789\ k_c^2)\ I && \text{for } 0.48 \le k_c < 1.10 \\ I_d &= 0.20\ I && \text{for } k_c \ge 1.10 \end{aligned} \qquad (2.12)$$

where k_c has been defined.

Beam radiation is calculated by subtracting diffuse from global radiation as written below

$$I_b = I - I_d. \tag{2.13}$$

2.5 Solar radiation on a tilted surface

In practical situations such as in a solar heat collector, the surface of the collector is not usually horizontal but tilted toward the sun. Therefore solar radiation falling on a tilted surface must be considered. Bugler (1977) and Jimenez and Castro (1982) have developed a method to calculate solar radiation on a tilted surface oriented in any direction and at any time. A procedure to express an equation to calculate the incident angle of beam radiation on a tilted surface relating it to other solar angles is described by Coffari (1977) and the equation is written in the form of

$$\text{Cos}\,\theta = X1 - X2 + X3 + X4 + X5 \tag{2.14}$$

where $X1 = \text{Sin}\,\delta\ \text{Sin}\,\varphi\ \text{Cos}\,\beta$

$X2 = \text{Sin}\,\delta\ \text{Cos}\,\varphi\ \text{Sin}\,\beta\ \text{Cos}\,\gamma$

$X3 = \text{Cos}\,\delta\ \text{Cos}\,\varphi\ \text{Cos}\,\beta\ \text{Cos}\,\omega$

$X4 = \text{Cos}\,\delta\ \text{Sin}\,\varphi\ \text{Sin}\,\beta\ \text{Cos}\,\gamma\ \text{Cos}\,\omega$

$X5 = \text{Cos}\,\delta\ \text{Sin}\,\beta\ \text{Sin}\,\gamma\ \text{Sin}\,\omega$

where θ is the incident angle of beam radiation on the tilted surface (figure 2.4), β is the slope of the surface (figure 2.4), φ is the latitude at the collector site, γ is the azimuth angle and ω is the hour angle.

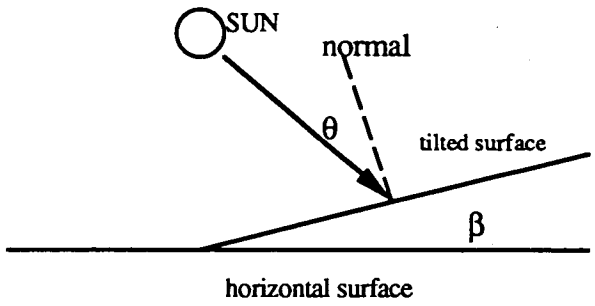

Figure 2.4 Beam radiation on a tilted surface

Equation (2.14) is only valid for $\theta < 90°$ and $\beta < 90°$. Another condition that should be considered is related to the azimuth angle γ. If the surface faces South, $\gamma = 0°$ and if it faces West, $\gamma = 90°$. If the surface faces East, $\gamma = -90°$ and finally if it faces North, $\gamma = 180°$.

For a horizontal surface, $\beta = 0°$ and equation (2.14) can be written as follows

$$\text{Cos } \theta z = \text{Cos } \delta \text{ Cos } \varphi \text{ Cos } \omega + \text{Sin } \delta \text{ Sin } \varphi. \qquad (2.15)$$

This is the same as equation (2.3) because Sin $\beta = 0$ and Cos $\beta = 1$ in equation (2.14). The ratio between (Cos θ) in equation (2.14) and (Cos θz) in equation (2.15) gives a geometric factor R_b. This is given below

$$R_b = \frac{\text{Cos } \theta}{\text{Cos } \theta z}. \qquad (2.16)$$

Liu and Jordan (1963), in Duffie and Beckman (1980) have developed the concept of solar radiation on tilted surfaces. They noted that there are three components of solar radiation falling on tilted surfaces; beam, diffuse and ground reflected radiation. A factor affecting the diffuse and ground-reflected radiation on the tilted surface is named the view factor. For diffuse radiation, the view factor labelled by R_d is predicted by equation (2.17) below

$$R_d = \frac{1.0 + \text{Cos } \beta}{2}. \qquad (2.17)$$

The view factor for the ground-reflected radiation denoted by R_g is written as follows

$$R_g = \frac{1.0 - \text{Cos}\ \beta}{2}. \qquad (2.18)$$

For horizontal surfaces, the view factors $R_d = 1$ and $R_g = 0$. For this situation, there is no ground-reflected radiation incident on the surface. For a vertical surface the view factors $R_d = 0.5$ and $R_g = 0.5$. It is clear that only 50 % of both diffuse and ground-reflected radiation are received by the surface. The remaining 50 % is reflected to the surroundings.

The total radiation on tilted surfaces is now obtained by adding the three components ($I_b R_b$), ($I_d R_d$) and (($I_b + I_d$) $R_g \rho$ as follows

$$I_T = I_b R_b + I_d R_d + (I_b + I_d) \rho R_g. \qquad (2.19)$$

where ($I_b + I_d$) is the global radiation and ρ is the reflectance of the surrounding area. The value of ρ is dependent of the area where the measurements are made. For example, ρ is equal to 0.2 if there is no snow cover and it is 0.7 when the ground is completely covered by snow.

The total radiation I_T described above is the radiation on the tilted surface with beam incident angle θ. When it passes through transparent material its intensity will be reduced due to absorption and reflection by the material. For transmitted radiation, parameters such as index of refraction and thickness of material will become the main factors and will be described later.

2.6 Solar radiation as electromagnetic waves

Solar radiation propagates as electromagnetic waves which consist of the combination of electric (**E**) and magnetic (**H**) waves. These two waves are known

as the polarization components which are dependent on and perpendicular to each other and perpendicular to the direction of propagation. Therefore solar radiation as electromagnetic waves is considered in three dimensions.

When solar radiation is incident on a smooth surface of a transparent material such as the plastic or glass cover of a solar heat collector, it is separated into three fractions; reflected, absorbed and transmitted. To describe these, one needs to know concepts of electromagnetic theory given by Snell's law and Fresnel's equations. The fractions of reflected and transmitted solar radiation can be found by considering energy flow across an interface of the material.

2.6.1 Snell's law and Fresnel's equations

When incident solar radiation from medium 1 with index of refraction n1 passes through an interface into medium 2 with index of refraction n2 where n1 is smaller than n2, some solar radiation will be reflected and some will be transmitted in a different direction.

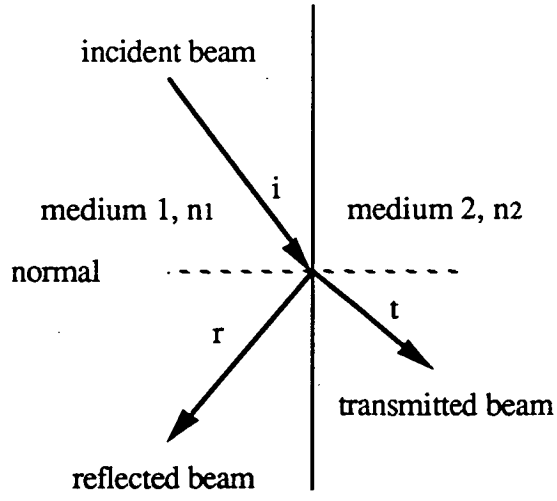

Figure 2.5 Incident, reflection and refraction of beam

If the incident solar radiation makes an angle with the normal to the surface (say i) and the refracted angle is t as shown in figure 2.5, an equation to relate parameters n1, n2, i and t is given as follows

$$n1 \sin i = n2 \sin t . \tag{2.20}$$

This equation is known as Snell's law.

Using the boundary conditions from electromagnetic theory the polarization components can be described as tangential or parallel to the boundary (Stratton, 1942). When an electric wave is parallel to a plane formed by an initial wave and the normal to the surface (called the plane of incidence) as shown in figure 2.6a, the tangential components of magnetic and electric waves at the interface are given by

$$H_i + H_r = H_t$$

or $$k_i (E_i + E_r) = k_t E_t$$

and $$E_i \text{ Cos } i - E_r \text{ Cos } i = E_t \text{ Cos } t \tag{2.21}$$

where H and E represent magnetic and electric waves respectively, kt/ki = n2/n1 for non-magnetic materials, k represents the wave number and the subscripts indicate incident for i, reflected for r and transmitted for t.

When equation (2.20) is substituted into equation (2.21) and solved for Er and Et then one may obtain the reflected and transmitted amplitude coefficients of solar radiation

$$\left(\frac{E_r}{E_i}\right)_P = \frac{n1 \text{ Cos } t - n2 \text{ Cos } i}{n1 \text{ Cos } t + n2 \text{ Cos } i} \tag{2.22a}$$

$$\left(\frac{E_t}{E_i}\right)_P = \frac{2\, n1 \text{ Cos } i}{n1 \text{ Cos } t + n2 \text{ Cos } i} \tag{2.22b}$$

where the subscript P indicates that E_i is parallel to the plane of incidence (defined above).

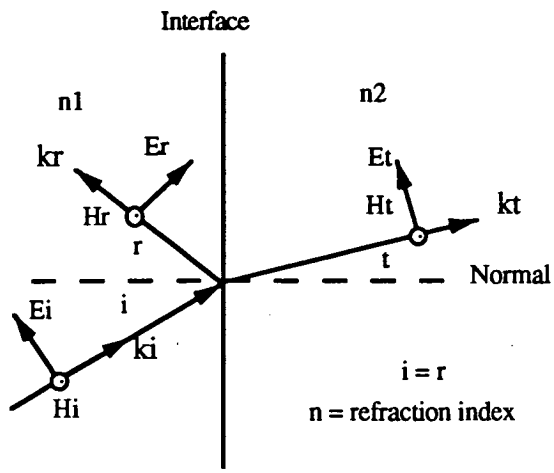

Figure 2.6a
Parallel polarized wave

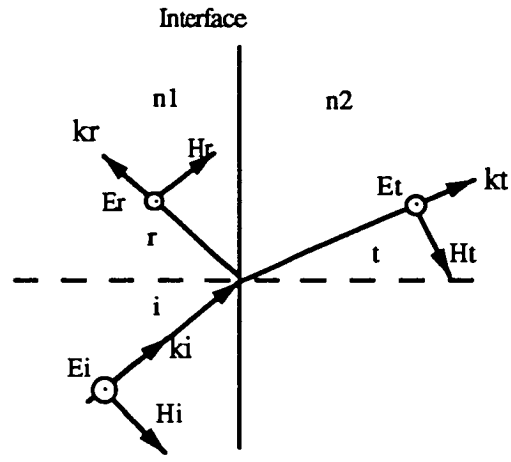

Figure 2.6b
Tangential polarized wave

When an electric wave is perpendicular to the plane of incidence as shown in figure 2.6b, the tangential components of electric and magnetic waves at the interface require that

$$E_i + E_r = E_t$$

and $$H_i \cos i - H_r \cos i = H_t \cos t. \qquad (2.23)$$

Using the same method to find equations (2.22a, b) one may obtain expressions for the reflection and transmission amplitude coefficients as follows

$$\left(\frac{E_r}{E_i}\right)_N = \frac{n1 \cos i - n2 \cos t}{n1 \cos i + n2 \cos t} \qquad (2.24a)$$

$$\left(\frac{E_t}{E_i}\right)_N = \frac{2\, n1 \cos i}{n1 \cos i + n2 \cos t}. \qquad (2.24b)$$

The subscript N indicates that E_i is perpendicular to the plane of incidence. Equations (2.22a), (2.22b), (2.24a) and (2.24b) are called Fresnel's equations.

2.6.2 Transmission coefficient of a non-absorbing material

As noted earlier the concept of energy flow is used to find the coefficients of the energy reflection and transmission through an interface of material. The average energy flux per unit area in the incident wave is given by the average value of the Poynting vector (**E** x **H**) (see Stratton, 1942). The energy reflection coefficient R and energy transmission coefficient T (figures 2.6a,b) are defined as the ratios of the average energy fluxes per unit area and per unit time at the interface. This reduces to

$$R = \frac{E_r^2}{E_i^2} \tag{2.25a}$$

for the energy reflection coefficient and

$$T = \frac{E_t^2 n2 \text{ Cos } t}{E_i^2 n1 \text{ Cos } i} \tag{2.25b}$$

for the energy transmission coefficient.

When equations (2.22a), (2.22b), (2.24a) and (2.24b) are substituted into equations (2.25a) and (2.25b) one may obtain

$$R_P = \left\{\frac{n1 \text{ Cos } t - n2 \text{ Cos } i}{n1 \text{ Cos } t + n2 \text{ Cos } i}\right\}^2 \tag{2.26a}$$

$$T_P = \frac{4\, n1\, n2 \text{ Cos } i \text{ Cos } t}{(n2 \text{ Cos } i + n1 \text{ Cos } t)^2} \tag{2.26b}$$

$$R_N = \left\{\frac{n1 \text{ Cos } i - n2 \text{ Cos } t}{n1 \text{ Cos } i + n2 \text{ Cos } t}\right\}^2 \tag{2.27a}$$

$$T_N = \frac{4\, n1\, n2 \text{ Cos } i \text{ Cos } t}{(n1 \text{ Cos } i + n2 \text{ Cos } t)^2} \tag{2.27b}$$

where R + T = 1, since there must be conservation of energy.

To simplify the problem, we only consider the components of reflection coefficients given by equations (2.26a) and (2.27a). When equation (2.20) is

substituted into these two equations, refraction indices n1 and n2 will be eliminated. Hence we may write

$$R_N = \left\{\frac{\text{Sin } (t - i)}{\text{Sin } (t + i)}\right\}^2 \tag{2.28a}$$

$$R_P = \left\{\frac{\tan (t - i)}{\tan (t + i)}\right\}^2. \tag{2.28b}$$

The other two components can be obtained using the same technique. However, by these components R_N and R_P we could determine the parallel and perpendicular components of the transmission coefficient. To show this, a ray-tracing method is applied (Duffie and Beckman, 1980). Let us consider the transmission through a smooth non-absorbing material in figure (2.7). The material has two interfaces. When a ray is incident on the first interface, the ray is then reflected and transmitted. If the intensity of the incident ray is unity then the reflected and transmitted intensity are r_1 and r_2 respectively. The transmitted ray becomes an incident ray for the second interface. The intensity of the reflected ray is equal to r_4 and the transmitted intensity is equal to r_3, and so on. The fractions r_1, r_2, and so on are described below.

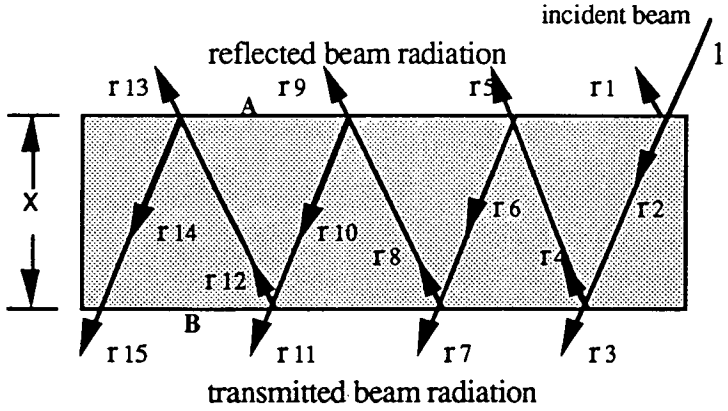

A and B represent the first and second interfaces and x is the thickness

$r_1 = r$, $r_2 = 1\text{-}r$, $r_3 = (1\text{-}r)^2$, $r_4 = (1\text{-}r)r$, $r_5 = (1\text{-}r)^2 r$, $r_6 = (1\text{-}r)r^2$, $r_7 = (1\text{-}r)^2 r^2$ $r_8 = (1\text{-}r)r^3$, $r_9 = (1\text{-}r)^2 r^3$, $r_{10} = (1\text{-}r)r^4$, $r_{11} = (1\text{-}r)^2 r^4$, $r_{12} = (1\text{-}r)r^5$, and so on.

Fig 2.7 Reflection, refraction and transmission on a non absorbing cover

When the transmitted rays (r_3, r_7,...and r_∞) at the second interface are added together, the transmission coefficient τ of the non absorbing material is obtained as written below

$$\tau = (1 - r)^2 \sum_{n=0}^{\infty} r^{2n} = \frac{(1 - r)^2}{1 - r^2}$$

or $$\tau = \frac{1 - r}{1 + r}. \qquad (2.29)$$

Here r is given by equation (2.26a) for the parallel component and equation (2.27a) for the perpendicular component of reflection coefficient of polarization.

2.7 Optical properties of an absorbing material

When solar radiation with intensity I_0 passes through a transparent material of thickness x normal to an interface, the absorbed radiation dI is proportional to I_0 and x. This consideration is referred to as Bouguer's law and given below

$$dI = - I C dx \qquad (2.30)$$

where C is the extinction coefficient. For the solar spectrum, C is assumed to be constant with solar radiation spectrum (wavelengths ranging from 0.29 to 2.5 μm). The intensity of solar radiation transmitted I_t through the transparent material can be calculated by integrating equation (2.30) with respect to the distance from zero to the thickness x, and we write

$$I_t = I_0 \exp(- C x). \qquad (2.31)$$

When incident solar radiation makes an angle i with the normal to the surface as indicated in figure 2.8, the distance travelled by solar radiation through

the material is equal to the thickness of material divided by the cosine of the refracted angle (r). Hence the transmitted radiation is then obtained as follows

$$I_t = I_o \exp\left(-\frac{C\ X}{\cos r}\right). \tag{2.32}$$

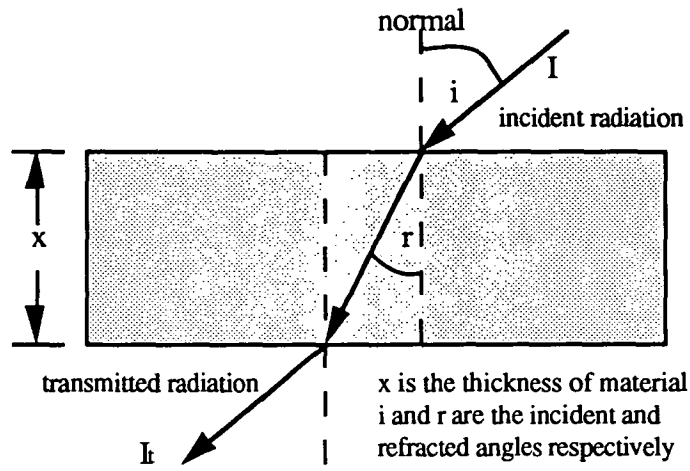

Figure 2.8 Absorption of solar radiation

The transmission coefficient of the transparent material is obtained as the ratio between I_t and I_o. This reduces to

$$\tau_a = \exp\left(-\frac{C\ X}{\cos r}\right). \tag{2.33}$$

To obtain the coefficient of the two components, the ray-tracing method described in section (2.6.2) can be applied again. The transmission, reflection and absorption coefficients of the perpendicular component of the polarization are written as follows

$$\tau_N = \frac{\tau_a\,(1 - R_N)^2}{1 - (R_N\tau_a)^2} = \tau_a \left(\frac{1 - R_N}{1 + R_N}\right)\left(\frac{1 - R_N^2}{1 - (R_N\tau_a)^2}\right) \tag{2.34a}$$

$$\rho_N = R_N + \frac{(1 - R_N)^2\,\tau_a^2\,R_N}{1 - (R_N\tau_a)^2} = R_N\,(1 + \tau_a\,\tau_N) \tag{2.34b}$$

$$\alpha_N = (1 - \tau_a)\left\{\frac{1 - R_N}{1 - (R_N\tau_a)}\right\}. \tag{2.34c}$$

For practical purposes, each of the last terms of equation (2.34a) and equation (2.34c) is close to unity, because "τ_a is seldom less than 0.9 and R_N is of the order of 0.1 for practical collector cover" (Duffie and Beckman, 1980). Hence we may write the transmission coefficient of a single cover as

$$\tau = \tau_a \{0.5 (\frac{1 - R_N}{1 + R_N} + \frac{1 - R_P}{1 + R_P})\} \tag{2.35}$$

where R_P and R_N are calculated from equations (2.26a) and (2.27a). The value of τ_a is determined from equation (2.33). Hence, the value of the transmission coefficient is clearly dependent on the incidence angle of incoming radiation on the surface.

The absorption coefficient of a single cover is written as

$$\alpha \cong (1 - \tau_a). \tag{2.36}$$

Finally, the reflection coefficient for a single cover is obtained as

$$\rho = 1 - \alpha - \tau. \tag{2.37}$$

Those three parameters ρ, α and τ indicate the optical properties of the material (cover of the solar collector) which are dependent on the incident angle of beam radiation at the interface.

2.8 Effective angle

As described in section (2.5), there are three components of solar radiation absorbed by a tilted surface. The incident angle of beam radiation is different from the incident angle of the others. The incident angles of diffuse sky and ground-reflected radiation are also different from each other and are dependent on the angle of the tilted surface. These two angles are called effective angles. The variation of

these angles is obtained from experimental measurements. From these data the relationship between effective angle and the angle of the tilted surface is formulated. Brandemuehl and Beckman (1980) estimated this variation. They found that the effective beam radiation incident angle for diffuse ground radiation is

$$\theta_e = 90 - 0.5788\,\beta + 0.002693\,\beta^2. \tag{2.38}$$

For diffuse sky radiation, it is

$$\theta_e = 59.68 - 0.1388\,\beta + 0.001497\,\beta^2. \tag{2.39}$$

These two equations will be used when we begin to determine the three optical properties of the material (cover of the solar collector) particularly for diffuse sky and ground-reflected radiation.

2.9 Determination of the transmittance-absorptance product

In section (2.5) we have presented a method to determine total radiation on a tilted collector surface in terms of beam, diffuse and ground-reflected radiation including the view factors of the tilted surface itself. However we have not shown how much solar energy is absorbed and converted to heat energy. To describe this, one needs to describe what we call the transmittance-absorptance product ($\tau\alpha$). This parameter exists due to the existence of multiple reflections of solar radiation between the absorbing plate and cover of a solar heat collector. Some transmitted radiation (beam, diffuse and ground-reflected radiation) reaching the absorbing plate is reflected back to the cover. Some of this reflected radiation is reflected back again to the plate. These multiple reflections occur continuously as long as the solar radiation is present. The multiple reflections between absorbing plate and cover are presented in figure 2.9.

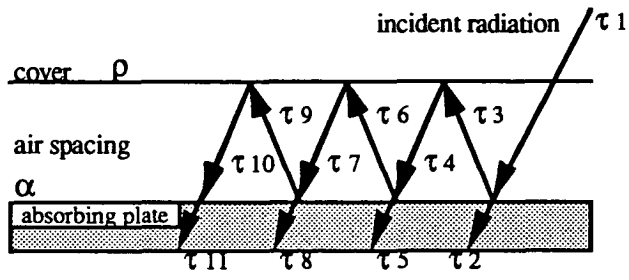

$\tau_1 = \tau$, $\tau_2 = \tau\,\alpha$, $\tau_3 = (1-\alpha)\tau$, $\tau_4 = (1-\alpha)\,\rho\,\tau$, $\tau_5 = (1-\alpha)\rho\,\tau\,\alpha$, $\tau_6 = (1-\alpha)^2\,\rho\,\tau$, $\tau_7 = (1-\alpha)^2\rho^2\,\tau$, $\tau_8 = (1-\alpha)^2\rho^2\,\tau\,\alpha$, $\tau_9 = (1-\alpha)^3\rho^2\,\tau$, $\tau_{10} = (1-\alpha)^3\rho^3\,\tau$, $\tau_{11} = (1-\alpha)^3\rho^3\tau\,\alpha$ and so on.

Figure 2.9 Solar radiation absorbed by absorbing plate

To determine the transmittance-absorptance product ($\tau\alpha$) of the solar collector, we need to apply the ray-tracing technique again (Duffie and Beckman, 1980). Hence we obtain

$$(\tau\alpha) = \tau\,\alpha \sum_{n=0}^{\infty}\{(1-\alpha)\rho_c\}^n = \frac{\tau\,\alpha}{1-(1-\alpha)\rho_c}. \qquad (2.40)$$

If we calculate the value of ($\tau\alpha$) using equation (2.40) we obtain nearly 1.01 times the product of τ times α. Hence we can simplify equation (2.40) into equation (2.41) below

$$(\tau\alpha) \cong 1.01\,\tau\,\alpha \qquad (2.41)$$

where α is the absorption coefficient of the plate and τ is the transmission coefficient of the collector's cover. τ and α are calculated from equations (2.35) and (2.36) respectively.

The total radiation absorbed by a collector with a single cover is now obtained by multiplying the total radiation on the tilted surface in equation (2.19) and the transmittance-absorptance product ($\tau\alpha$) in equation (2.41). Hence we write as follows

$$I_T = I_b\,R_b(\tau\alpha)_b + I_d\,R_d\,(\tau\alpha)_d + (I_b+I_d)\,\rho\,R_g\,(\tau\alpha)_g \qquad (2.42)$$

where subscript b refers to beam radiation, d represents diffuse radiation and g indicates ground-reflected radiation.

This absorbed total radiation will be used as a source of energy for the present simulation of the solar drier. The symbol I_T will be replaced by H in the next chapters.

CHAPTER 3

SOLAR HEAT COLLECTOR

As described in the introduction (chapter.1) a solar drier is an alternative means of drying agricultural products, for example fruits, paddy, fish, etc, using solar energy. Solar radiation is absorbed by a solar heat collector and used to dry the wet product.

This chapter aims to review several aspects which relate to the collector. Discussion commences with concepts of heat transfer (conduction, convection and radiation). The discussion is extended to the application of the concepts to calculate all of the heat transfer coefficients which take place in the collector. Finally a method to calculate the characteristics of the collector such as an efficiency factor (section 3.8), etc are described.

3.1 Fundamental concepts of heat transfer

The transfer of heat from one point to another within a medium is usually in terms of conduction, convection and radiation processes. These three modes will be met in discussion of a solar collector because not all incoming radiation can be converted into useful heat energy. Some energy is lost to the environment by these three modes. Hence, it is necessary to describe these modes briefly as basic tools to derive equations for any heat transfer occuring in the collector. The concept of an electrical network is also included as a tool to determine a combination of thermal resistances (heat transfer coefficients) in the collector.

3.1.1 Conduction heat transfer

Heat transfer by conduction is the most important mode of heat transfer in solids. Conduction heat transfer in both gases and fluids is excluded from this study. According to Fourier, who made a lot of observations of this heat transfer, the conduction heat transfer for one dimension in any conductor is dependent on two main factors : the cross-section (A) of the material and the gradient of the material's temperature (dT/dx). In other words, that conduction heat transfer q_{cond} is proportional to A, proportional to temperature difference dT and inversely proportional to the length of conductor dx. This leads to the equation

$$q_{cond} = - k A \frac{dT}{dx} \tag{3.1}$$

where k is the thermal conductivity of the material in W/(m ^{o}C) which is assumed to be uniform and constant. The negative sign indicates that heat is transferred in the opposite direction to the gradient of temperature.

For the case of conduction through a uniform slab, or along an insulated rod, equation (3.1) is modified into the simple relation

$$q_{cond} = \frac{1}{L} k A (T_1 - T_2) \tag{3.2}$$

where (T_1-T_2) is the temperature difference between two points along the conductor in degrees Celsius and L is the length of conductor in m.

3.1.2 Convection heat transfer

Fluid is the medium of heat transfer by convection. Based on the nature of fluid flow, convective heat transfer is classified into two modes. When fluid flow is created by some external forces, such as a fan, atmospheric wind, etc, the flow is called forced convection. When fluid flow is caused by bouyancy forces, it is

named free or natural convection. An example of natural convection is the heat transfer which takes place between a hot horizontal surface and cooler air. Air that is in contact with the hot surface has a higher temperature, hence lower density than air above the surface. Because of gravitation, a circulation movement is created in which the cooler air moves downward close to the hot surface and the warm air moves upward. If the air surrounding the hot surface is not quiescent then the convective heat transfer may be dominated by forced convection.

In general, the rate of heat transfer by convection q_{conv} is proportional to to the difference between the surface and fluid temperatures and proportional to the surface area A and can be written

$$q_{cond} = h\,A\,(T_S - T_F) \tag{3.3}$$

where h is the average convective heat transfer coefficient in $W/(m^2\,K)$ and assumed to be constant. T_F and T_S are the temperatures of the fluid and the surface in degrees Celsius. This equation is known as Newton's law of cooling.

3.1.3 Radiation heat transfer

As described in sections (3.1.1) and (3.1.2) the media for conductive heat transfer can be either solids, liquids or gases and the media for convective heat transfer are gases and liquids. Heat transfer by radiation can occur in a vacuum, fluids and transparent solids. Heat radiation incident on a non transparent medium is absorbed and reflected. For a transparent medium such as a cover of a collector, radiation is not only absorbed and reflected but also transmitted through the cover. Those three fractions of radiation are indicated by absorption α reflection ρ and transmission τ coefficients (see section.2.7).

When discussing radiation of real surfaces, it is necessary to introduce the concept of an ideal blackbody briefly because the characteristics of real surfaces are

always compared with the characteristics of an ideal blackbody. The ideal blackbody is defined as a surface which can absorb all incoming radiation regardless of wavelength and direction. This indicates that the absorption coefficient α is equal to unity. It also emits more energy at any particular temperature and wavelength than other surfaces. The ideal blackbody is known as a diffuse emitter because it emits energy in all directions with emission coefficient ε equal to unity.

The ideal blackbody emits energy at a rate that is proportional to the fourth power of its absolute surface temperature T. Stefan-Bolztmann's law for the ideal blackbody thermal radiation indicates that

$$E_b = \sigma T^4 \tag{3.4}$$

where E_b is the total emissive power for the ideal blackbody and σ is the Stefan-Boltzmann constant, 5.67×10^{-8} W/(m^2 K^4).

The application of Stefan-Bolztmann's law for non-blackbody thermal radiation is now considered. If a non-blackbody material has surface temperature T which is higher than the temperature of its surroundings then it radiates energy per unit surface area at the rate

$$E_{nb} = \varepsilon \sigma T^4 \tag{3.5}$$

where E_{nb} is in W/m^2, ε is the emission coefficient of the material which ranges from zero to unity. If ε is equal to unity then it represents a blackbody.

Using equation (3.5) one can find the rate of thermal radiation between two non-blackbody surfaces either parallel or non-parallel flat plates. For non parallel flat plates, the thermal radiation is not completely absorbed by each surface. There is a geometric effect which is called thermal radiation shape factor. For instance, for two perpendicular surfaces with the same geometry, the thermal radiation emitted

from one surface is less than 20 % absorbed by the other surface (Thomas, 1980). The rest of the thermal radiation is absorbed by the surroundings.

To describe the exchange of thermal radiation between two surfaces, one may assume that the surface is gray where all radiation properties are independent of wavelength, the surface temperature and the incident energy over the surface are uniform.

Based on the method given by Thomas again one may derive the rate of the exchange of thermal radiation between two surfaces. For example, if two flat plates have surfaces A_1 and A_2 with surface temperatures T_1 and T_2 respectively then the following relationship is obtained.

$$q_{rad} = \frac{\sigma (T_1^4 - T_2^4)}{\frac{1 - \varepsilon_1}{A_1 \varepsilon_1} + \frac{1}{A_1 F_{1-2}} + \frac{1 - \varepsilon_2}{A_2 \varepsilon_2}} \tag{3.6}$$

where q_{rad} is in watts, F_{1-2} is the thermal radiation shape factor, ε_1 and ε_2 are the emission coefficients of surfaces A_1 and A_2 respectively.

From equation (3.6), two approximations can be employed. The first is when thermal radiation occurs between two infinite flat plates such as in flat plate collectors, the shape factor F_{1-2} is unity because it is assumed that all thermal radiation from surface A_1 will be absorbed by surface A_2 and the thermal radiation leaving the surface A_2 will be absorbed by the surface A_1 again. For a solar collector the surface areas A_1 and A_2 are usually the same and given by A. Under these conditions the rate of thermal heat transfer leads to

$$q_{rad} = \frac{\sigma A (T_1^4 - T_2^4)}{\frac{1}{\varepsilon_1} + \frac{1}{\varepsilon_2} - 1}. \tag{3.7a}$$

The second approximation is related to the ratio of the surface area of these two surfaces. If A_1 is a very small area and placed inside an enclosure with surface area A_2 then the value of A_1/A_2 is approximately zero. In addition, all thermal radiation from A_1 will be absorbed by A_2, depending on its absorption coefficient. This gives the factor equal to unity. Under these conditions, equation (3.6) reduces to

$$q_{rad} = \varepsilon \sigma A (T_1^4 - T_2^4) \tag{3.7b}$$

where q_{rad} is in watts, $\varepsilon_1 = \varepsilon_2 = \varepsilon$, $A_1 = A_2 = A$ and other quantities have been defined.

Equation (3.7b) can be employed when one determines the radiative heat transfer coefficient between the cover of a solar collector and the sky (section 3.5).

The other way to show the rate of thermal radiation transfer is in terms of the temperature difference, say (T_1-T_2) where T_1 and T_2 are the uniform temperatures in K of the first and the second surface respectively. The relation is written as

$$q_{rad} = h_r A (T_1 - T_2) \tag{3.8}$$

where h_r is the radiative heat transfer coefficient in $W/(m^2 K)$.

By combining equation (3.7b) and equation (3.8) one may obtain

$$h_r = \varepsilon \sigma (T_1 + T_2) (T_1^2 + T_2^2). \tag{3.9}$$

3.1.4 Electrical analogue for heat transfer

In electrical networks, a basic law for a simple network is described by the Ohm's law. If the potential difference between two points (A and B) at each end of

a resistance R is ΔV and the electric current is I, the resistance R is then equal to the potential difference divided by the electric current as shown in figure 3.1.

Figure 3.1. A simple electrical network

Conductive, convective and radiative heat transfers are described by equations (3.2), (3.3) and (3.8) respectively and can be written in a general form as

$$q = \frac{\Delta T}{R} \tag{3.10}$$

where q is the rate of heat transfer in watts, ΔT is the temperature difference in K and R is the thermal resistance in K/W.

If one relates this equation to the concept of an electrical network, the temperature difference is analogous to the potential difference ΔV and q is analogous to the electric current I. Hence the resistance R is obtained to be in terms of $(\frac{1}{A_S h})$.

In electrical networks, several resistances may be connected in series or parallel arrangements or a combination of series and parallel arrangements. Similar processes occur in heat transfer systems with the transfer of heat from one medium to another. Therefore the total thermal resistance can be calculated by using the same method as in the electrical system. This method will be used for the calculation of a combination of loss coefficients of a solar collector in section (3.6).

3.2 Free convection in enclosed spaces

The space between an absorbing plate and the innermost cover of a solar collector can be assumed to be an enclosed space. As the plate absorbs solar

radiation, its temperature becomes higher than both the cover and the air in the space. Being in an enclosed space, heat loss by free convection from the absorbing plate to its surrounding may take place.

For free convection within a flat plate collector, three dimensionless numbers (Nusselt number Nu, Rayleigh number Ra, and Prandtl number Pr) are used to calculate the convective heat transfer coefficient. The relationship between each dimensionless number and the characteristics of an enclosed air is given by

$$Nu = h_{p\text{-}c}\frac{s}{k}$$

$$Ra = g\,V''\frac{\Delta T\, s^3}{\upsilon\,\alpha} \qquad (3.11)$$

$$Pr = \frac{\upsilon}{\alpha}$$

where $h_{p\text{-}c}$ is the heat transfer coefficient by free convection in $W/(m^2\,K)$, s is the air space in m, ΔT is the temperature difference between the absorbing plate and the cover in K, α is the thermal diffusivity of air in m^2/sec, υ is the kinematic viscosity in m^2/sec, g is the gravitational constant, 9.80 m^2/sec, V" is the volumetric coefficient of expansion of an ideal gas in K^{-1} and $V'' = \frac{1}{273+T}$ for T in °C.

For evaluation of the air properties in the space, the average of the two plate temperatures may be used.

Hollands et al (1976) developed a method to correlate the Nusselt number, Rayleigh number and the tilt angle of a solar collector. The relationship is based on experimental data at atmospheric air temperature and tilt angle 0 - 75 degrees range. The relationship is expressed as follows

$$Nu = 1 + 1.44\,A\,B + C \qquad (3.12)$$

where A, B and C are parameters defined as follows

$$A = \{1 - \frac{1708}{Ra\ Cos\ \beta}\}^{(+)}$$

$$B = 1 - \left\{\frac{\text{Sin } 1.6\beta^{1.6}}{\text{Ra Cos } \beta}\right\}$$

$$C = \left\{\left(\frac{\text{Ra Cos } \beta}{5830}\right)^{1/3} - 1\right\}^{(+)}.$$

The exponent (+) near the brackets indicates that positive values are to be used (negatives are assumed to be zero). Ra is the Rayleigh number and β is the tilt angle of the collector.

3.3 Forced convection

Heat loss by forced convection from a solar collector is mainly caused by wind. Other factors, for example orientation with respect to the wind and geometry can influence the value of the convective heat transfer coefficient and hence the heat loss to the environment. In general the forced convective coefficient h_w in W/(m^2 K) due to wind speed can be written in the form of

$$h_w = a + b\,v \tag{3.13}$$

where a and b are the constants and v is the wind speed in m/sec.

Whillier (1977) used equation (3.13) to determine the forced convective coefficient when he calculated the combination of heat transfer coefficients (top loss coefficient) of several different collector covers without restrictions. He used the constants a = 5.7 and b = 3.8 for glass cover, plastic cover and for the combination of glass and plastic covers. Test et al (1981) estimated the forced convective heat transfer coefficient for tilted smooth surfaces in the natural environment as a function of wind speed. They indicated that the first constant a on the right side of equation (3.13) is related to free convection and the second constant b refers to the forced convection. From measured data, they obtained the constants in equation (3.13) a = (8.55 $\pm$ 0.86) and b = (2.56 $\pm$ 0.32) for the tilt angle $\geq$ 40 degrees. If

wind speed is around 2.30 m/sec the forced convective heat transfer is the same figure either calculated from Whillier's constants or Test et al.

Equation (3.13) indicates that the heat transfer coefficient increases linearly with increase in wind speed. The effect of other parameters such as collector dimensions is not taken into consideration. Ramsey and Charmchi (1980) indicated that the heat transfer coefficient due to wind speed is very much different from forced convective coefficient which was determined by equation (3.13). They determined the forced convective coefficient h_w of four combinations of collector covers using a correlation equation quoted by Sparrow et al (1979). They recommended using the following equations :

$$h_w = 0.86 \frac{k}{Lc} Re^{1/2} Pr^{1/3}$$

$$Lc = \frac{4\,Ac}{C} \qquad (3.14)$$

$$Re = v \frac{Lc}{\upsilon}$$

where k is the thermal conductivity of air in W/(m^2 K), C is the circumference of the collector in m, Lc is the characteristic dimension of the collector surface area in m, v is the wind speed in m/sec, Ac is the collector surface surface in m^2, Re and Pr are Reynolds and Prandtl numbers respectively (dimensionless).

Equation (3.14) gives a heat transfer coefficient due to wind speed which is smaller than the heat transfer coefficient calculated from equation (3.13). For example, equation (3.13) gives the heat transfer coefficient around 22.8 W/(m^2 K) and equation (3.14) results 6.0 and 5.9 W/(m^2 K) for ambient temperatures 20 and 0 ^{o}C (Ramsey and Charmchi, 1980).

Equation (3.14) was preferred in the present study because not only wind speed is included into the calculations but also the characteristics of ambient air and the collector dimensions.

3.4 Radiation transfer between absorbing plate and cover

The method described in section (3.1.3) is used to determine the heat transfer coefficient by radiation between an absorbing plate and a cover (such as the present simulation). However, there is a modification when a solar collector uses a clear plastic cover. Whillier (1977) recommended that the radiative heat transfer coefficient be expressed as follows

$$h_{rp\text{-}c} = \sigma \varepsilon_c \varepsilon_p \left\{ \frac{T_p^4 - T_c^4}{(1 - \rho_c \rho_p)(T_p - T_c)} \right\} \tag{3.15}$$

where ε_c, ε_p, ρ_c and ρ_p are emissivities and reflectances of the cover and absorbing plate respectively.

Whillier also considered that some infrared radiation transfers directly to the absorbing plate through the plastic cover. The net radiation transfers between the absorbing plate and the surroundings were described through the expression

$$q_{rp\text{-}s} = \sigma A \tau_c \varepsilon_p \left\{ \frac{T_p^4 - T_{sky}^4}{(1 - \rho_c \rho_p)} \right\} \tag{3.16}$$

where τ_c is the transmission coefficient of the cover determined from equation (2.35) and the heat transfer coefficient by radiation between the absorbing plate and surroundings is expressed as

$$h_{rp\text{-}s} = \frac{q_{rp\text{-}s}}{T_p - T_a} . \tag{3.17}$$

3.5 Radiation to the environment

An outer surface of a solar collector can be assumed to be surrounded by a large environment, hence radiation between the surface and the surroundings : air,

earth, buildings, the sky, etc takes place. For radiative heat transfer, the effective temperature of the surroundings (called the effective sky temperature) is dependent on atmospheric conditions. For example, the effective sky temperature is about 230 K under cold and clear sky conditions and it is approximately 285 K under warm and cloudy conditions (Incropera and DeWitt, 1985). Swinbank (1963), in Duffie and Beckman (1980) recommended that the effective sky temperature be determined by the local absolute air temperature T_a using

$$T_{sky} = 0.0552\, T_a^{1.5}. \tag{3.18}$$

The collector surface can be thought of as a small surface surrounded by an enclosure with a larger surface (see the second approximation used in equation 3.6). The enclosure here is the surroundings such as the sky. If the temperatures of the sky and the cover of the collector are T_{sky} and T_c respectively then the radiative heat transfer coefficient between the two surfaces is given by

$$h_{rc\text{-}s} = \sigma \varepsilon (T_c + T_{sky})(T_c^2 + T_{sky}^2) \tag{3.19}$$

where ε is the emission coefficient of the cover.

3.6 Top loss coefficient

Solar energy absorbed by a solar collector is not completely converted into useful energy. Some will be lost. Heat loss through the top of the collector is the largest fraction of overall heat loss and it occurs through convection, conduction and radiation as shown in figure (3.2a). Heat loss by convection and radiation takes place between the cover and the surroundings and between the cover and the absorbing plate. Radiation loss also can occur between the absorbing plate and the sky. Heat loss through conduction occurs from the cover sheet. It is however a very small loss by comparison with convection and radiation. The top loss

coefficient is defined as the summation of all heat transfer coefficients which take place through the top of the collector.

Determination of the top loss coefficient is based on a method used in the calculation of the total resistance of a series-parallel network in an electrical circuit. From this point of view, the top loss coefficient is then redefined as the reciprocal of the net effective resistance of the thermal circuit as described in section (3.1 4). For a single collector cover, an analogy diagram of the top loss coefficient of the collector is shown in figure 3.2b. Heat transfer through conduction is negligible as the cover is thin.

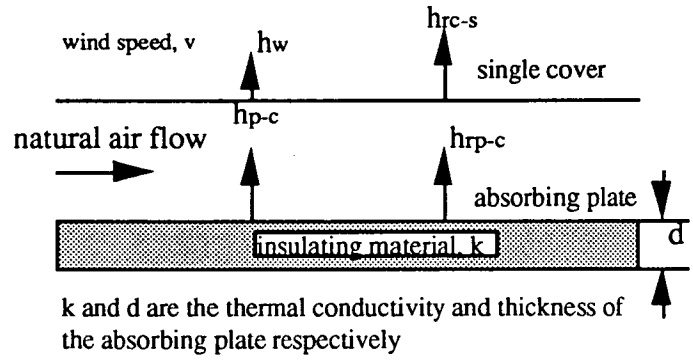

Figure 3.2a. Solar heat collector

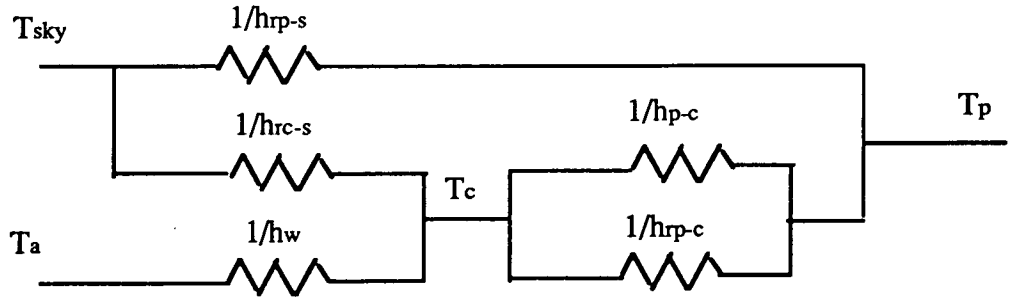

Figure 3.2b Network analogy

Using the method given by Whillier (1963) the top loss coefficient is then written as

$$U_t = h_{rp\text{-}s} + \left(\frac{1}{h_{p\text{-}c} + h_{rp\text{-}c}} + \frac{1}{h_w + h_{rc\text{-}s}}\right)^{-1}. \tag{3.20}$$

The top loss coefficient can be determined when all of the heat transfer coefficients are known. Each heat transfer coefficient is calculated at an appropriate temperature. For instance, the heat transfer coefficient between the absorbing plate and the cover is obtained using the temperatures of the plate T_p and the cover T_c. Sometimes these temperatures are not known but are assumed initially and then calculated using an iterative process. To determine the temperature of the cover the following equation is used.

$$T_c = T_p - \left\{\frac{U_t\,(T_p - Tf_i)}{h_{p\text{-}c} + h_{rp\text{-}c} + h_{rp\text{-}s}}\right\} \tag{3.21}$$

where $h_{p\text{-}c}$, $h_{rp\text{-}c}$ and $h_{rp\text{-}s}$ are determined from equations (3.11), (3.15) and (3.17) respectively, Tf_i is the temperature of the inlet air. The process of recalculating the temperature of the cover uses an iterative method.

3.7 Bottom loss coefficient

Usually a solar collector uses insulating material under an absorbing plate. The insulating material is shown in figure (3.2a). The bottom loss coefficient U_b of the collector is defined as the ratio of the thermal conductivity of the insulation material k to its thickness d. The bottom loss coefficient is approximately expressed as

$$U_b = \frac{k}{d}. \tag{3.22}$$

From this equation one may state that heat loss through the bottom can be reduced by using a low thermal conductivity and increasing the thickness. In the

present work, there was no insulating material placed under the absorbing plate but the thickness of the absorbing plate itself (made of wood) was considered as insulating.

3.8 Collector efficiency factor and overall loss coefficient

Consider a solar collector such as the one illustrated in figure (3.3) which is directly in contact with ambient air with ambient temperature T_a. A transparent material is employed for a cover to allow solar radiation to heat an absorbing plate. The heating process is assumed to be uniform. The result is that the temperature of the plate increases up to a certain temperature, say T_p. As the plate surface temperature is higher than its surroundings, the surface emits thermal radiation to the ambient air through the enclosed air and the cover. Useful energy gain used to increase the temperature of the enclosed air is given by

$$q = H - U_L (T_p - T_a) \tag{3.23}$$

where q is in W/m^2, H is the solar radiation intensity in W/m^2, U_L is the overall loss coefficient in $W/(m^2 K)$ and the temperatures of the absorbing plate T_p and ambient air T_a are in K. This equation is usually called a generalized equation.

Bliss (1959), in Parker (1981) noted that the generalized performance equation is more conveniently written in terms of fluid temperature (enclosed air) than in terms of plate temperature as described in equation (3.23). Using this new idea, the efficiency factor of the collector is introduced as a new parameter into the equation which is defined through the equation

$$q = F' \{H - U_L(T_f - T_a)\} \tag{3.24}$$

where T_f is the enclosed air temperature in K.

For the derivation of both the efficiency factor and the overall loss coefficient (Duffie and Beckman), one may use a concept of heat loss from an absorbing plate to ambient air through the top and bottom of a solar collector (figure 3.3). The losses can occur through conduction, convection and radiation. The air flow within the collector is natural flow and assumed to be in a steady state condition.

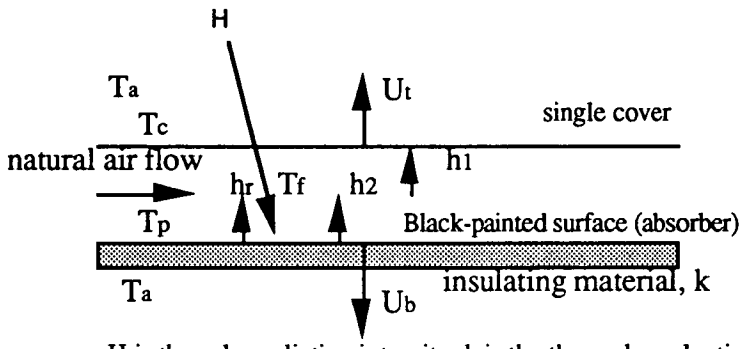

H is the solar radiation intensity, k is the thermal conductivity
Ut and Ub are the top and bottom loss coefficients.
Tc, Tp, Tf and Ta are the temperatures of the cover, absorbing plate, enclosed air and ambient respectively.
hr, h1 and h2 are the heat transfer coefficients by radiation and convection.

Figure 3.3 Solar heat collector with a single cover

Heat from the absorbing plate will be transferred to the enclosed air and ambient air through the convective heat transfer coefficient h_2 and bottom loss coefficient U_b respectively. Heat is also lost from the enclosed air to the collector cover through the convective heat transfer coefficient h_1. Heat is transferred from the absorbing plate to the cover through the radiative heat transfer coefficient h_r. Heat loss to the ambient air can also occur through the top by the mixed convection and radiation which is called top loss coefficient U_t. If H is the solar radiation intensity, T_f is the enclosed air temperature and T_a is the ambient air temperature, the energy balance for the absorbing plate, enclosed air and collector cover are written respectively as follows

$$H - U_b(T_p-T_a) - h_r(T_p-T_c) - h_2(T_p-T_f) = 0 \tag{3.25}$$

$$U_t(T_c-T_a) - h_1(T_f-T_c) - h_r(T_p-T_c) = 0 \tag{3.26}$$

$$h_2(T_p-T_f) + h_1(T_c-T_f) - q = 0 \tag{3.27}$$

where q is the useful energy gain in W/m^2 and calculated from equation (3.24).

Equations (3.25) and (3.26) are solved in terms of (T_c-T_f) and (T_p-T_f) then substituted into equation (3.27) to obtain the useful energy gain in terms of H and $(T_f - T_a)$ (Parker, 1981). This results in the same expression as the useful energy gain in equation (3.24) and given by

$$q = F' \{H - U_L(T_f - T_a)\} \tag{3.28a}$$

where

$$F' = \frac{h_1h_r + h_2(U_t+h_r+h_1)}{(U_t+h_r+h_1)(U_b+h_r+h_2) - h_r^2} \tag{3.28b}$$

$$U_L = \frac{\{(U_b+U_t)(h_1h_r+h_2h_r+h_1h_2)\} + U_bU_t(h_1+h_2)}{h_1h_r+h_2(U_t+h_r+h_1)}. \tag{3.28c}$$

Basically, the convective heat transfer coefficient within the collector is dependent on the Nusselt, Prandtl and Raleigh numbers in which the three dimensionless numbers are actually dependent only on the temperature of the enclosed air, as indicated in equation (3.11). However, this does not indicate that the convective heat transfer coefficient h_1 is equal to h_2. Equation (3.11) is only used for calculating h_{p-c} where the transfer of heat occurs from the absorbing plate to the cover. The two convective heat transfer coefficients h_2 and h_1 which are from the plate to enclosed air and from the enclosed air to the cover respectively are found by considering that the overall loss coefficient is equal to the top plus the bottom loss coefficients. This assumption leads to the expression

$$U_L = U_b + U_t. \tag{3.29}$$

If equation (3.28c) is substituted into equation (3.29) the expression below is obtained.

$$h_1 = \frac{U_t}{U_b} h_2. \tag{3.30}$$

It would be better to use the same symbols as used in previous equations to avoid confusion about equations (3.28b), (3.28c) and (3.30). We replace the symbol h_1 with $h_{1p\text{-}c}$ and h_2 with $h_{2p\text{-}c}$ for the convective heat transfer coefficients between the absorbing plate and the cover and hr with $h_{rp\text{-}c}$ for the radiative heat transfer coefficient. The collector efficiency factor F' and the overall loss coefficient U_L reduce to the expressions below

$$F' = \frac{F}{(U_t+h_{rp\text{-}c}+h_{1p\text{-}c})(U_b+h_{rp\text{-}c}+h_{2p\text{-}c}) - h_{rp\text{-}c}^2} \tag{3.31}$$

$$U_L = \frac{(U_b+U_t)(h_{1p\text{-}c}h_{rp\text{-}c}+h_{2p\text{-}c}h_{rp\text{-}c}+h_{1p\text{-}c}h_{2p\text{-}c})+U_bU_t(h_{1p\text{-}c}+h_{2p\text{-}c})}{F} \tag{3.32}$$

where $F = h_{1p\text{-}c}h_{rp\text{-}c}+\{h_{2p\text{-}c}(U_t+h_{rp\text{-}c}+h_{1p\text{-}c})\}$.

The values of $h_{1p\text{-}c}$ and $h_{2p\text{-}c}$ are not known. However, there should be a relationship with other parameters, such as the top loss coefficient and convective heat transfer coefficient between the absorbing plate and cover. To obtain this relationship, we may use the concept of the electrical analog again. Let us consider the heat transfer system between the absorbing plate and the cover as shown in figure (3.3). The convective heat transfer is the sum of the heat transfer coefficients from the absorbing plate to the enclosed air and from the enclosed air to the cover. This is represented by the series arrangement. Hence we obtain

$$h_{p\text{-}c} = \frac{h_{1p\text{-}c}\, h_{2p\text{-}c}}{h_{p\text{-}c}+h_{2p\text{-}c}}. \tag{3.33}$$

Alternatively we can write

$$h_{p\text{-}c} = \frac{h_{1p\text{-}c}}{1+\frac{h_{1p\text{-}c}}{h_{2p\text{-}c}}} \tag{3.34}$$

and equation (3.30) can also be written as

$$\frac{h_{1p\text{-}c}}{h_{2p\text{-}c}} = \frac{U_t}{U_b}. \tag{3.35}$$

By inserting equation (3.34) into equation (3.35) we obtain

$$h_{1p\text{-}c} = h_{p\text{-}c}(1 + \frac{U_t}{U_b}). \tag{3.36}$$

Using the same method the heat transfer coefficient from the absorbing plate to the enclosed air is given by

$$h_{2p\text{-}c} = h_{p\text{-}c}(1 + \frac{U_b}{U_t}) \tag{3.37}$$

where $h_{p\text{-}c}$ is determined from equation (3.11) and (3.12). Both equations are evaluated using the average temperature between the absorbing plate and cover.

According to equations (3.23) and (3.24), the collector efficiency factor F' represents the ratio between the useful energy gain and the useful energy gain at which the surface temperature of the absorbing plate is the same as the enclosed air temperature. In addition to this, if we define the total heat transfer coefficient from the enclosed air to ambient air as U_o and the overall heat transfer coefficient from the absorbing plate to ambient air as U_L (Duffie and Beckman, 1980) then the collector efficiency factor F' is obtained by dividing U_L into U_o. This reduces to the following expression

$$F' = \frac{U_o}{U_L}. \tag{3.38}$$

3.9 Heat removal and flow factors of collector

As described in section (3.8) the absorbing plate of the collector is uniformly heated by solar radiation. This creates a uniform temperature of the absorbing plate surface and produces natural convection. The air flow within the collector is assumed to be in a steady state condition. Under this condition one may develop the temperature distribution of enclosed air along the collector.

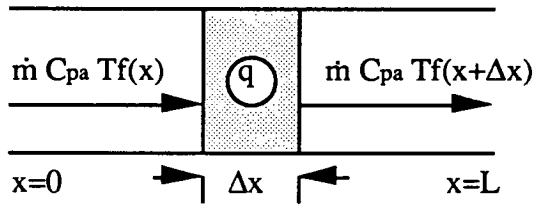

Figure (3.4) Heat balance on an element of air

Now consider an element of air within a collector in figure (3.4). After the air passes a certain distance, say Δx along the collector, the energy balance equation is given by

$$\dot{m}\, C_{pa} Tf(x) - \dot{m}\, C_{pa}\, Tf(x+\Delta x) - q\, y\, \Delta x = 0 \qquad (3.39)$$

where $\dot{m}$ is the flow rate in kg/sec, C_{pa} is the specific heat of the enclosed air at temperature Tf in J/(kg K), y is the width of the collector in m, L is the collector length in m, q is the useful energy gain (equation 3.24) in W/m^2, Tf(x) is the temperature of the enclosed air at position x and $Tf(x+\Delta x) = Tf(x) + \frac{\Delta Tf}{\Delta x}\Delta x$.

To solve this equation, one may substitute equation (3.28a) into equation (3.39) for q, then take the limit as Δx ---> 0 and finally integrate with respect to x to obtain the temperature distribution of the enclosed air at any location along the collector as follows

$$\frac{Tf - T_a - \frac{H}{U_L}}{Tf_i - T_a - \frac{H}{U_L}} = \exp\left(-\frac{U_L F' y\, x}{\dot{m}\, C_{pa}}\right). \qquad (3.40)$$

If the inlet fluid temperature at x = 0 is Tf_i and the outlet temperature at x=L is Tf_o, then equation (3.40) becomes

$$\frac{Tf_o - T_a - \frac{H}{U_L}}{Tf_i - T_a - \frac{H}{U_L}} = \exp\left(-\frac{U_L F' Ac}{\dot{m} C_{pa}}\right) \tag{3.41}$$

where Ac = L y, is the collector surface area in m^2.

As the distribution of the enclosed air temperature is known, hence the outlet air temperature (Tf_o), one may obtain the actual energy gain q" of the collector as follows

$$q'' = \dot{m} C_{pa} (Tf_o - Tf_i). \tag{3.42}$$

q" in equation (3.42) is actually equal to the useful energy gain in equation (3.23) when the absorbing plate temperature is at the inlet air temperature. Under this condition, the energy gain is called the maximum possible energy gain q_U and is given by

$$q_U = F_R Ac \{H - U_L(Tf_i - T_a)\}. \tag{3.43}$$

Hence, the ratio of the actual energy gain q" to the maximum possible energy gain q_U is called the collector heat removal factor F_R, and is given by

$$F_R = \frac{\dot{m} C_{pa} (Tf_o - Tf_i)}{Ac \{H - U_L(Tf_i - T_a)\}}. \tag{3.44}$$

If equation (3.44) is rearranged to the same form as equation (3.41), the collector heat removal factor is rewritten in the form of

$$F_R = \frac{\dot{m} C_{pa}}{Ac U_L} \{1 - \exp\left(-\frac{U_L F' Ac}{\dot{m} C_{pa}}\right)\}. \tag{3.45}$$

The flow factor F" of the collector is defined as the ratio between the heat removal factor F_R and the efficiency factor F'. This leads to the expression

$$F'' = \frac{F_R}{F'}$$

or one can write

$$F'' = \frac{\dot{m}\, C_{pa}}{Ac\ U_L\ F'} \{1 - \exp(-\frac{U_L F' Ac}{\dot{m}\, C_{pa}})\} \cdot \tag{3.46}$$

3.10 Average air and plate temperatures

When the three dimensionless numbers (Nusselt, Raleigh and Prandtl numbers) are computed, the properties of the enclosed air between an absorbing plate and the innermost cover of a solar collector can be evaluated at an average of the absorbing plate and cover temperatures. The average air temperature in this section is the temperature of the enclosed air along the collector. The same situation is applied to the average plate temperature, i.e. the temperature of the absorbing plate along the collector. These are the temperatures used to determine all kinds of heat transfer coefficients existing in the collector.

The average air temperature is calculated from equation (3.40). This equation is integrated with respect to the length of the collector from 0 to L. The integration form is as follows

$$Tf_{ave} = \frac{1}{L} \int_0^L Tf_{ave}\, dx$$

or one may write as

$$Tf_{ave} = Tf_i + \frac{\frac{q_U}{Ac}}{F_R\ U_L} (1 - F'') \cdot \tag{3.47}$$

The average absorbing plate temperature is calculated from the relation given by the useful energy gain in equation (3.23). This is created by the temperature difference between the absorbing plate and the ambient air. This relationship is expressed as follows

$$q_U = Ac \{H - U_L(Tp_{ave} - T_a)\}. \tag{3.48}$$

Equation (3.48) is actually equal to the maximum possible energy gain given by equation (3.43). If these two equations are rearranged, one may obtain the following expressions

$$\frac{\frac{q_U}{Ac}}{U_L F_R} = \frac{H}{U_L} - (Tf_i - T_a) \tag{3.49a}$$

$$\frac{F_R \frac{q_U}{Ac}}{U_L F_R} = \frac{H}{U_L} - (Tp_{ave} - T_a). \tag{3.49b}$$

From equations (3.49a) and (3.49a) the average plate temperature is obtained as follows

$$Tp_{ave} = Tf_i + \frac{\frac{q_U}{Ac}}{U_L F_R} (1 - F_R) \tag{3.50}$$

where q_U is determined either from equations (3.42) or (3.48).

The relationship between the average air temperature and the average plate temperature is obtained by substituting equation (3.50) into equation (3.47) and is expressed as

$$Tf_{ave} = Tp_{ave} - \frac{\frac{q_U}{Ac}}{U_L F_R} (F'' - F_R). \tag{3.51}$$

This equation indicates that the average plate temperature is always greater than the average air temperature because the collector flow factor F" is always greater than the collector heat removal factor F_R.

3.11 Outlet air temperature

The main function of a solar collector is to increase the air temperature for practical purposes. Fresh inlet air with an initial temperature Tf_i enters the collector through a lower vent. This air is heated while passing through the collector. Warm air moves out through an upper vent of the collector with temperature Tf_o. This is called the outlet air temperature. The relationship between Tf_o and other parameters is given by

$$Tf_o = Tf_i + \frac{q_U}{\dot{m}\, C_{pa}} \tag{3.52}$$

where q_U is determined either from equations (3.42) or (3.48).

CHAPTER 4

DRYING CHAMBER AND CHIMNEY

This chapter contains a general discussion about drying processes. The concept of heat and mass transfer is included to formulate mathematical models of the processes. For instance, computations of the humidity and temperature of outlet air and the temperature of fish being dried within a chamber at any time are discussed. Calculations of moisture concentration, the end of the constant rate period and water activity are reviewed. There is also a discussion of the flow rate through the chamber and chimney. Finally, there is information about the optical properties of the absorbing plate and cover of the collector.

4.1 Introduction to a drying chamber

A diagram of a simple drying chamber used for drying fish is depicted in figure (4.1). The fish are placed inside the chamber with an initial surface temperature equal to the ambient air temperature. Air from a solar collector with inlet temperature T_i, humidity Y_i, enthalpy h_i and air flow rate $\dot{m}$, enters the chamber from a bottom vent and increases the air temperature within the chamber. Heat q_s from surrounding air is absorbed by the fish through convective heat transfer. Some heat Q_L is transferred into the walls of the chamber resulting in heat loss.

While free moisture remains on the surface of the fish, air adjacent to the fish is saturated with humidity Y_{sat} and temperature T_{sat}. Evaporation of moisture from the surface of the fish takes place through convective mass transfer into the surrounding air. Because of this evaporation the amount of water vapor within the

chamber increases. The temperature of water vapor is indicated by T_{av}, where temperature T_{av} is higher than temperature T_{sat}.

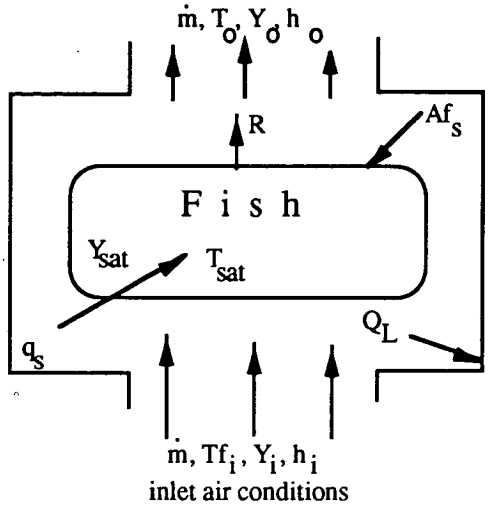

Figure 4.1. Drying chamber

The rate of mass transfer from the surface A_{fs} is denoted by R. The characteristics of outlet air leaving the chamber are indicated by temperature Tf_o, absolute humidity Y_o, enthalpy h_o and constant air flow rate $\dot{m}$.

4.2 Concept of mass and heat transfer

Mathematical models of the movement of a mixture of water vapor and dry air within a chamber are based on mass and heat balance equations (Palancz, 1984). Mass transfer from fish to the surroundings during the drying process is divided into two periods: constant and falling rate periods. In the constant rate period, the evaporation rate is strongly dependent on the external conditions of fish, such as air flow rate. This period continues so long as there is sufficient water from the interior of the fish to saturate the fish surface. When the amount of water is insufficient to

maintain this process then the evaporation rate is determined by internal diffusion which is influenced by salt and fat contents. This is called the falling rate period.

Consideration now is focussed on the mass balance for the moisture content of the air. The drying rate through the chamber is determined by the inlet air humidity, outlet air humidity and air flow rate. This is described by the equation

$$R = \dot{m} (Y_o - Y_i) \tag{4.1}$$

where all variables in this equation have been indicated in figure (4.1).

Usually, the drying rate is not measured experimentally but is calculated from the flow rate and inlet and outlet air humidities. To find the outlet humidity, it is necessary to express the drying rate in terms of other parameters. Another form of the drying rate equation is the moisture drying rate from the fish where it is a function of surface area, saturated surface humidity of the fish, inlet and outlet air humidities during the constant rate period. An approximation to the drying rate leads to the equation

$$R = h_m A_{fs}(Y_{sat} - \frac{Y_i + Y_o}{2}). \tag{4.2}$$

The surface mass transfer coefficient h_m changes during drying (Doe and Heruwati, 1988). They described that the coefficient varies with the speed of air flow through the chamber, particularly when the speed of air flow is larger than 0.6 m/sec. The effect of air speed can be seen through the general equation below

$$h_m = k \{1 + (c\ v)\}^{0.8} \tag{4.3}$$

where v is the speed of air flow in m/sec, k = 0.006 W/(m^2 K) and c = 1 sec/m. When $v \leq 0.6$ m/sec, the surface mass transfer coefficient h_m is approximately 0.005 W/(m^2 K).

For the constant rate period, the mass of fish M in kg after an increment of time Δt in seconds is given by

$$M = M_o - R\,\Delta t \tag{4.4}$$

where M_o is the initial mass of fish in kg and R is the drying rate during the constant rate period in kg/sec.

When equation (4.1) is inserted into equation (4.2) the outlet humidity form the drying chamber Y_o can be obtained from the equation

$$Y_o = \frac{2\,Y_{sat} + (\frac{2\,\dot{m}}{h_m\,A_{fs}} - 1)\,Y_i}{\frac{2\,\dot{m}}{h_m\,A_{fs}} + 1}. \tag{4.5}$$

If one defines $K_1 = \{2\dot{m}/(h_m\,A_{fs}) - 1\}$ and $K_2 = K_1 + 2$, then equation (4.5) reduces to

$$Y_o = \frac{2\,Y_{sat} + K_1 Y_i}{K_2} \tag{4.6}$$

where Y_{sat} is the humidity of saturated air at the surface of fish in kg (H_2O)/kg dry air.

The relationship between temperature and humidity of saturated air is calculated through an expression which is formulated from a psychrometric chart (Doe and Heruwati, 1988) as follows

$$Y_{sat} = 0.001 \exp (0.063\,T_{sat} + 1.41) \tag{4.7}$$

where T_{sat} is the temperature (^oC) of saturated air on the surface of the fish.

The derivation of equations (4.2) to (4.6) is based on the mass balance which reduces to give the outlet air humidity. Outlet temperature is determined by combining several relationships. To do this the energy balance for the air and fish must be considered. The energy balance for the air is given by

$$\dot{m}\,(h_i - h_o) + R\,h_v = q_s\,A_{fs} + Q_L \tag{4.8}$$

where h_i and h_o are the enthalpies of air at the inlet and outlet in J/kg, q_s is the heat absorbed by the wet fish in W/m^2, A_{fs} is the fish surface area in m^2, Q_L is the heat loss to the walls of the chamber in watts, R is the drying rate in kg/sec and h_v is the moisture enthalpy in J/kg.

Warm air from the collector increases the air temperature within the chamber. Fish initially at lower temperature will absorb heat from the warm air. The amount of heat transfer to the fish is dependent on the surrounding air temperature, the surface area and heat transfer coefficient of the fish. An equation to relate the heat transfer q_s with these parameters is expressed as

$$q_s = h_t A_{fs} \left(\frac{Tf_i + Tf_o}{2} - T_{sat}\right) \tag{4.9}$$

where h_t is the surface heat transfer coefficient in W/(m^2 K), T_{sat} is the saturated surface temperature in ^oC, Tf_o is the temperature of the outlet air in ^oC and Tf_i is the temperature of air entering the chamber in ^oC. Note that $\frac{Tf_i + Tf_o}{2}$ is an approximation for the air temperature in the chamber.

The surface heat transfer coefficient h_t of the fish is approximately 10 W/(m^2 K) (Doe and Heruwati, 1988). When the speed of air flow within the drier is larger than 0.6 m/sec, the surface heat transfer coefficient is determined using the same method as for the mass transfer coefficient in equation (4.3) with k = 6.0, and c = 1 sec/m.

The enthalpy of inlet air h_i at temperature Tf_i is expressed as

$$h_i = C_{pa} Tf_i + \lambda Y_i \tag{4.10}$$

and the enthalpy of outlet air h_o at temperature Tf_o is given by

$$h_o = C_{pa} Tf_o + \lambda Y_o \tag{4.11}$$

The enthalpy of moisture h_v at temperature T_{sat} is written as

$$h_v = \lambda + C_{pv} T_{sat} \tag{4.12}$$

where C_{pa} is the specific heat of the air in J/(kg K), λ is the latent heat of evaporation of water in J/kg and C_{pv} is the specific heat of water vapor at constant pressure in J/(kg K).

When equations (4.2) to (4.12) are inserted into equation (4.8) one may obtain an expression for the outlet air temperature Tf_o

$$Tf_o = \frac{(C_{pa} - \frac{h_t A_{fs}}{2\dot{m}})\, Tf_i + \{ (Y_o - Y_i)\, C_{pv} + \frac{h_t A_{fs}}{\dot{m}} \}\, T_{sat} - \frac{Q_L}{\dot{m}}}{C_{pa} - \frac{h_t A_{fs}}{2\dot{m}}} . \qquad (4.13)$$

If one defines

$$K_3 = C_{pa} - \frac{h_t A_{fs}}{2\ \dot{m}}$$

$$K_4 = (Y_o - Y_i)\, C_{pv} + \frac{h_t A_{fs}}{\dot{m}}$$

$$K_5 = C_{pa} + \frac{h_t A_{fs}}{2\ \dot{m}}$$

equation (4.13) leads to

$$Tf_o = \frac{K_3 Tf_i + K_4 T_{sat} - \frac{Q_L}{\dot{m}}}{K_5} . \qquad (4.14)$$

The average temperature of the mixture of air and water vapor within the chamber is obtained from the inlet and outlet temperature as given by

$$T_{av} = \frac{T_i + T_o}{2} . \qquad (4.15)$$

This average temperature T_{av} will be used for calculating the characteristics of the mixture of air and water vapor within the chamber. The values of T_{av} from measurements indicate not very much difference between Tf_i and Tf_o. For example (Tf_i=42.8°C and Tf_o=40.6°C at 13:00 P.M. on Dec, 2nd, 1990).

Basically, the temperature of the fish surface is less than the temperature T_{av} of the surrounding air. This fact has been found experimentally by Jason (1958).The temperature of the fish surface can be obtained by looking at the heat balance between the warm air and the fish. Heat transfer from the warm air to the fish has been indicated in equation (4.9). This heat transfer must be equal to heat absorbed q_{ab} and latent heat for evaporation q_{Lh} of the water in the fish. These two processes are represented by the equations

$$q_{ab} = M_{fs}\, C_{pf}\, (T_{fs(t+\Delta t)} - T_{fs(t)}) \tag{4.16}$$

$$q_{LH} = R\, \lambda\, \Delta t \tag{4.17}$$

where $T_{fs(t)}$ and $T_{fs(t+\Delta t)}$ represent the temperatures of the fish at the beginning of drying (t) and after $(t+\Delta t)$ in each day, M_{fs} is the mass of fish in kg, C_{pf} is the specific heat of the fish in J/(kg ^{o}C), Δt is the time increment in seconds and other quantities have been defined.

The temperature of the fish surface at time Δt can be obtained by combining equation (4.9), equation (4.16) and equation (4.17) to obtain $T_{fs(t+\Delta t)}$ as follows

$$q_s = q_{ab} + q_{Lh}$$

or we may write

$$T_{fs(t+\Delta t)} = T_{fs(t)} + \frac{h_t\, A_{fs}(T_{av} - T_{fs(t)}) - (R\, \lambda\, \Delta t)}{M_{fs}\, C_{pf}} \tag{4.18}$$

where T_{av} is the average temperature obtained from equation (4.15). The temperature of the fish surface may be assumed to be valid for both constant and falling drying rate periods.

As described in previous paragraphs, the initial drying rate from the surface of the fish into the surrounding air is found from the mass balance. This period ends when the supporting free water from the interior of the fish is insufficient. Then the falling rate period commences. To determine the end of the constant rate

period, several factors must be considered. These include factors such as the equilibrium moisture content and so on (see equation 4.30).

4.3 Moisture concentration

The moisture concentration of fish is defined as the mass of water in a unit volume of fish which can be expressed in terms of the moisture, salt and fat contents. Representation of the moisture content of the fish can be in terms of a wet or dry basis. Doe and Olley (1989) showed the conversions of the moisture content of the fish from wet basis to dry basis and vice versa. They assume the total mass of the fish consists of four components, mass of water M_w, mass of salt M_s, mass of fat M_f and dry mass M_b. If the total mass is M, then we may write

$$M = M_w + M_s + M_f + M_b \tag{4.19}$$

and the fraction of each content is described as follows

$$\begin{aligned} mc &= \frac{M_w}{M} & md &= \frac{M_w}{M_b} \\ sc &= \frac{M_s}{M} & sd &= \frac{M_s}{M_b} \\ fc &= \frac{M_f}{M} & fd &= \frac{M_f}{M_b} \end{aligned} \tag{4.20}$$

where mc, sc and fc represent moisture, salt and fat contents on a wet basis. The symbols md, sd and fd indicate moisture, salt and fat contents of the fish on a dry basis.

If we define $M_d = 1 + md + sd + fd$ and $M_c = 1 - mc - sc - fc$ then we may write

$$\begin{aligned} mc &= \frac{md}{M_d} & md &= \frac{m_c}{M_c} \\ sc &= \frac{sd}{M_d} & sd &= \frac{s_c}{M_c} \end{aligned} \tag{4.21}$$

$$fc = \frac{fd}{M_d} \qquad sd = \frac{f_c}{M_c}.$$

We may also present the relationship below

$$M_b = M\ M_c$$

$$M = M_b\, M_d. \tag{4.22}$$

In order to compute the evaporation rate from the fish it is necessary to determine moisture concentration within the fish. The initial moisture concentration is dependent on the three contents of the fish (moisture, fat and salt contents). An equation used to relate these three contents on the dry basis with initial moisture concentration is

$$C_o = \frac{md}{1 + md + sd + fd} \times 1000 \tag{4.23}$$

where C_o is the moisture concentration of the fish during the drying process in kg/m^3 and the quantity 1000 refers to the density of water in kg/m^3.

The values of md, sd and fd are computed from equation (4.20 or 4.21). The moisture concentration of the fish changes from the beginning of drying to the end because it depends on the change in the fish moisture content. If the moisture content of the fish decreases due to evaporation of moisture from the fish surface then its moisture concentration also decreases as shown in equations (4.24) and (4.25).

Before the equilibrium moisture concentration of the fish being dried is determined, it is necessary to calculate the equilibrium moisture contents md_e on a dry basis at air temperature T_a through the equation (Doe and Heruwati, 1988)

$$md_e = md\ (\frac{286}{T_a})^{0.8} \tag{4.24}$$

where T_a is the absolute air temperature (^oK) and md is also the equilibrium moisture content which is computed from the relative humidity of the surrounding air on the dry basis (see Appendix A).

The relationship between the equilibrium moisture concentration C_e in kg/m^3 and the equilibrium moisture, salt and fat contents is written as

$$C_e = \frac{md_e}{1 + md_e + sd + fd} \times 1000 \qquad (4.25)$$

where the figure 1000 represents the density of water in kg/m^3.

If the air temperature increases then the relative humidity of the air decreases. Hence the equilibrium moisture concentration also decreases and vice versa (see equations 4.24 and 4.25). The relationship between an equilibrium mass of the fish (M_e) and the equilibrium moisture content (md_e) is given by

$$M_e = M_b (1 + md_e + sd + fd) \qquad (4.26)$$

where all parameters have been defined.

4.4 Determination of the end of the constant drying rate period

As noted in section (4.2), falling rate drying begins when the rate at which free water diffuses to the surface of the fish is not enough to support the evaporation from the surface of the fish. The drying rate at this stage decreases exponentially with time. The movement of free water to the surface of the fish is dependent on the diffusivity of the fish itself. An Arrhenius-type equation (Jason, 1958) is used to estimate the value of the diffusivity which is a function of temperature and energy of activation for diffusion. An equation to relate these parameters is

$$D_e = D_o \exp\left(-\frac{E}{R\,T}\right) \tag{4.27}$$

where D_o is the constant in cm^2/sec or m^2/sec which is independent of temperature, E is the energy of activation for diffusion in J/(kg Mol), R is the gas constant in J/(kg Mol K) and T is the absolute air temperature (K).

Jason (1958) obtained the value of the ratio between the energy of activation and gas constant to be approximately 3620 K. He also found the constant D_o to be approximately 5.4×10^{-5} m^2/sec for non salted fish. Doe and Heruwati (1988) considered the effect of salt content on the constant D_o. They found that D_o varies from 8×10^{-5} to 10×10^{-5} m^2/sec when the salt content on a dry basis ranges from 0.66 to 0.05. This variation was used in the present simulation. Jason (1965) investigated the effect of fat content (fc) on the diffusivity (D). An equation to relate these two parameters is given by

$$D^{-1} = \alpha + \beta\, fc \tag{4.28}$$

where α is the intercept between D^{-1} and fc and β is the slope of the line.

For non-fatty fish, fc = 0 and the diffusivity $D^{-1} = D_o^{-1} = \alpha$. When we substitute this condition into the equation we obtain the diffusivity of the fish in the form of

$$D = \frac{D_o}{1 + D_e \beta\, fc} \tag{4.29}$$

where D_o is equal to D_e in equation (4.27) in which the effect of fat content is not involved.

The end of the constant rate period of drying fish has been considered by Jason (1958) using a mathematical approach. The result is given by

$$\varepsilon = \frac{\dfrac{D\,(C_o - C_e)}{a}}{\dfrac{D\,t_c}{a^2} + \dfrac{1}{3} - \dfrac{2}{\pi^2}\displaystyle\sum_{1}^{\infty} \frac{1}{n^2} \exp\left(-\frac{D\,n^2\,\pi^2\,t_c}{a^2}\right)} \tag{4.30}$$

where C_o, C_e and D are calculated from equations (4.23), (4.25) and (4.29) respectively, ε is the evaporation rate in kg/sec, a is the half thickness of the fish in m and t_c is the time at the end of the constant rate period in seconds.

The constant drying rate R in equation (4.1) or equation (4.2) may be compared with the evaporation rate ε in equation (4.30). When ε is the same or less than R the constant rate period terminates and the falling rate period commences.

During the falling rate period the drying rate is affected by the internal condition of the fish. Parameters for the constant rate period do not much influence the drying rate during the falling rate period. The movement rate of water from within the fish to the surface depends on the internal properties of the fish as shown symbolically in equation (4.30). An equation to compute the mass of the fish M at any time t during this stage may be written as follows

$$M = M_e + (M_c - M_e) \exp\left(-\frac{t - t_c}{\tau}\right) \tag{4.31}$$

where M_e and M_c are the equilibrium mass and the mass of the fish in kg at time t_c respectively, t_c is the time at the end of the constant rate period in seconds and τ is the drying time constant in seconds, which indicates that the rate of weight loss of fish is inversely proportional to the drying time constant (τ) (Jason, 1965).

Jason (1958) states that the drying time constant can be obtained from

$$\tau = \frac{4}{\pi^2 D\, f(x)} \tag{4.32}$$

where f(x) is a geometric factor. Doe and Heruwati (1988) derived $f(x)=a^{-2}$ where a is the half thickness of the fish in m.

4.5 Water activity

Water activity is a common concept in food technology since it is a measure of the free water in food available for the growth of micro-organisms. It is related to relative humidity which is defined as the ratio between the partial pressure of water vapor in air and the partial pressure of water vapor in saturated air at the same temperature. Relative humidity is usually written as a percentage, but water activity is presented as a fraction. In addition to this, one may say that water activity is equal to the relative humidity of the air in equilibrium conditions. Doe and Heruwati (1988) showed that if dried fish is exposed to air with humidity 80 %, the water activity of the dried fish is 0.80 when it reaches equilibrium. Doe et al (1982) studied the effect of salt content on the water activity of the fish. They determined from experiments that there are two components of water activity : a component due to salt and a component from fish muscle. Lupin (1986) fitted a linear expression to the data which were obtained by Doe et al. When these two forms of water activity are multiplied, the complete result of water activity is shown as follows

$$a_w = (1.007 - 0.684 \frac{M_s}{M_w}) (1.160 - 0.066 \frac{M_b}{M_w}) \qquad (4.33)$$

where M_s, M_w and M_b represent the mass of salt, the mass of water and the salt free, fat free dry mass of fish respectively in kg.

4.6 Chimney

The air flow rate in a solar drier using free convection is usually slower than in a solar drier using forced convection. The flow rate in free convection is dependent on the absorbed energy from incoming solar radiation. To increase the absorbed radiation the collector surface area must be increased. This increases the difference between the temperature of the air inside and outside of a chamber. If the

collector surface area is too large the air temperature inside the chamber may rise above 50 ^{o}C causing the fish to be cooked (Doe et al, 1977). One method of increasing the air flow rate without excessively increasing the air temperature inside the chamber is by constructing a chimney on the top of the chamber.

The chimney commonly has a rectangular cross-section which is constructed from a wood frame. It is often covered with a black plastic sheet over all surfaces to increase the absorption of solar energy (Exell, 1980). Sometimes only a half surface is covered with the black plastic sheet. The other half surface is covered with a clear plastic sheet to allow incoming radiation to enter through it and be absorbed by the black sheet. This way it may increase the air temperature inside the chimney faster than if the all surfaces of the chimney frame are covered with the black plastic sheet.

Solar radiation absorbed by the chimney can be predicted using the same procedures as those used for determining the solar radiation absorbed by a tilted surface (Chapter 2). The slope of the surface of the chimney is 90 degrees because it is positioned perpendicular to a horizontal surface.

For the purpose of this work the efficiency of the plastic chimney to absorb solar radiation is assumed to be approximately 25 %. This is due to the effect of its vertical position on the top of the chamber. For example, heat loss by convection to the environment may be faster from the chimney at a higher level than at a level close to the ground, since wind speed may be lower at a position close to the ground. If the temperature of the air from the chamber is T_i then the temperature T_o of the air which leaves the top of the chimney is given by

$$Tf_o = Tf_i + \frac{\frac{\eta}{100}\,\alpha\, A\, H}{\dot{m}\, C_{pa}} \qquad (4.34)$$

where η is the efficiency of the chimney in %, A is the half surface area in m^2, H is the solar radiation intensity in W/m^2, α is the absorption coefficient of the black plastic, $\dot{m}$ is the air flow rate in kg/sec and C_{pa} is the specific heat of air in J/(kg K).

4.7 Calculation of air flow rate

The combination of a collector, a chamber and a chimney is called a solar drying system. Air movement through the system can be expressed either as a volumetric flow rate or a mass flow rate. Mass flow rate is used in preference to volumetric flow rate because it is independent of air density.

The mass flow rate is usually called air flow rate or just flow rate which has a dimension in kg/sec or kg/hr. The flow rate through the system is affected by ambient air temperature, air temperature within the system, cross-sections of the inlet and outlet air vents and the slope of the collector. One method to relate these parameters is based on the pressure drop through the system. The pressure drop is comprised of two components. The first is a change in pressure due to a non-uniform cross section of a duct where the flow takes place (called a change in velocity head) as shown symbolically in equation (4.41). The second is a change in pressure due to elevation difference in the air column (called a change in static head) as indicated mathematically in equation (4.42).

The density of the air or mixture of the air and water vapor can be computed using the concept of a specific volume. For air the ideal gas law equation can be applied as given below

$$\upsilon = \frac{R\ T}{Ma\ P} \tag{4.35}$$

where υ is the specific volume of the air in m^3/kg, R is the universal gas constant in J/(kg Mol K), T is the absolute air temperature in K, Ma is the molecular weight of air in kg/(kg Mol) and P is the atmospheric pressure in N/m^2.

For water vapor, the analysis should be made with water vapor as if it were an ideal gas so that the ideal gas law equation can be used. The specific volume of the water vapor at atmospheric pressure and its relation to saturation pressure is computed from the equation

$$\upsilon_v = (\upsilon_v)_S \frac{P_S}{P} \tag{4.36}$$

where υ_v is the specific volume of water vapor in m^3/kg, P_S and P are the saturation and atmospheric pressure respectively in N/m^2 and $(\upsilon_v)_S$ is the specific volume of water vapor at the saturation pressure in m^3/kg.

The specific volume of the mixture of the air and water vapor is found by adding the two specific volume terms, written as

$$\upsilon(mix)_{1\ atm} = \upsilon_a + Y\ (\upsilon_v) \tag{4.37}$$

where Y is the humidity of the air in kg (H_2O)/kg dry air.

The specific volume of the mixture of the air and water vapor can also be written as

$$\upsilon(mix) = (\frac{1}{Ma} + \frac{Y}{Mv}) \frac{R\ T}{P} \tag{4.38}$$

where Ma = 29 kg/(kg Mol), Mv = 18 kg/(kg Mol) and R = 8314.4 J/(kg Mol K).

The density of the mixture of the air and water vapor is determined from this specific volume by

$$\rho = \frac{1}{\upsilon(mix)} . \tag{4.39}$$

To illustrate the pressure drop through the system, a simple diagram shown in figure (4.2) is used. The pressure drop between the inlet and outlet air is given by the equation

$$P_1 - P_2 = \sum_{n=1}^{8} P_n - P_{n+1} \tag{4.40}$$

The pressure drop due to the velocity head change is given by

$$P_n - P_{n+1} = \frac{0.5\ \dot{m}}{A^2 C^2 \rho} \tag{4.41}$$

where A is the inlet air cross-section in m^2 and C is the the discharge coefficient (see table 4.1).

The value of the discharge coefficient can be obtained from the ASHRAE Handbook (1985) as shown in table (4.1).

Table 4.1 Discharge coefficient at angle $\phi = 180$

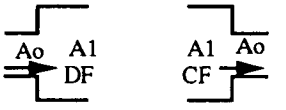

	Discharge coefficient	
A_1/A_o	C_1	C_2
2	0.30	0.26
4	0.64	0.41
6	0.79	0.42
>10	0.88	0.43

where DF and CF represent diverging and converging flows, A_1 and A_o are the cross-sections of outlet and inlet vents for the converging flow and the reverse for the diverging flow.

The change in pressure due to the static head change across the system is given by

$$P_n - P_{n+1} = \rho\, h\, g \tag{4.42}$$

where ρ indicates the air density in kg/m^3 at a position where the pressure is calculated, h is the height of the air column in m and g is the gravitational acceleration (= 9.80 m/sec^2).

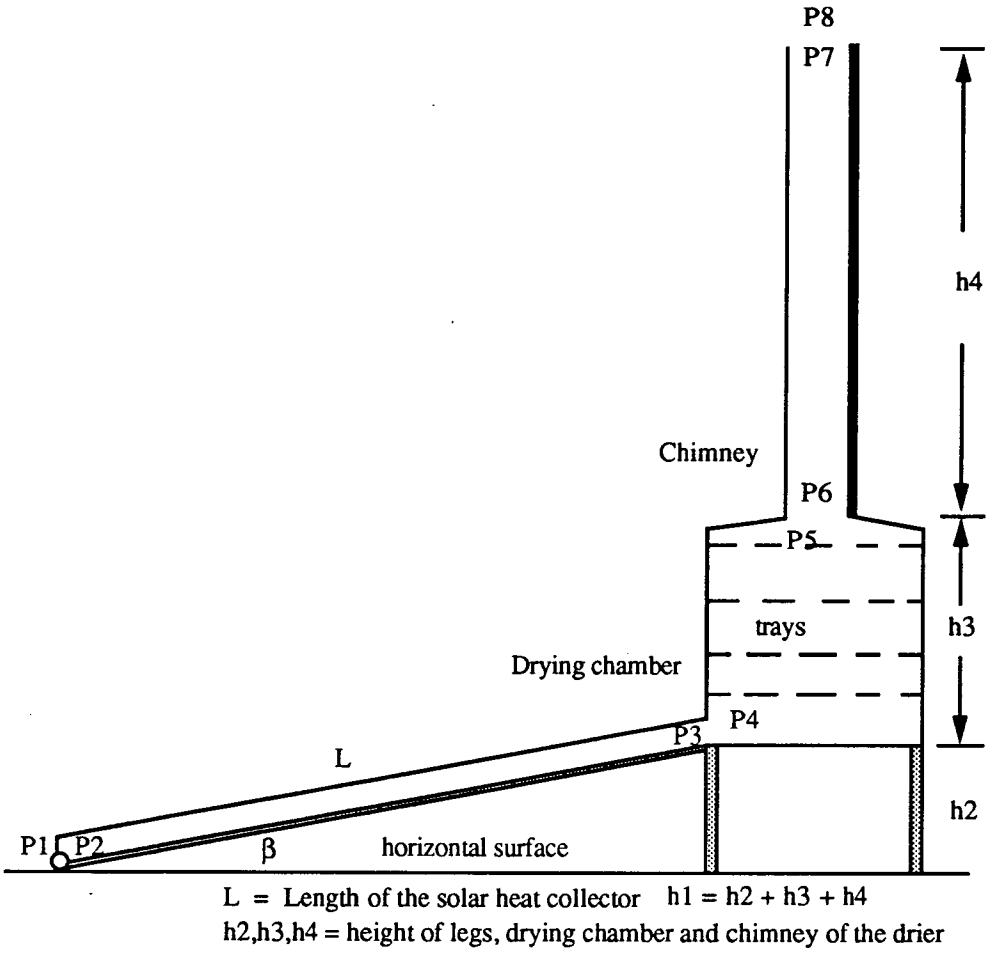

Figure 4.2 A simple diagram of a solar drier system

Let us consider a number of trays inside the chamber as shown in figure (4.2). Each tray is loaded with fish. The warm air moves from the base to the top through the layers of fish. This creates the pressure drop and changes the velocity head. On the other hand, the pressure drop can also be produced by a difference in h3 (i.e. between the base and the top, see figure 4.2). This alters the static head. The pressure drop within the chamber is determined by the average value of the two kinds of pressure drops because the other half is assumed to be lost due to friction among the fish and the walls of the chamber.

When the two expressions of the pressure drops (equations 4.41 and 4.42) are substituted into equation (4.40) then we obtain the air flow rate $\dot{m}$ through the system.

4.8 Properties of materials

Optical properties of the components of a solar heat collector such as extinction coefficient and absorptance are given by several authors. Basically, these properties are dependent on the wavelength of incident waves. However, for engineering purposes, the effects of the variation of the wavelengths can be assumed to be negligible. Robin and Spillman (1980), in Arinze et al (1986) give the optical properties of a clear polyethelene plastic material. The refractive index of the polyethelene plastic is 1.515 and its extinction coefficient is 0.0752/mm. These properties were used in the present work. The three other optical properties : absorption, reflection and transmission coefficients change with incident angle of beam radiation (see section 2.7). Robin and Spillman give the absorption, reflection and transmission coefficients as 0.011, 0.09 and 0.899 respectively.

Another optical property of the clear plastic material which should be known is its emissivity. It is defined as the ratio between absorbed energy and emitted energy by a surface. For an ideal blackbody, the emissivity of the surface is equal to its absorptivity. For non ideal blackbodies, such as a black-painted surface, its emissivity is different from its absorptivity. Whillier (1977) used 0.63 and 0.88 as the values of the emissivity of a clear plastic cover and a glass cover respectively. He also showed the emissivity of a black-painted absorber to be 0.95. Fohr and Figueiredo (1987) used 0.9 as the value of the emissivity of black polyethelene plastic. These data are satisfied for the solar radiation spectrum with wavelengths ranging from 0.28 to 2.5 μm. These emissivities of black and clear plastics were used for the computer simulation.

CHAPTER 5

MATERIAL AND METHOD

5.1 Process of simulation

A computer program was written by the author to simulate the operation of an indirect solar fish drier (appendix G). To carry out the process of simulation, there are three iteration processes employed in the program. First, there is the determination of the cover temperature; second, there is the calculation of the average temperature of the absorbing plate and finally, there is the computation of the air flow rate through the collector, the drying chamber and the chimney.

The first step is to estimate the top loss coefficient of the collector. It is estimated from the combination of the heat transfer coefficients, i.e. from free convection, forced convection and radiation. Free convection and radiation occur between the cover and absorbing plate. Radiation takes place between the cover and the environment (such as the sky). Forced convection occurs due to wind. The radiative heat transfer takes place between the absorbing plate and the sky due to infrared radiation passing through the cover to the absorbing plate. To compute the heat transfer coefficients the temperatures of the cover and absorbing plate are assumed. The results are added together through a series-parallel resistance network analog to find the top loss coefficient.

Using the value of the top loss coefficient, we calculate the temperature of the cover. This cover temperature is used to determine all heat transfer coefficients, giving a new top loss coefficient. The cover temperature is calculated again. This iteration is terminated when the new cover temperature does not differ from the previous value by more than ($\pm$ 0.01 ^{o}C), hence the top loss coefficient is obtained

temporarily because its value changes again when the temperature of the absorbing plate and the flow rate are calculated in the second and final iterations.

The second iteration is to compute the temperature of the absorbing plate. For this situation, we need the flow rate and the temperature of air in the collector. This temperature is initially assumed to be close to the temperature of the absorbing plate. Using the calculated cover temperature and top loss coefficient in the first iteration we can compute the temperature of the absorbing plate. Because this temperature changes, then the cover temperature and top loss coefficient change again. Hence the first iteration is repeated. When the difference between the new and old absorbing plate temperatures is within (± 0.01 ^{o}C), then the iteration is stopped.

The final iteration is to determine the air flow rate. As the flow rate changes the temperatures of the cover and absorbing plate and the top loss coefficient change again. As a result the first and second iterations must be carried out again. When there is little change between the last and previous computations (± 0.01 kg/sec) then the iteration ends. From the final iteration, we can calculate all parameters relating to the characteristics of the collector and the air inside the chamber. This enables us to calculate the drying rate as a function of the humidities of inlet and outlet air and the air flow rate. During the iteration processes the energy balance is always satisfied.

5.2 Drier design procedures

To obtain the maximum dimensions of the drier the following procedures were carried out :

1. The angle selected for the tilt of the collector was selected to maximize the absorption of solar radiation for a particular date.

2. The surface area and width of the air gap of the collector were calculated so that the tilted collector did not produce an outlet air temperature higher than 50 ^{o}C.

3. The heat energy available from the collector is computed to match the amount of fish to be dried.

4. The height of the chimney was determined to keep the average air temperature within the chamber less than 50 °C.

5. When those calculations were finished the drying rate was examined. If it was low then the calculations from 2 to 4 were repeated by changing the surface area and air spacing of the collector and the height and cross-section of the chimney. The iteration processes in section (5.1) were followed again. Results relating to the drier are described in section (5.3).

When drying simulation was carried out, we proposed to dry around 60 kg of fresh fish. In testing the prototype drier only 20.5 kg of fresh fish were used. This was because the thickness of the fish was smaller than the assumed thickness for the simulation (the surface area of the fish in the simulation was similar to the surface area of the fish in testing). Therefore the weight of fish in testing was less than in the simulation.

5.3 Equipment

The solar heat collector was constructed in a trapezoidal shape (figure E.1, in appendix E). Front and back widths were 2.50 m and 1.00 m respectively. The height of the walls was 0.075 metres. Cross sections of the air inlet and outlet were

respectively, (1.875 x 0.05 m) and (1.00 x 0.075 m). The base and innermost walls were blackened with blackboard paint in order to increase the amount of heat absorbed from incoming solar radiation. A clear polyethelene sheet about 0.20 mm thick was used as a cover. To keep the cover lying horizontally on the top of the collector, there were eight wire strings tensioned across the top of the walls.

The drying chamber was built from a wooden frame which was separate from the collector (figure E.1, in appendix E). The dimensions were 1.00 m in length, 0.80 m in width and 1.15 m in height. Sides, bottom and back walls were covered with a plywood material. At the lower back wall, there was an inlet door for the warm air from the collector. This inlet was 52 cm from a horizontal ground (the legs of the chamber were 52 cm each). An exhaust hole (0.40 x 0.40 m) was provided on the top of the chamber.

The door of the chamber was constructed from plywood sheets and positioned on the front side. It could be opened and closed easily when necessary during drying activities. Fish being dried could be seen through a small glass window in the door.

There were eight trays inside the chamber, as shown in figure E.3 in appendix E, positioned horizontally on small wooden rails attached to the vertical walls. The distance between trays was about 15 cm. The lowest tray was positioned about 20 cm from the bottom wall. The trays were made from plastic mesh on a wooden frame. A bent nail was stuck at each corner of those trays. When the weighing procedure was carried out, two pieces of string were connected to the four bent nails, and hung from a spring balance.

The chimney was also made from the wooden framing. It had a rectangular cross section (0.40 x 0.40 x 2.00 m). Black plastic sheeting less than 0.20 mm thick was used for the chimney. Two sides were covered with black plastic and the

other two were covered by clear polyethelene sheet as shown in figure E.3 in appendix E. There was a black plastic hat on the top of the chimney to prevent rain entering the chamber. Because the chimney was constructed separately from the chamber, it could be fitted to the top of the chamber and pulled off when necessary.

The solar drier was constructed by two local persons. Time for building was three 7 hour days. Work began at 9:00 AM and finished at 5:00 PM with one hour free in each day through three days. The cost for the materials and construction of the drier including labor is shown in appendix F.

Seven Micronta Digital Thermometers were used in the experiment. Each thermometer had a sensor which was separated from its indicator and connected by one metre of wire. Indoor and outdoor air temperatures ranging from -40 to 110 ^{o}C could be measured. Calibration of the thermometers was carried out in a laboratory before use. The calibration graph is shown in section C.1, in appendix C.

The other instruments were a Barometer, Hygrometer, Mercury-in-glass sling Psychrometer, Testoven 4000 vane anemometer, (0 - 3) and (0 - 6) kg spring balances and Solarimeter EKO Type MS-42 and indicator. The solarimeter sensor and its indicator are separated and connected by 3 metres of cable. The solarimeter was calibrated in the laboratory. The calibration procedures and the calibration factor are indicated in section C.2, in appendix C. Measured data were multiplied by this factor.

5.4 Method of measurements

The solar drier was set up near a place where local people conduct sun drying of fish. Fish drying was carried out in three trials. Each trial took different numbers of days due to weather conditions. The same species of fish dried by local

processors were used for the experiments. The fish were purchased from local fishermen. Fish were weighed to the nearest 0.01 kg using a (0 - 3) kg spring balance before and after salting processes and the mass of water and salt used for salting. Results are indicated in table (5.1).

Table (5.1) Mass of the fish, water and salt used for drying.

Trial	Species	m1 (kg)	m2 (kg)	m3 (kg)	Mw (kg)	Ms (kg)	Salting (hr)
1	P.Kelapa	13.75	-	12.90	4.00	0.50	14.0
2	Gulamah	-	12.70*	11.77	0.80*	2.50*	18.0
3	Gulamah	-	22.10*	20.50	0.60*	1.65*	20.0

A dash indicates mass of fish was not measured
m1 represents mass of gutted fish without head
m2 represent mass of gutted fish
m3 indicates mass of clean fish after salting
An * represents the total mass of the fish, water and salt from two containers (see in the text)

Detailed of the salting processes in the first, second and third trials are described as follows:

The first trial commenced on 24 th Nov. and ended on 27 th Nov.1990. The fish species was Pari Kelapa (Trygon sepheu). Salting was carried out before drying began with the same technique as used by local processors. The fish mass was 13.75 kg after gutting and removal of heads. A circular container of 1.0 m in diameter and 0.30 m in height was filled with 4 kg water. Salt (0.25 kg) was spread into the container and stirred. The fish were placed in the water and 0.15 kg salt was spread on top of the fish. More fish were placed in the container and 0.10 kg was spread again on the fish. Salting took around 14 hours. The salted fish (13.05 kg) were cut into 0.50 cm thick fillets and washed with fresh water (similar to the local process). The mass of the washed fillets was 12.90 kg.

The second trial was conducted on 28 th Nov. and finished on 2nd Dec.1990. The fish species used for this trial was Gulamah (Pseudociena

amoyensis). There were 163 fresh fish weighing 15 kg, bought from local fishermen. The fish were classified into three groups based on their dimensions, i.e. small, medium and large (table B.1, in appendix B).

The dimensions of the fish were measured, i.e. mass, length, width and thickness. The fish were cleaned by skinning and gutting, conducted by three workers. The clean fish mass was 12.70 kg. During the cleaning period, the fish were covered with ice to prevent spoilage until salting commenced. Two circular containers 0.50 m in diameter and 0.20 m in height were used for salting. The same method was used as for the first trial. The first container was filled with 7.00 kg fish, 1.35 kg salt and 0.5 kg water. In the second container, there were 5.70 kg fish, 1.16 kg salt and 0.5 kg water. The amount of water used for salting was only 0.40 kg per container because the washed fish contained a lot of water. This was noticed at the end of salting when the fish were immersed in the containers. Salting lasted about 18.00 hours and salted fish weighed 11.77 kg. The mass of salted fish was less than before salting. This may be because the mass of water extracted from the fish was larger than the mass of salt penetrated into the fish. There were 11 fish spoiled during salting and these were excluded from drying. 152 fish weighting 10.86 kg were dried.

The final trial took place from 7 th to 10 th Dec.1990. The fish species and their dimensions were similar to those in the second trial. The fish were weighed before preservation. To avoid spoilage, the fish were gutted, split and washed with fresh water by several workers as soon as possible. The clean fish mass was 22.10 kg.

The same procedures as in the second trial were used for salting. The first container contained 13.35 kg fish, 0.90 kg salt and 0.30 kg water. The second contained 8.75 kg fish, 0.75 kg salt and 0.30 kg water. Salting took around 20

hours. The salted fish were washed with water to remove excess salt. Final mass was 20.50 kg.

Before loading on to trays the fish on all trays were hung inside a plastic mesh for few minutes to reduce the amount of water on the skin. The fish were not exposed to solar radiation during this period.

Each tray was numbered and weighed before being loaded with salted fish. The same number of fish were arranged on each tray. There were typically 36 fish for Gulamah sizes per tray. The trays were put into the drying chamber and then the chamber was closed.

There was one hole drilled under each tray through the wall. Each sensor of the thermometers was passed through the holes to measure local air temperature. The indicators were hung on the wall outside the chamber. Measured temperatures were corrected using the calibration graph. Ambient air temperature was also measured by an electrical thermometer. A Testoven 4000 vane anemometer was used to measure wind speed. The average wind speed was recorded.

The collector was set up at the tilted angle 10 degrees from the horizontal surface. It was faced to the East in the morning and turned to the West in the afternoon so that solar radiation intensity was maximized. This work was carried out at 1:00 PM after weighing all fish and recording other data.

The solarimeter was placed beside the collector and was set to a horizontal position using its adjustable legs. The horizontal position was indicated by a spirit bubble on the side of the equipment. The glass envelope of the solarimeter was cleaned with a piece of soft tissue when measurement commenced.

A Barometer and Hygrometer were used to measure the atmospheric pressure and air relative humidity respectively. These instruments were not exposed

to solar radiation in order to reduce inaccuracy of measurements. The sling psychrometer was positioned vertically on the ground near the solarimeter to measure dry and wet bulb temperatures. When the mass of trays including fish was measured, the nearest 0.1 kg using a 0-6 kg spring balance was used.

All quantities outside the chamber were measured every 30 minutes. The temperature of the air underneath each tray was measured hourly throughout the day. The mass of the fish was measured three times every day so that there was not too much heat loss. The first was at the beginning of drying (at 9:00 AM but not always), the second was at 1:00 PM or 2:00 PM and the last was at the end of drying (5:00 PM). The time taken for weighing all trays was around 15 minutes. The measurements were conducted by two persons in order to save time.

At the end of each trial, five dried fish from each tray were put inside a double storage plastic bag. These fish were brought to a laboratory for chemical assessment, particularly to determine their moisture, salt and fat contents and their water activity. The storage plastic bags were checked for leaks and tied tightly in order to prevent ambient air humidity increasing the moisture content of the dried fish inside the bags.

The analysis of the dried fish was carried out at the Research Institute of Fish Technology (RIFT) Jakarta. The author was not involved in this work.

CHAPTER 6

RESULTS AND DISCUSSION

6.1 Weather conditions and solar radiation intensity

Very bad weather occurred during the first trial. There were three hours of clear sky in the first day. The second day there was continuous rain. Hence there was no drying during daylight hours. The sky was clear for just four hours and cloudy for four hours on the third day. There were five hours of clear sky on the final day. Average ambient air temperature varied from 28 to 30 ^{o}C and air temperature within the chamber was around 38 ^{o}C.

Because of rain, some water entered the chamber through leaks in the exhaust of the chamber. Fish inside the chamber became wet again and some fish, particularly the fish on trays near the top, were spoiled. Four trays containing fish were removed. The spoiled fish on the other trays were also removed. With the bad weather conditions the fish had only 16 hours drying, i.e. 3 hours in the first day, no drying in the second day, 8 hours in the third day and 5 hours in the final day.

Weather conditions during the second trial were not very much better than during the first trial. Drying on the first day amounted to only 2.5 hours in the morning because there was rain in the afternoon. On the second day, there was no rain but the sky was covered by cloud throughout the daylight hours. Cloud cover also occurred during the third day and was followed by rain; the sky cleared for around two hours. On the fourth and fifth days there was cloud cover but no rain.

Due to the poor weather conditions during the first and second trials, these results are not included in this study because it was not possible to simulate the weather conditions with the computer program. Other measurements such as salt,

fat and final moisture contents are included for information (see tables B.2.1 and B.2.2, in appendix B).

In the final trial, the weather conditions were much better than in the other two. Even though there was some cloud cover, the drying continued until the fourth day. Solar radiation during the four days was measured using the solarimeter. Results of measurements are indicated in table 6.1.

The irregular variation of solar radiation intensity due to cloud cover throughout the daylight cannot be used directly in the simulation because the program cannot follow rapidly varying solar radiation. A single equation for global radiation intensity is required as outlined below.

To find the equation, we first selected solar radiation from each day under clear sky conditions. All chosen values were assumed to be the highest intensity of solar radiation during the time interval. The results are presented in table D.1, in appendix D. Those values were then plotted using an analytical method to find a smooth graph (figure D.1, in appendix D) giving the power-series polynomial equation (equation D.2, in appendix D) as below

$$I(t) = - 10661 + 2384.3\ t - 151.33\ t^2 + 2.8231\ t^3 \qquad 6.1$$

where I is solar radiation intensity on a horizontal surface (W/m^2) and t is day time from 8:30 to 17:00. The polynomial equation was selected because it was simple and gave an adequate fit to the data.

To evaluate equation (6.1) we need the time t in terms of an hour fraction. For example, if the time t is at 9:30 AM then it represents 9.5 and so on, because the program is run using an increment time of the hour fraction (0.1 hour). When the time t from 9.0 to 17.0 is substituted into equation (6.1) the figures under I in table (6.1) are obtained and called maximum possible solar radiation intensity.

Because the figures under I are obtained from equation (6.1), they are possibly in some places less than the measured radiation (I_1, I_2, I_3 and I_4).

Table 6.1 Measured solar radiation (1990)
Location : Bagan Siapi-api, Riau - Sumatra Indonesia
Latitude : 2° 8' N
Longitude : 100° 10' E
Altitude : 1.8 - 7.0 m

Time (hr)	Solar radiation (W/m^2)				
	Day 1 7 Dec	Day 2 8 Dec	Day 3 9 Dec	Day 4 10 Dec	
	I_1	I_2	I_3	I_4	I
8:30	-	-	-	-	-
9:00	-	*	138.4	-	598.0
9:30	-	655.2	711.7	758.2	752.8
10:00	-	725.8	812.6	810.5	872.1
10:30	-	168.0	148.3	847.9	958.1
11:00	*	273.9	119.3	883.2	1012.9
11:30	827.4	773.1	1100.7	68.5	1038.6
12:00	656.6	1041.4	921.3	9.9	1037.4
12:30	193.4	1008.2	1051.9	-	1011.3
13:00	406.7	38.8	97.4	-	962.5
13:30	753.3	748.4	829.6	-	893.0
14:00	739.9	754.0	725.8	-	805.1
14:30	761.1	679.9	599.4	-	700.8
15:00	182.2	590.2	488.6	-	582.2
15:30	64.2	151.1	427.1	-	451.5
16:00	10.6	125.7	252.8	-	310.7
16:30	12.0	101.0	128.5	-	162.1
17:00	12.7	38.8	10.6	-	7.6

A dash indicates that solar radiation was not measured and no drying. An * indicates that solar radiation was not measured but drying commenced. I_1, I_2, I_3 and I_4 represent converted-measured solar radiation for day 1, day 2, day 3 and day 4 respectively. I indicates maximum possible solar

radiation based on the values of the highest intensity of selected-measured solar radiation during experiments.

6.2 Solar collector performance

The characteristics of a solar collector can be examined when an air flow rate through the collector is known. When drying was carried out we were not able to measure air speed inside the collector because it was too slow. Accordingly, the flow rate was not discussed

6.3 Solar drier performance

The most important parameter used to assess performance of the solar fish drier in this study is drying rate. This is determined from measurements of the mass of fish at intervals during drying. Results including percentage mass of fish are presented in the first and second columns of table B.3, B.4,.. and B.10, in appendix B. Figure 6.1 is a plot of the reduction of mass of the fish against time. Figure 6.2 shows the percentage of the original mass of the fish. The eight graphs refer to eight trays inside the chamber. Trays were numbered from tray 1 to tray 8. Tray 1 was located at the lowest position and followed by tray 2 and so on to tray 8 on the top position as shown in figure E.3 in appendix E. It can be seen that evaporation of water from the fish surfaces is fastest on tray 1 followed by tray 2. This is principally because these trays were both placed in the warmest air so the fish on the trays were heated rapidly. The fish on the other trays show similar but slower drying performance. There is no discernible difference from one graph to another.

One of the most interesting aspects of figure 6.2 is that the graphs of percentage mass end at a similar figure. Hence one can state that average drying rate is identical for all trays. Hence, it may be possible to increase the amount of fish to

be dried (see section 5.2). A possible technique would be to add a number of trays inside the drying chamber.

Table 6.2 Dimensions of solar drier

Specifications	**Drier A**	**Drier B**	**Units**
Absorbing material	wood*	plastic**	
Absorbing surface area	5.25	8.00#	m^2
Height of black chimney	2.00	2.00#	m
Cross-section of chimney	0.16	0.04#	m^2
Solar radiation (24.5 hr)	43.42	larger##	MJ/m^2

An * represents a blackened wood surface with blackboard paint
A ** indicates a black PVC sheet
An # indicates a calculated figure from a diagram of the SCD solar drier
A ## indicates that a predicted value from data is larger than the figure under drier A

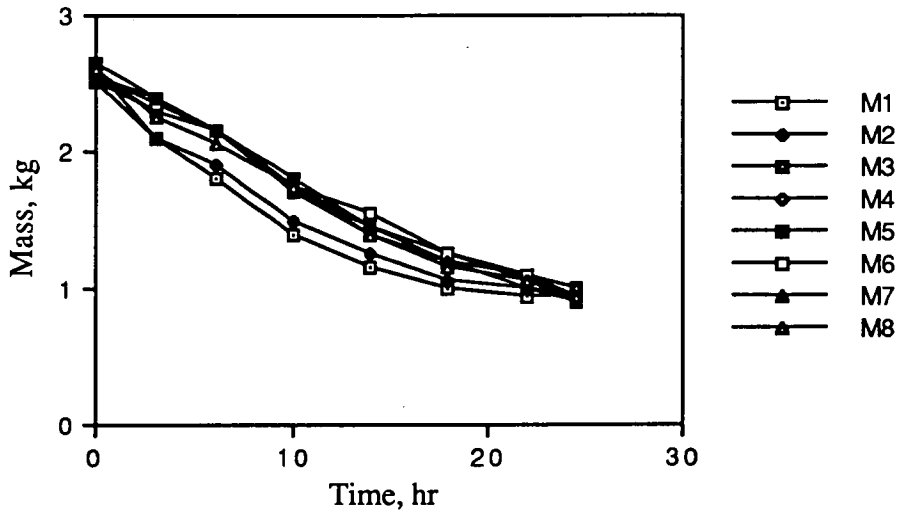

M1,.., M8 represent mass of fish on trays 1,.., 8, respectively

Figure 6.1 Mass versus time

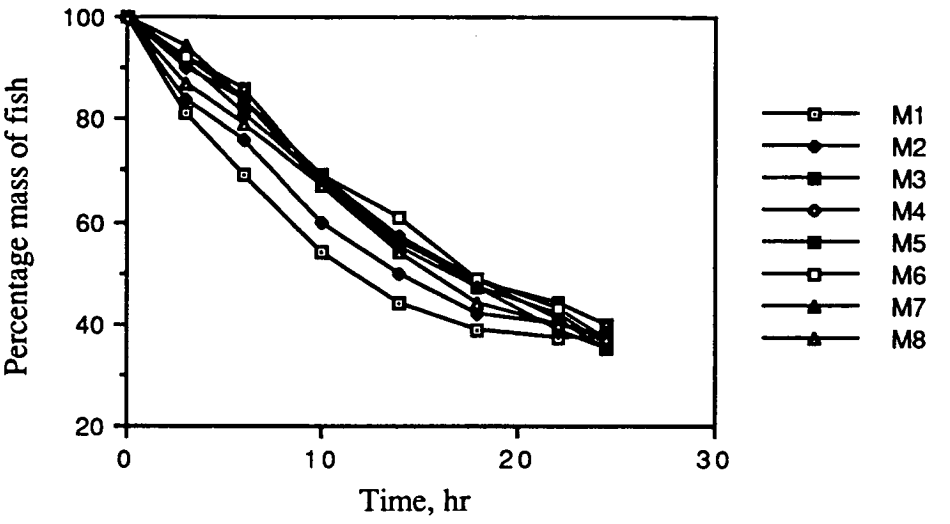

M1,.., M8 indicate percentage mass of original of fish on trays 1,.., 8, respectively

Figure 6.2 Percentage mass versus time

The drying rate from the present study can also be compared with results given by previous researchers into solar drier design, for example measurements obtained by Trim and Curran (1983). They constructed and tested three driers (tent, cabinet and SCD driers). From these three kinds of driers we select the performance of the SCD drier (designated drier B, shown in figure E.2 in appendix E) which is similar in shape to the drier (designated drier A, shown in figure E.1 in appendix E) of the present study. The diagrams of both driers are shown in appendix E. Dimensions and other parameters relating to the two driers are shown in table 6.2.

The time used to dry the fish in the final trial was 24.5 hours through four days. Because the mass of the fish, particularly the fish from the lowest tray, did not change very much from the previous measurement, we assumed that the fish were dry.

Trim and Curran did ten trials to dry Pampano (Trachinotus paitensis) and Lisa (Xenomugil thoburni) fish with three kinds of salting processes (dry salted split, brined split and dry salted fillet fish). Trial no.7 (brined split Lisa) are

selected for comparison, as the fish in this trial had salt and fat contents similar to those in trial 3 of this study. Data relating to the fish are indicated in table 6.3 below.

Table 6.3 Fish conditions

Components	**Drier A**	**Drier B**
Fish species	Gulamah	Lisa
Preservation	split and salting	split and brine
Initial mass Mo (kg)	20.50	8.00
Salt content (%,wet.basis)	9.99	11.20
Fat content (%, wet.basis)	11.57	*
Mi/Mo (%) after 24.5 hr	38.05	40.64#

* The fat content was not reported but the fish is categorised as a medium fat content (Sidwell et al, 1974), in Trim and Curran (1983). Curran and Poulter (1983) obtained the fat content of brined lisa fish to be approximately 3.09 (%, wet basis) when its moisture content and water activity are 29.93 (%,wet basis) and 0.73 respectively. Mi/Mo is the ratio between the mass (Mi) of the fish after drying for about 24.5 hours and initial mass (Mo).

The figure here represents (Mi/Mo) computed from a graph given by trial no 7 from drier B. Figures under drier A are obtained from table B.11, in appendix B. Figures from both driers are averaged from several values.

If two fish have similar fat and salt contents, the effect of moisture diffusivity (De) on drying, particularly during the falling rate phase, should be the same for both kinds of fish. On the other hand, if the salt content or fat content is different from one fish to another then the drying rate is lower for the fish with the higher fat and salt contents. Jason (1965) stated that there is a significant effect of the fat content on the diffusivity (section 4.4) and hence the drying rate. In addition, Doe and Heruwati (1988) indicated that the salt content can influence the diffusivity through its proportional constant (Do). According to Doe and Heruwati

as noted in section (4.4), the value of the constant ranges from 8.0 x 10^{-5} to 10 x 10^{-5} m^2/sec when the salt content varies from 66.0 to 5.0 (%, wet basis).

Based on table 6.3, fish in drier A has a slightly lower salt content and very much higher fat content than the fish in drier B. These conditions suggest that the value of Mi/Mo should be lower in the fish from drier B than drier A, but the reverse is true. Mi/Mo is lower in drier A than drier B. Thus the amount of moisture evaporated from the surface of the fish is larger from the fish in drier A than the fish in drier B, even though the total insolation used by drier A is lower than drier B (table 6.2). In other words the drying rate in the drier built and tested in Indonesia is slightly faster than the drying which was carried out by Trim and Curran in Ecuador.

The moisture content of the fish was not measured at the time of drying, but was computed from the measured mass and from salt, fat and final moisture contents. These contents were measured subsequently at the Research Institute of Fish Technology (RIFT), Jakarta. A technique described by Doe and Olley (1989) was used to calculate the moisture content. The computation technique is described as follows : we take fish conditions from tray 1, as an example. Measurements indicated that initial mass Mo = 2.60 kg and final mass Mf = 0.95 kg. From chemical assessment we obtained the salt content sc = 8.15 (%, wet basis), fat content fc = 12.05 (%, wet basis) and final moisture content, mcf = 23.97 (%, wet basis). The bone dry mass of the fish is the dry mass of the fish (fat-free, salt free) which is computed by subtracting the masses of fat and salt from the mass remaining after oven drying. It is also determined as follows :

Bone dry mass Mb = Mf(1-mcf-sc-fc)= 0.53 kg.

The salt and fat contents on a dry basis were computed as follows :

Salt content sd = sc/(1-mcf-sc-fc) = 0.15 (dry basis).

Fat content fd = fc/(1-mcf-sc-fc)= 0.22 (dry basis).

To determine the initial moisture content of the fish we first compute its moisture content on a dry basis. This is dependent on its initial mass as follows :

Moisture content md = (Mo/Mb)-1-sd-fd = 3.54 (dry basis) and the initial moisture content is

mci = md/(1+md+sd+fd) = 72.22 (%, wet basis).

Because the salt content, fat content on a dry basis and bone dry mass of the fish are constant, it is possible to calculate its moisture content at any time using the measured mass. The moisture content is called calculated moisture content. The same technique is employed to calculate the moisture content of the fish on each tray. The results are presented in tables B.3, B.4,... and B.10, in appendix B.

When the calculated moisture contents from table B.3 to table B.10 in appendix B are plotted, figure 6.3 is obtained. Because the fish have different salt and fat contents on each tray a slight difference in initial moisture content occurs. There were eight trays inside a drying chamber. The moisture content graphs of the fish on trays 4, 5, 6 and 7 show a similar pattern. This is probably due to the fact that all these trays were placed in the middle of the chamber. Hence the moisture from the fish on the lower trays saturated the air in the lower part of the chamber and reduced drying rate in the upper trays.

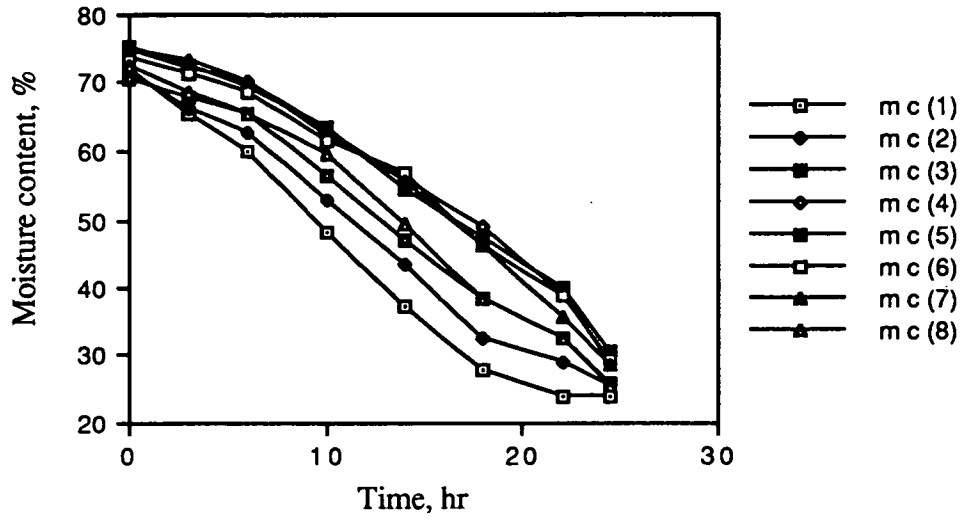

mc(1),.., mc(8) represent moisture contents of fish on trays 1,.., 8, respectively

Figure 6.3 Moisture content versus time

The moisture content of the fish on the top tray (tray 8) reduced more rapidly than the fish on trays 4, 5, 6 and 7 because of increasing local air temperature which was due to the absorption of solar radiation on the chimney. Because tray 8 was located in the highest position the moisture could exit from the chamber unimpeded.

The fastest reduction of moisture content took place from the fish on trays 1 and 2, followed by tray 3. This may be explained using similar reasoning to that used earlier for data given in figure 6.2. The positions of these trays were located in the warmest and driest air. Hence the moisture from these fish evaporated more rapidly than from the others.

6.4 Water activity and storage life of the dried fish from each tray

As noted in section (4.5), the water activity of fish is a measure of the amount of free water within the fish which is used by micro-organisms to grow. It is also a measure of the storage life of the fish. The lower the water activity of the

fish shows, the longer its storage life. Based on Doe et al (1982) the water activity of dried fish is dependent on its moisture and salt contents provided these are calculated on a fat-free basis. The water activity of the dried fish was calculated using the values of both moisture and salt contents. Results are tabulated in the last column of tables B.3, B.4, .. and B.10 in appendix B and indicated graphically in figure 6.4.

The most interesting aspect of figure 6.4 is that all water activity graphs decrease at similar rates. This can be explained by looking at the ratio of salt to moisture contents as a salt contribution factor (sd/md) and an inverse moisture content in dry basis as a fish muscle contribution factor (1/md). Both factors have been described by Lupin (1986).

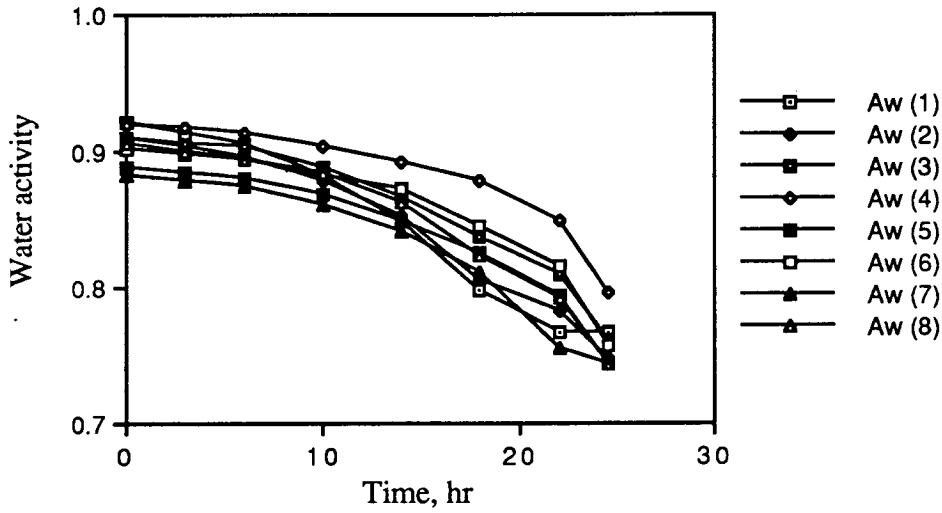

A(1),.., A(8) represent water activities of fish on trays 1,.., 8, respectively

Figure 6.4 Water activity versus time

The water activity of fish from tray 4 in figure 6.4 reduces slower than the others with respect to the drying time. This is caused by the salt contribution factor (sd/md) of the fish on tray 4 is always less than for the fish on the other trays, while the fish muscle contribution (l/md) is similar for the fish from all trays.

Using calculated water activities, the storage life of the dried fish can be predicted, based on a technique outlined by Poulter et al (1982). Results are shown in table 6.5. The lowest storage life of dried fish is given for the fish on tray 4, because the fish have the highest water activity. The second lowest storage life is given for the fish on tray 1, where the fish have the lowest moisture content (see table B.3, in appendix B). This occurs because the fish have the second highest water activity. Hence, one can state that lower moisture content does not necessarily indicate a higher storage life.The three contents (moisture, salt and fat contents) determine the storage life of the fish through its water activity.

Table 6.4 Prediction of the storage life of the dried fish

Tray No.	Water activity a_w *	Storage life (days) *
1	0.767 ± 0.032	19.4 ± 4.7
2	0.743 ± 0.030	32.0 ± 6.4
3	0.761 ± 0.028	21.9 ± 4.5
4	0.797 ± 0.028	10.5 ± 2.6
5	0.743 ± 0.025	32.0 ± 5.4
6	0.753 ± 0.026	23.8 ± 4.6
7	0.743 ± 0.029	32.0 ± 6.2
8	0.743 ± 0.031	32.0 ± 6.5

* Calculations of the estimate of the error were based on the instrumental errors.

6.5 Comparison between measurements and simulation

6.5.1 Air temperature

The temperature and relative humidity of the ambient air used in the process of simulation are not constant but change regularly from time to time throughout the day. The technique employed to find a general equation for the temperature and

relative humidity of the air is similar to that used for the solar radiation. Measured air temperature and relative humidity are shown in table D.2 and the equations are given by equations (D.2 and D.3), in appendix D.

The outlet air temperature from the collector increased as the solar radiation intensity increased. Prediction from the computer simulation sometimes gave identical figures and sometimes different figures from the measurements. An example from the best day (day 3 of the final trial) of drying activities is given in table 6.5.

Table 6.5 Measured and estimated air temperatures

Time	Ambient Temperature (°C)		To1 °C		To2 °C	
	Est	Mea	Est	Mea	Est	Mea
9:00	29.3	29.3	36.8	35.6	32.8	31.9
10:00	30.7	32.9	41.9	44.6	37.7	37.8
11:00	32.0	34.1	44.9	46.2	40.5	38.4
12:00	33.4	36.5	46.0	48.8	42.2	40.0
13:00	34.7	33.6	47.0	43.4	43.5	40.1
14:00	36.1	36.1	46.4	48.3	43.4	42.4
15:00	34.8	34.4	42.1	44.2	39.9	41.7
16:00	33.5	34.5	37.0	44.7	35.3	41.3
17:00	32.1	32.1	32.1	38.1	30.5	38.2

To1 : outlet air temperature from a solar collector
To2 : outlet air temperature from a drying chamber
est and mea represent estimated and measured results

A different figure between measured and estimated data as shown in table 6.6 is explained as follows: Solar radiation intensity in the simulation changes regularly and never drops to a very low intensity or increases suddenly to a high intensity. Hence estimated outlet air temperature increases or decreases regularly

according to the variation of the assumed solar radiation intensity. On the other hand, the actual solar radiation intensity sometimes dropped to a very low value due to cloud cover or increased to a high value. Therefore the outlet air temperature changed irregularly. Sometimes the measured data were higher and sometimes lower than the estimated data.

6.5.2 Drying rate and moisture content

The drying performance described above refers to fish on separate trays. In the computer simulations, bulk conditions of the fish are used. Bulk salt, fat and final moisture contents of the fish on all trays are approximately 9.99, 11.57 and 27.31 (%, wet basis) respectively (table B.11, in appendix B). Initial moisture content is approximately 73.23 (%, wet basis), computed from measured mass, salt, fat and final moisture contents.

As noted earlier, because salt and fat contents on a dry basis are always constant during drying, the moisture content of fish at any time can be calculated from its measured mass. The technique used to compute the moisture content is the same as the technique employed in the previous section. Results, including simulated results after drying for about 24.5 hours are indicated in table B.11, in appendix B.

The mass and moisture content on a wet basis of the fish from estimated and measured data plotted against time are shown in figure 6.5 and figure 6.6 respectively. These two figures indicate that the reduction of mass and moisture content of the fish calculated from measured data are slightly faster than simulated

results. The main factor affecting this situation may be due to inaccurate dimensions (surface area and thickness) of the fish used in the computer simulation. The computed moisture evaporation from the fish can be increased by increasing the surface area and reducing the thickness.

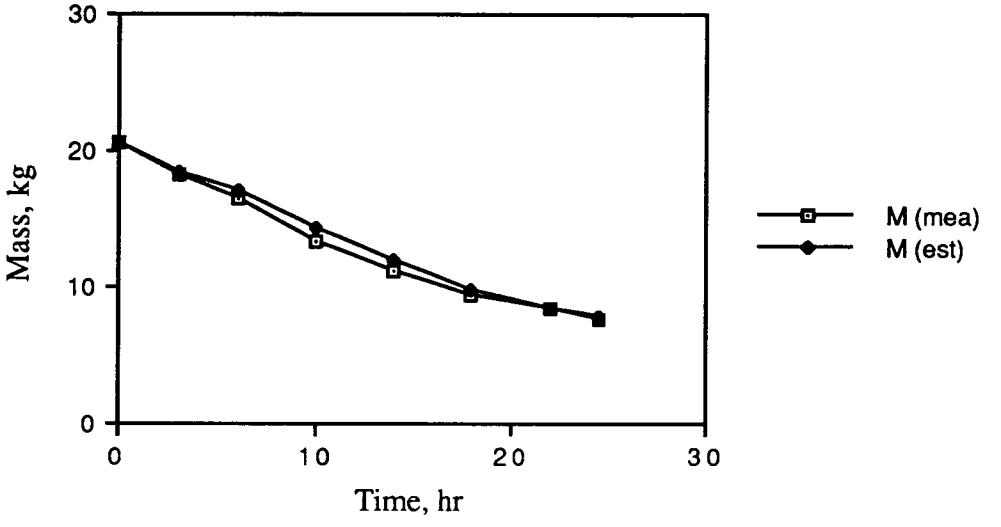

Figure 6.5 Measured and estimated mass versus time

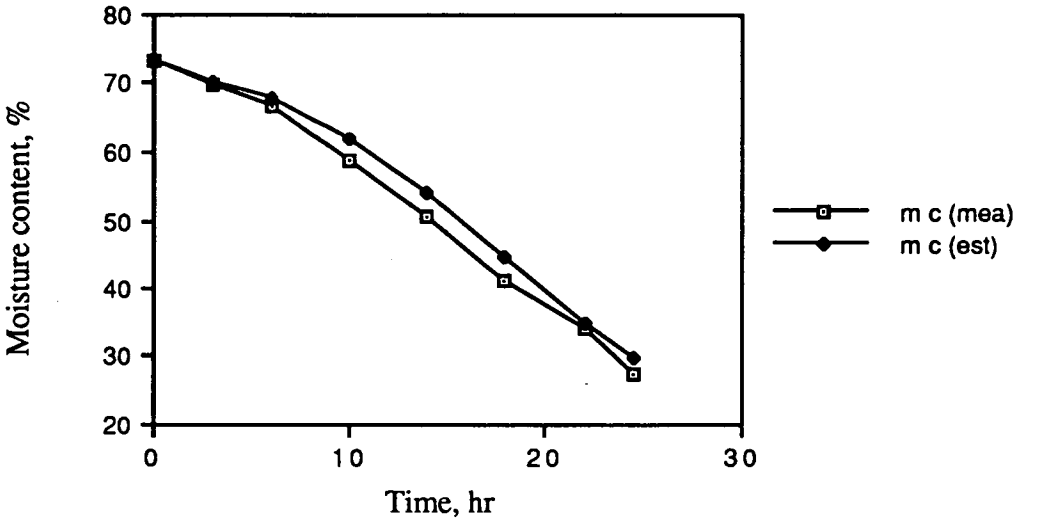

Figure 6.6 Measured and estimated moisture contents versus time

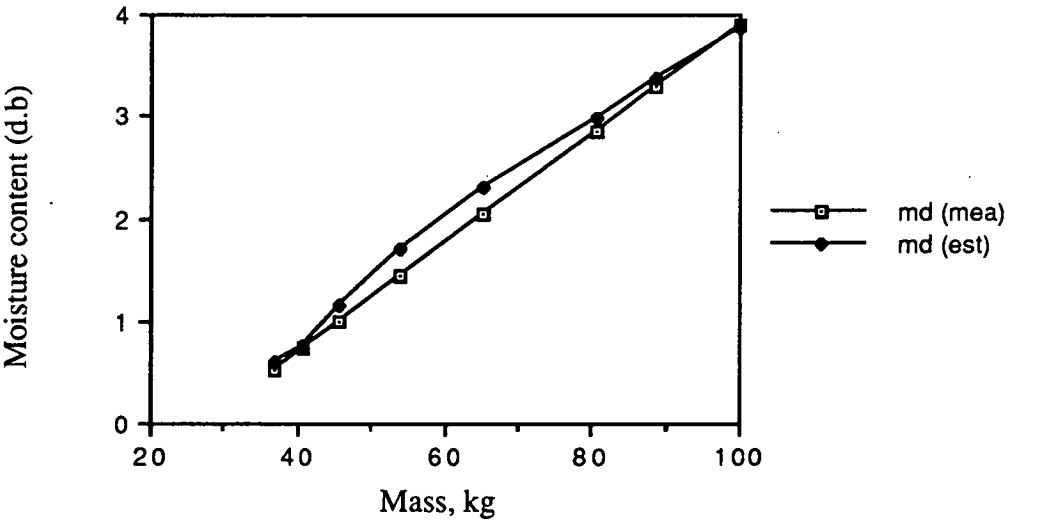

Figure 6.7 Measured and estimated moisture contents (dry basis) versus mass

Figure 6.7 shows the relationship between the measured and estimated moisture contents on a dry basis of the fish and its mass. The moisture content from estimated results decreased more slowly than from measurements because the mass from measurements reduced faster than from simulation.

To examine the limitations of the computer simulation we apply the Student's t test (Hoel, 1958). Data from table B.11, in appendix B are used for the test. When calculations are carried out, the values of $t_{0.025, 6}$ are 0.315 and 0.956 for the mass and moisture content (wet basis) of the fish respectively, while the 5 per cent critical value of t is found from the Student's distribution table to be 2.447 ($t_{0.025, 6} = 2.447$). Because both the calculated figures are less than ($t_{0.025, 6} = 2.447$) one can state that the reduction of the mass and moisture content of the fish per hour from simulation and measurements is at similar rates, at 95 per cent confidence limits. This result leads to the conclusion that the computer simulation is consistent with measurements, i.e. there is no significant difference between the measured and simulated data.

6.5.3 Water activity and storage life

The water activities of dried fish calculated from measured data (called $a_{w\ mea}$) and from simulated data (called $a_{w\ est}$) are presented in the last two columns of table B.11 in appendix B. These two kinds of water activity are plotted against time and indicated graphically in figure 6.8. The graph given by measured data is below the graph plotted from the simulated data. Moisture content is the main factor affecting the position of the two graphs as salt and fat contents are the same for both calculations.

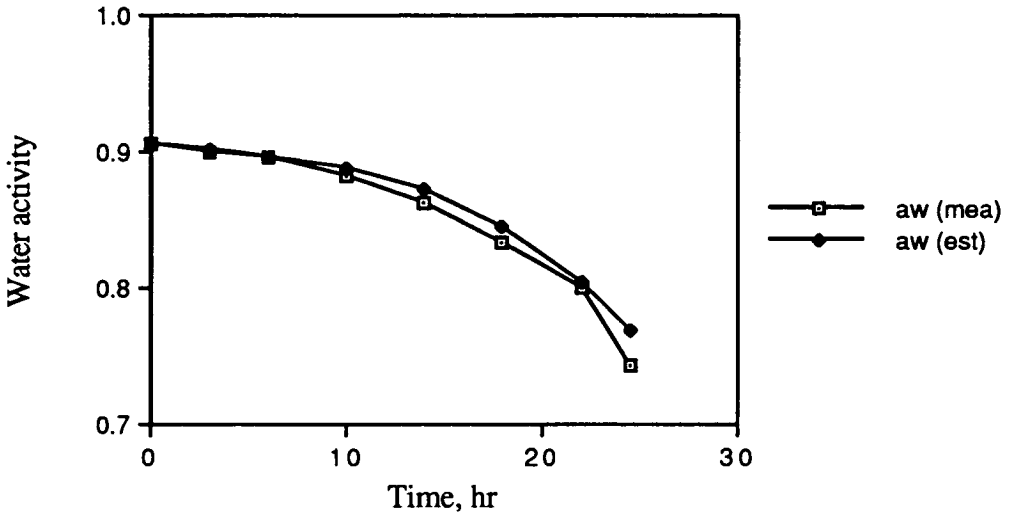

Figure 6.8 Measured and estimated water activities versus time

There is not a significant distinction between the two graphs in figure 6.8. To show this, the same statistical analysis as on the mass and moisture content used in section (6.4.2) is applied. Data are obtained from the last two columns of table B.11, in appendix B. The result indicates that the value of the t test with 6 degrees of freedom is 1.922 which is falling considerably at a region less than 5 per cent critical value of the t ($t_{0.025,\,6} = 2.447$). This implies that the values of a_w from measurements reduce at identical rates as from the simulation, at 95 per cent confidence limits. Thus, the computer simulation indicates again a reliable prediction for the water activity.

Based on Poulter et al again, the storage lives are calculated from measured ($a_w = 0.743 \pm 0.004$) and simulated data ($a_w = 0.769 \pm 0.003$) to be approximately (32.0 ± 0.8) days and (18.6 ± 0.5) days respectively where the estimate of the errors were computed from the instrumental errors.

CHAPTER 7

CONCLUSION

7.1 Fish conditions from each tray

Evaporation of moisture content from the fish surface throughout the eight trays inside the drying chamber indicated generally similar rates during drying. The drying rate occurred slightly faster from the fish at the first- and second-lowest trays because of the warmest and driest air. However, the percentage mass on the dried fish from each tray ended at a similar figure.

The final water activity of the dried fish from those trays was calculated from the method of Doe and Heruwati (1988). The results ranged from (0.743 ± 0.025) to (0.797 ± 0.028). The fish from trays 2, 3, 5, 7 and 8 had the similar water activity which is lower than that of the fish from the other trays. The fish from tray 4 had the highest water activity.

Based on the calculated water activity we can predict the storage life of the dried fish (Poulter et al, 1982). The highest water activity of the dried fish gives the lowest storage life and inversely the longest storage life is given by the lowest water activity. Hence the dried fish from trays 2, 3, 5, 7 and 8 have the longest predicted storage life, i.e. (32.0 ± a, where the values of a are indicated in table 6.4) days because those fish have the similar lowest final water activities. The storage life of the dried fish from tray 4 with the highest water activity was computed to be (10.5 ± 2.6) days.

7.2 Measured and estimated results

7.2.1 Air temperature

The air temperatures in the collector were sometimes lower and sometimes higher than the simulated data. This was because the intensity of solar radiation during measurements varied irregularly. The air temperature was very much influenced by the amount of solar radiation and also wind speed.

7.2.2 Drying rate, moisture content and water activity

Based on the statistical analysis (the Student's t test), the calculated drying rates from the measured and simulated mass of the fish indicate similar rates, with 95 per cent confidence limits. Using the same test for the moisture content and water activity, we established that the reduction of the moisture content and water activity of the fish from measurements is consistent with the results from simulation. From these results one may state that the results show close agreement between measurements and simulation. In the other words, the mathematical models used to simulate the performance of the solar drier are adequate for this study.

7.2.3 Drier performance and effectiveness

The percentage mass of the dried fish after 24.5 hours was 38.05 % from the present study compared with 40.64 % from the results obtained by Trim and Curran (1983) in Ecuador. These figures indicate the drying rate in the drier constructed and tested in Indonesia was slightly faster than the drying which was done by Trim and Curran in Ecuador.

It can be concluded from the present study that there is benefit in making a computer simulation before building a solar fish drier. This leads us to obtain optimum dimensions of the drier, the amount of fish to be dried and results in increase in the drying rate.

REFERENCES

Ad hoc panel of the board on science and technology for international development.(1988). *Fisheries Technologies for Developing Countries, 149-155*. Washington DC : National Academic Press.

Anderson,E.E.(1983). *Fundamentals of Solar Energy Conversion*. Massachusetts : Addison-Wesley Publishing Company, Inc.

Anonymous.(1985). *ASHRAE Fundamentals Handbook*. Atltanta : American Society of Heating, Refrigerating and Air-Conditioning Engineers, Inc.

Arienze,E.A., Schoenau,G.J. and Besant,R.W.(1986). Prediction of incident and transmitted solar irrandiance or irrandiation for a tilted surface with double-layered plastic covers. *Solar Energy, 36(2), 191-195*.

Brace Research Institute.(1973). *How to Make a Solar Cabinet Dryer for Agricultural Produce*. Quebec : McGill University.

Brandemuehl,M.J. and Beckman,W.A.(1980). Transmission of diffuse radiation through CPC and flat plate collector glazings. *Solar Energy, 24, 511-513*.

Bugler,J.W.(1977). The determination of hourly insolation on an inclined plane using a diffuse irradiance model based on hourly measured global horizontal insolation. *Solar Energy, 19, 477-491*.

Coffari,E.(1977). The sun and the celestial vault. *Solar Energy Engineering, 5-36*, Sayigh, A.A.M (Ed). New York : Academic Press.

Curran,C.A. and Poulter,R.G.(1983). Isoholic sorption isotherms : III. Application to a dried salted tropical fish (*Xenomugil thoburni*). *Journal of Food Technology, 18, 739-746*.

Doe,P.E., Ahmed,M., Muslemuddin,M. and Sachithananthan,K.(1977). A polythene tent drier for improved sun drying of fish. *Food Technology in Australia, 29(11), 437-441*.

Doe,P.E.(1979). The polyethylene tent fish drier : A progress report. *International Conference Agricultural Engineering in National Development, Serdang, Selangor, Malaysia.* Paper No:79-12.

Doe,P.E., Poulter,R.G. and Olley,J. (1982). Isoholic sorption isothers. I. Determination dried salted cod (*Gadus morrhua*), *Journal of food Technology, 17, 125-134.*

Doe,P.E.(1986). Principles of fish drying and spoilage. *Cured Fish Production in the Tropics. In Preceedings of a Workshop, 14-25 April 1986 at University of the Philippines in the Visayas, Diliman Quezon City, Philippines,* Reilly.A and Barile.L.E (Ed).

Doe,P.E. and Heruwati,E.S.(1988). A model for the prediction of the microbial spoilage of sun-dried tropical fish. *Journal of Food Engineering, 8, 47-72.*

Doe,P.E. and Olley,J.(1989). Drying and dried fish products, Seafood: *Resources, Nutritional Composition and Preservation,*.Sikorski.Z.E (Ed). Boca Raton : CRC Press Inc.

Duffie,J.A. and Beckman,W.A.(1980). *Solar Engineering of Thermal Processes.* New York : John Wiley & Sons, Inc.

Exell,R.H.B. and Kornsakoo,S.(1978). A low cost solar rice dryer. *Appropriate Technology, 5(1), 23-24.*

Exell,R.H.B.(1980). A simple solar rice dryer : Basic design theory. *Sunworld, 4(6), 186-191.*

Erbs,D.G., Klein,S.A. and Duffie,J.A.(1982). Estimation of the diffuse radiation fraction for hourly, daily and monthly-average global radiation. *Solar Energy, 28(4), 293-302.*

Fohr,J.P. and Figueiredo,A.R.(1987). Agricultural solar air collectors : Design and performances. *Solar Energy, 38(5), 311-321.*

Hoel,P.G.(1958). *Introduction to Mathematical Statistics.* New York : John Wiley and Sons, Inc.

Hollands,K.G.T., Unny,T.E., Raithby,G.D. and Konicek,L.(1976). Free convective heat transfer across inclined air layers. *ASME Journal of Heat Transfer, 98, 189-193.*

Hottel,H.C.(1976). A simple model for estimating the transmittance of direct solar radiation through clear atmospheres. *Solar Energy, 18, 129-134.*

Incropera,F.P. and DeWitt,D.P.(1985). *Fundamentals of Heat and Mass Transfer.* New York : John Wiley and Sons, Inc.

Jansen,T.J.(1985). *Solar Engineering Technology.* New Jersey : Prentice-Hall, Inc.

Jason, A.C.(1958). A study of evaporation and diffusion processes in the drying of fish muscle. *Fundamental Aspects of the Dehydration of Foodstuffs, Torry Memoir No.2, 103-135.*

Jason,A.C.(1965). Effects of fat content on diffusion of water in fish muscle. *Journal of Science Food Agriculture, 16, 281-288.*

Jimenez,J.I. and Castro,Y.(1982). Solar radiation on sloping surfaces with different orientations in Granada, Spain. *Solar Energy, 28(3), 257-262.*

Lupin,H.M.(1986). Water activity in preserved fish products. *Cured fish production in the tropics. In Proceedings of a Worrkshop, 14-25 April 1986 at University of the Philippines in the Visayas, Diliman Quezon City, Philippines,* Reilly.A and Barile.L.E (Ed).

Orgill,J.F. and Hollands,K.G.T.(1977). Correlation equation for hourly diffuse radiation on a horizontal surface. *Solar Energy, 19, 357-359.*

Palancz,B.(1984). Analysis of solar-dehumidification drying. *International Journal of Heat and Mass Transfer, 27(5), 647-655.*

Parker,B.F.(1981). Derivation of efficiency and loss factors for solar air heaters. *Solar Energy, 26, 27-32.*

Poulter,R.G., Doe.P.E. and Olley,J.(1982). Isohalic sorption isothemrs.II.Use in the prediction of storage life of dried salted fish. *Journal of Food Technology, 17, 201-210.*

Ramsey,J.W. and Charmchi,M.(1980). Variancies in solar collector performance predictions due to different methods of evaluating wind heat transfer coefficients. *ASME Journal of Heat Transfer, 102, 766-768.*

Sparrow,E.M., Ramsey,J.W. and Mass,E.A.(1979). Effect of finite width on heat transfer and fluid flow about an inclined rectangular plate. *ASME Journal of Heat Transfer, 101, 199-204.*

Stratton,J.A.(1944). *Electromagnetic Theory.* New York : McGraww-Hill Book Company, Inc.

Test,F.L.,Lessmann,R.C. and Johary,A.(1981). Heat transfer during wind flow over rectangular bodies in the natural environment. *ASME Journal of Heat Transfer, 103, 262-267.*

Thomas,L.C.(1980). *Fundamentals of Heat Transfer.* New Jersey : Prentice-Hall, Inc.

Trimm,D.S. and Curran,C.A.(1983). A comparative study of solar and sun drying of fish in Ecuador. *Report of the Tropical Products Institute, L60.*

Williams,J.R.(1983). *Design and Installation of Solar Heating and Hot Water Systems.* Michigan : Ann Arbor Science Publishers.

Whillier,A. (1963). Plastic covers for solar collectors. *Solar Energy, 7(3), 148-151.*

Whillier,A.(1977). Prediction of performance of solar collectors. *ASHRAE GRP 170, Applications of Solar Energy for Heating and Cooling of Buildings, VIII (1-13),* Jordan,R.C. and Liu,B.Y.H (Ed).

APPENDIX A

A.1 Water activity

As defined in section 4.5, water activity is a measure of unbound water inside fish in which micro-organisms can grow. It is also defined as an equilibrium moisture content of dried fish with the surrounding air. The water activity of the dried fish in relating to salt and moisture contents (Lupin, 1986) is written as follows

$$a_w = (1.007 - 0.684 \frac{M_s}{M_w}) (1.160 - 0.066 \frac{M_b}{M_w}) \cdot \quad \text{A.1}$$

Define M_s/M_b = sd, M_b/M_w = md then equation (A.1) is written as follows

$$a_w = (1.007 - 0.684 \frac{sd}{md}) (1.160 - \frac{0.066}{md}) \cdot \quad \text{A.2}$$

A.2 Calculation of equilibrium moisture content

Using equation (A.2) the equilibrium moisture content can be evaluated from given value of the water activity (a_w), salt (sc) and fat (fc) contents. Equation (A.2) is solved using the method developed by Doe and Heruwati (1988). If the water activity $a_w \geq 0.50$ the moisture content of the fish is

$$md = \frac{0.066}{1.160 - a_w} \quad \text{A.3}$$

where sd = 0. If $0 < a_w < 0.50$ then the moisture content is given by

$$md = \frac{a_w}{5.0} \cdot \quad \text{A.4}$$

A.3 Salt content effect

Consider the effect of the salt content sd and define x=sd/md where md is computed from equation (A.3) or equation (A.4). If $x \leq 0.075$ then the moisture content is given by equation (A.3) or (A.4) depending on a_w. To determine the moisture content md (dry basis) and equilibrium moisture content md_e we apply the method given by Doe and Heruwati (1988) as outlined below.

If $x > 0.075$ the equation (A.2) is solved again. For water activity $a_w > 0.50$ equation (A.2) reduces to a quadratic equation in terms of md, the value of which can be determined from the equation below

$$md = = \frac{- B + \sqrt{B^2 - 4AC}}{2A} \qquad A.5$$

where $A = 1.1681 - a_w$, $B = - (0.7934\ sd + 0.0665)$ and $C = 0.0451\ sd$. For water activity $a_w \leq 0.50$ the moisture content md is calculated from

$$md = \frac{3.42 + a_w}{5.035} . \qquad A.6$$

When $x \leq 0.36$ and $md \leq 0.40$ then the moisture content md is calculated from equations (A.5) or (A.6) depending on a_w. If $md > 0.40$ then the moisture content is determined from

$$md = \frac{0.684\ sd}{1.007 - a_w} . \qquad A.7$$

Now we look at the moisture content under condition $x > 0.36$. When the water activity $a_w \geq 0.375$ the moisture content is calculated by

$$md = \frac{a_w}{3.75} . \qquad A.8$$

When the water activity $0.375 < a_w \leq 0.75$ the moisture content is given by

$$md = \frac{0.066}{1.160 - 1.33\ a_w} . \qquad A.9$$

For water activity a_w>0.75 the moisture content is computed from the equation below

$$md = \frac{0.684\ sd}{1.007 - a_w} \cdot \qquad \text{A.10}$$

The equilibrium moisture content of the dried fish md_e is the moisture content in equilibrium with air at a particular relative humidity rh. Thus we can compute the equilibrium moisture content using the equations above by replacing a_w with rh throughout. The relationship between the equilibrium moisture content and air temperature Ta is given by

$$md_e = md \left(\frac{298}{273 + Ta}\right)^{0.8} \qquad \text{A.11}$$

where md is computed from equation (A.3) to equation (A.10) under appropriate conditions.

APPENDIX B

Table B.1 Dimensions of Gulamah fish

Size	Whole	Gutted	Length	Width	Thickness
	kg	kg	mm	mm	mm
Small	0.080	0.075	180	50	35
Medium	0.110	0.100	210	60	40
Large	0.230	0.200	250	70	45

Table B.2.1 Fish conditions on trial 1 (Pari Kelapa fish)

Tray	mc	sc	fc	a_w
	(%, w.b)	(%,.w.b)	(%, w.b)	
1	19.21	3.14	4.43	0.813
2	22.34	6.71	3.47	0.770
3	25.29	3.49	2.61	0.895

Where mc, sc and fc represent the the moisture, salt and fat content respectively, (w.b) represents the wet basis and a_w is the water activity.

Table B.2.2 Fish conditions on trial 2 (Gulamah fish)

Tray	mc	sc	fc	a_w
	(%, w.b)	(%, wb)	(%, w.b)	
1	23.27	18.65	4.54	0.742
2	28.20	18.88	5.74	0.742
3	26.74	19.39	3.82	0.742
4	26.76	20.79	3.92	0.742
5	27.83	18.38	4.15	0.742
6	26.10	16.95	3.32	0.742
7	25.99	17.54	5.38	0.742

Fish conditions on trial 3 (Gulamah fish) are presented from table B.3 to table B.11

Table B.3 Fish conditions on tray 1

	sc = 8.15	% (w.b)		fc =12.05	% (w.b)	
Time	**mi**	**mi**	**mc**	**sd/md**	**1/md**	**a_w**
(hr)	(kg)	(%)	(%, w.b)			
0.0	2.60	100.00	72.22	0.1128	0.2825	0.921
3.0	2.10	80.77	65.81	0.1242	0.3846	0.913
6.0	1.80	63.23	59.87	0.1361	0.4926	0.905
10.0	1.40	53.85	48.41	0.1684	0.7813	0.883
14.0	1.15	44.23	37.19	0.2192	1.2346	0.849
18.0	1.00	38.46	27.77	0.2935	1.9231	0.798
22.0	0.95	36.54	23.97	0.3400	2.3256	0.767
24.5	0.95	36.54	23.97	0.3400	2.3256	0.767

Where md, mi and a_w are the moisture content on dry basis, the mass in kg and the water activity of the fish respectively. Other quantities have been defined.

Table B.4 Fish conditions on tray 2

	sc = 9.23	(%, w.b)		fc =15.42	(%, w.b)	
Time	**mi**	**mi**	**mc**	**sd/md**	**1/md**	**a_w**
(hr)	(kg)	(%)	(%, w.b)			
0.0	2.50	100.00	71.67	0.13	0.27	0.910
3.0	2.10	84.00	66.27	0.14	0.34	0.903
6.0	1.90	76.00	62.72	0.15	0.40	0.897
10.0	1.50	60.00	52.78	0.18	0.60	0.879
14.0	1.25	50.00	43.34	0.21	0.88	0.853
18.0	1.05	42.00	32.55	0.28	1.39	0.805
22.0	1.00	40.00	29.18	0.32	1.61	0.783
24.5	0.95	38.00	25.45	0.36	1.96	0.743

Table B.5 Fish conditions on tray 3

	sc = 9.07	(%, w.b)		fc =10.07	(%, w.b)	
Time	**mi**	**mi**	**mc**	**sd/md**	**1/md**	**a_w**
(hr)	(kg)	(%)	(%, w.b)			
0.0	2.50	100.00	70.40	0.13	0.31	0.910
3.0	2.30	92.00	67.83	0.13	0.35	0.906
6.0	2.15	86.00	65.58	0.14	0.39	0.903
10.0	1.70	68.00	56.47	0.16	0.57	0.888
14.0	1.40	56.00	47.14	0.24	1.19	0.867
18.0	1.20	48.00	38.33	0.24	1.19	0.837
22.0	1.10	44.00	32.73	0.28	1.52	0.809
24.5	1.00	40.00	26.00	0.35	2.13	0.761

Table B.6 Fish conditions on tray 4

	sc = 8.56	(%, w.b)		fc =12.68	(%, w.b)	
Time	**mi**	**mi**	**mc**	**sd/md**	**1/md**	**a_w**
(hr)	(kg)	(%)	(%, w.b)			
0.0	2.55	100.00	74.96	0.11	0.23	0.920
3.0	2.30	90.20	72.24	0.12	0.27	0.917
6.0	2.15	84.31	70.30	0.12	0.30	0.914
10.0	1.70	66.67	62.44	0.14	0.42	0.904
14.0	1.45	56.86	55.97	0.15	0.55	0.893
18.0	1.25	49.02	48.92	0.18	1.73	0.878
22.0	1.05	41.18	39.19	0.22	1.87	0.849
24.5	0.90	35.29	29.06	0.30	1.92	0.797

Table B.7 Fish conditions on tray 5

Time (hr)	sc=11.96 mi (kg)	(%, w.b) mi (%)	mc (%, w.b)	fc = 8.47 sd/md	(%, w.b) 1/md	a_w
0.0	2.65	100.00	75.17	0.16	0.23	0.889
3.0	2.40	90.57	72.59	0.17	0.27	0.885
6.0	2.15	81.13	69.40	0.17	0.31	0.880
10.0	1.80	67.92	63.45	0.19	0.41	0.869
14.0	1.45	54.72	54.63	0.22	0.59	0.849
18.0	1.25	47.17	47.37	0.25	0.79	0.826
22.0	1.10	41.51	40.19	0.30	1.05	0.795
24.5	0.95	35.85	30.75	0.39	1.60	0.743

Table B.8 Fish conditions on tray 6

Time (hr)	sc =10.40 mi (kg)	(%, w.b) mi (%)	mc (%, w.b)	fc =11.92 sd/md	(%, w.b) 1/md	a_w
0.0	2.25	100.00	73.66	0.14	0.25	0.901
3.0	2.35	92.16	71.42	0.15	0.27	0.898
6.0	2.15	84.31	68.76	0.15	0.31	0.895
10.0	1.75	68.63	61.63	0.17	0.43	0.883
14.0	1.55	60.78	56.67	0.18	0.52	0.873
18.0	1.25	49.02	46.28	0.25	0.79	0.845
22.0	1.10	43.14	38.95	0.28	1.08	0.816
24.5	0.95	37.25	29.31	0.36	1.70	0.753

Table B.9 Fish conditions on tray 7

	sc =12.74	(%, w.b)		fc =10.52	(%, w.b)	
Time	**mi**	**mi**	**mc**	**sd/md**	**1/md**	**a_w**
(hr)	(kg)	(%)	(%, w.b)			
0.0	2.55	100.00	74.78	0.17	0.23	0.882
3.0	2.40	94.12	73.21	0.17	0.25	0.879
6.0	2.15	84.31	70.09	0.18	0.29	0.874
10.0	1.75	68.63	63.25	0.20	0.39	0.861
14.0	1.45	56.86	55.65	023	0.54	0.842
18.0	1.20	47.06	46.41	0.28	0.78	0.811
22.0	1.00	39.22	35.69	0.36	1.22	0.755
24.5	0.90	35.29	28.55	0.45	1.70	0.743

Table B.10 Fish conditions on tray 8

	sc = 9.81	(%, w.b)		fc =11.40	(%, w.b)	
Time	**mi**	**mi**	**mc**	**sd/md**	**1/md**	**a_w**
(hr)	(kg)	(%)	(%, w.b)			
0.0	2.60	100.00	72.74	0.14	0.27	0.906
3.0	2.25	86.54	68.50	0.14	0.33	0.900
6.0	2.05	78.85	65.42	0.15	0.39	0.895
10.0	1.75	67.31	59.50	0.17	0.49	0.885
14.0	1.40	53.85	49.37	0.20	0.74	0.862
18.0	1.15	44.23	38.37	0.26	1.15	0.824
22.0	1.05	40.38	32.50	0.30	1.49	0.793
24.5	0.95	36.54	25.39	0.39	2.08	0.743

Table B.11 Fish conditions from measured and estimated data

	sc= 9.99 (%, w.b)		fc=11.57 (%, w.b)			
Time	**Mass of fish**		**Moisture**		**Water activity**	
(hr)	**m** (kg)		**content**		(a_w)	
			mc (%, w.b)			
	mea	**est**	**mea**	**est**	**mea**	**est**
0.0	20.50	20.50	73.23	73.23	0.905	0.905
3.0	18.20	18.53	69.85	70.37	0.900	0.901
6.0	16.50	17.02	66.74	67.76	0.896	0.897
10.0	13.35	14.40	58.89	61.90	0.882	0.888
14.0	11.10	12.01	50.56	54.29	0.863	0.872
18.0	9.35	9.86	41.30	44.36	0.833	0.844
22.0	8.35	8.43	34.27	34.87	0.800	0.803
24.5	7.55	7.80	27.31	29.64	0.743	0.769

A **mea** represents the calculated results from measured data
An **est** indicates the calculated results from estimated data

APPENDIX C

C.1 Calibration graph for the air temperature

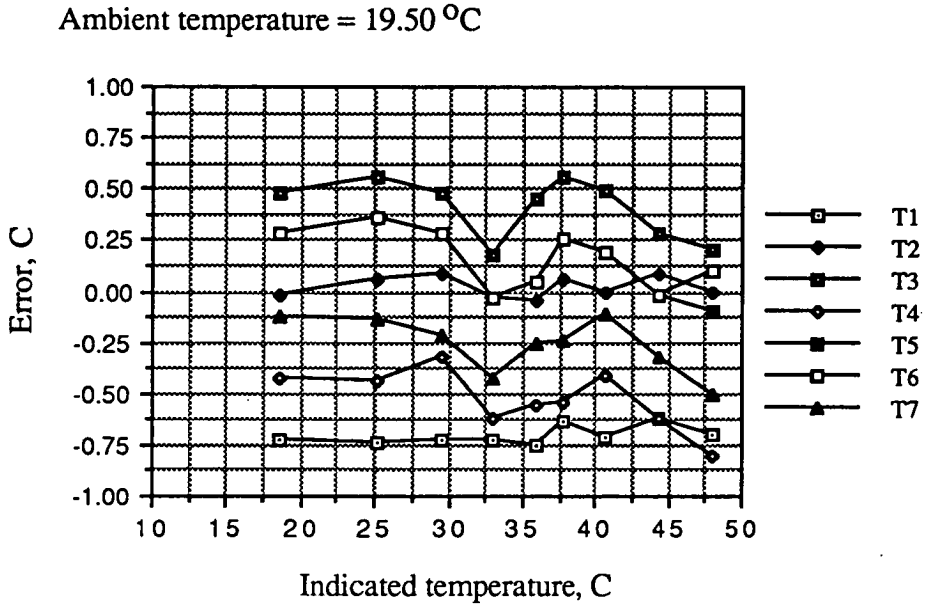

T1, T2,..and T7 represent Thermometers 1, 2,..and 7 used to measure the air temperatures under trays 2, 3,..and 8, respectively inside the chamber during measurements. The air temperature under tray 1 was measured using thermometer 2 (T2).

C.2 Calibration factor for solar radiation intensity

Brief procedures to calibrate the solarimeter are described as follows : When the voltage output from solarimeter V = 0.0 mV the indicator reading s = 2.9 and when V = 9.75 mV the value of s = 194.5. A multiplication factor f is calculated as follows f = (9.75-0.0)/(194.5-2.9) = 0.050887. Because the voltage output of 1 mV from the solarimeter is equivalent to 13.95 W/m^2 the multiplication factor f =

$(0.71 \pm 0.03) W/m^2$, where the estimate of the error refers to the instrumental accuracy.

APPENDIX D

Table D.1 Selected solar radiation intensity

Date (1990)	Time	Solarra diation Intensity (W/m^2)	
		Measured	Calibrated
2 Dec	8:30	500	355.0
2 Dec	9:00	1001	701.7
26 Nov	10:00	1159	822.9
26 Nov	11:00	1334	947.1
8 Dec	12:00	1475	1047.3
30 Nov	13:00	1512	1073.5
8 Dec	14:00	1068	758.3
8 Dec	15:00	836	593.6
9 Dec	16.00	358	254.2
8 Dec	17:00	55	39.1

The relationship between the calibrated solar radiation and time is shown graphically in figure D.1

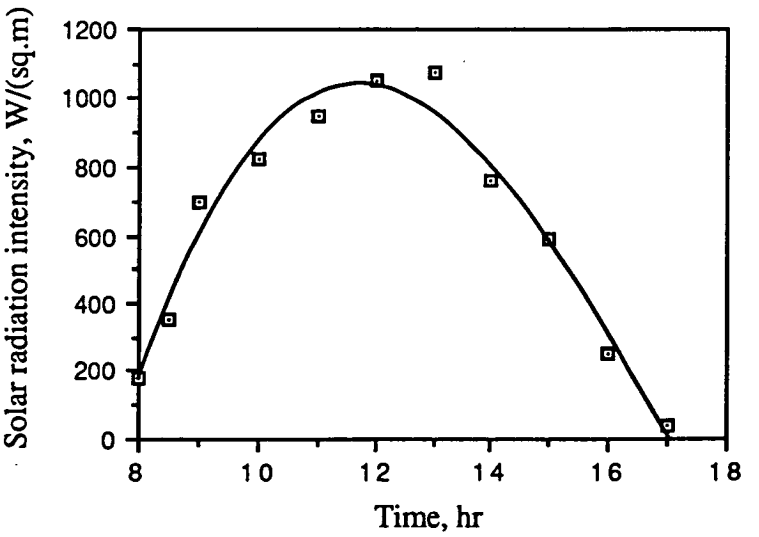

An power-series polynomial equation from this graph is given by

$$I(t) = -10661 + 2384.3\,t - 151.33\,t^2 + 2.8231\,t^3 \qquad \text{for } 8.0 \le t \le 17.0 \qquad \text{D.1}$$

where I is the solar radiation intensity in W/m^2 and t is the time in hours.

Table D.2 Measured ambient temperature, humidity and atmospheric pressure

Time	**Ta**	**rh**	**P**
(hr)	^oC	%	mbar
9:00	29.32	59.0	1028.9
10:00	32.92	42.40	1028.5
11:00	34.14	37.90	1027.9
12:00	36.50	31.20	1026.8
13:00	33.57	44.00	1027.5
14:00	36.13	47.60	1027.5
15:00	34.44	44.40	1027.5
16:00	34.54	49.80	1026.5
17:00	32.10	51.00	1027.0

From table D.2 we write linear equations for air temperature and relative humidity as follows

$$Ta = 1.36\,t + 17.06 \qquad \text{for } 8.5 \le t \le 14.0$$

$$Ta = -1.34\,t + 54.89 \qquad \text{for } 14 < t \le 17.0 \qquad \text{D.2}$$

$$rh = 127.8 - 6.6\,t \qquad \text{for } 8.5 \le t < 13.0$$

$$rh = 13.4 + 2.2\,t \qquad \text{for } 13 < t \le 17.0 \qquad \text{D.3}$$

where t represents time in hours. The atmospheric pressure was used an average value P = 1027.6 mbar.

APPENDIX E

Diagram of solar drier

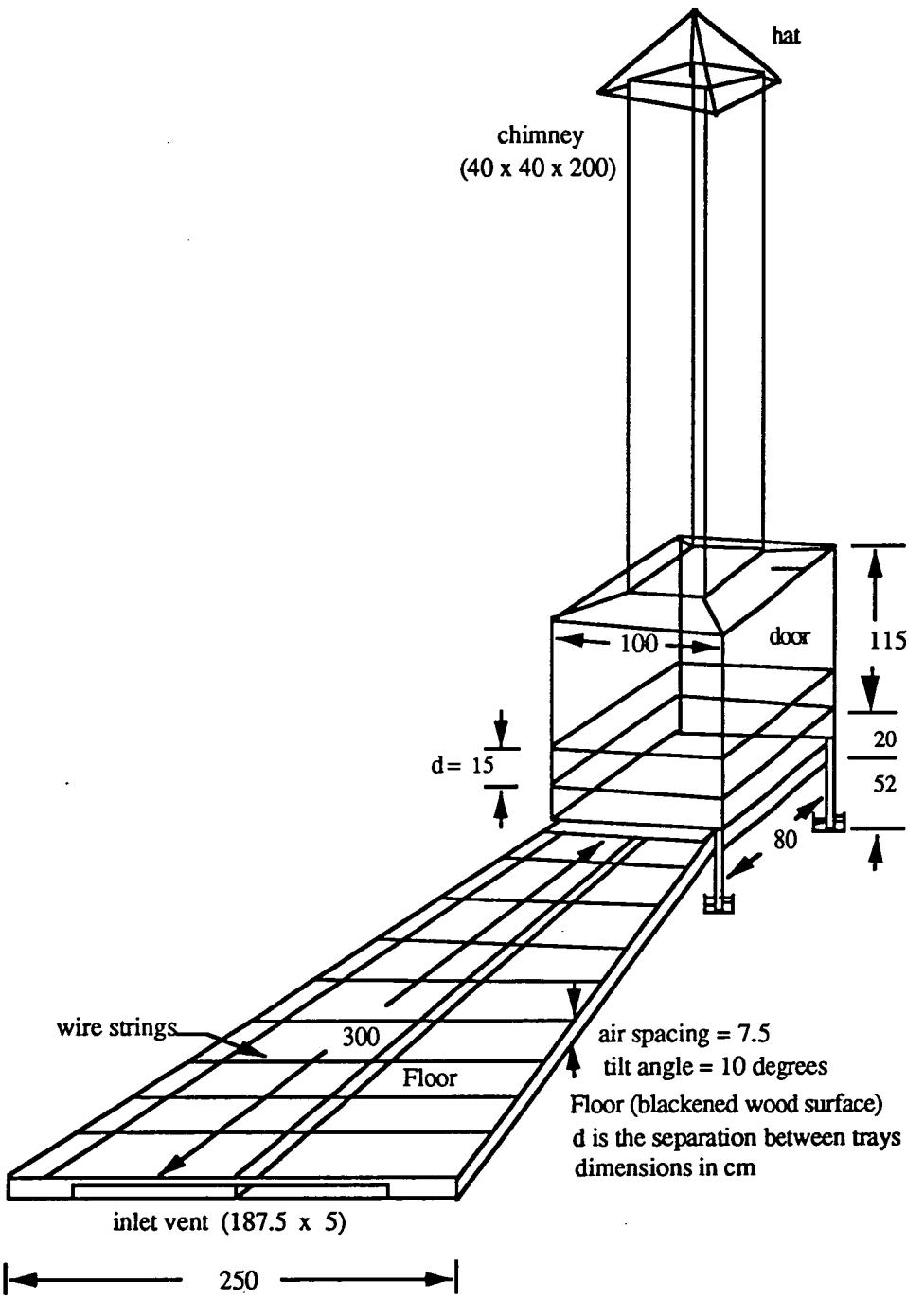

Figure E.1 Solar drier A built by Barsong (1990)

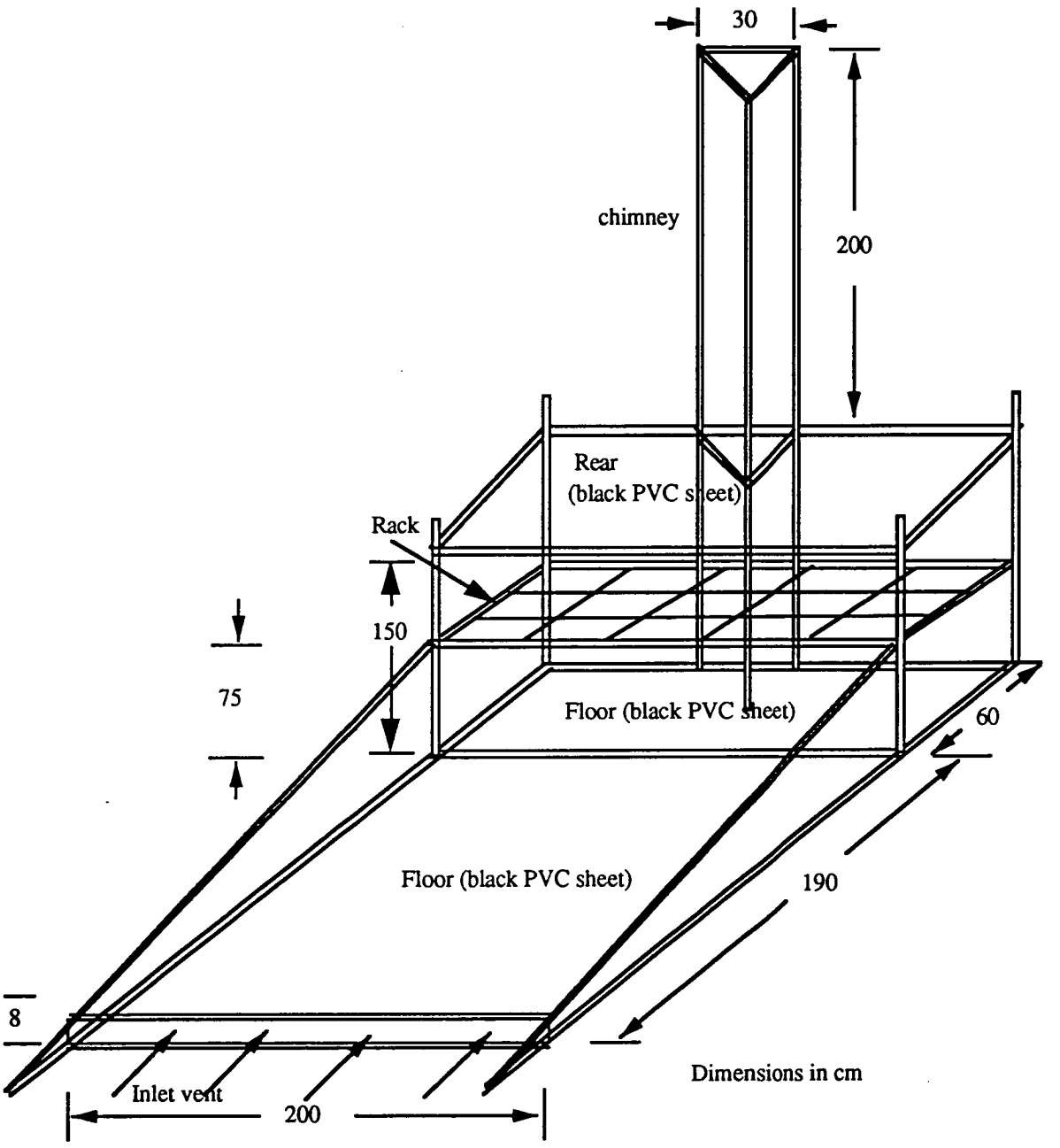

Figure E.2 Solar drier B built by Trim and Curran (1983)

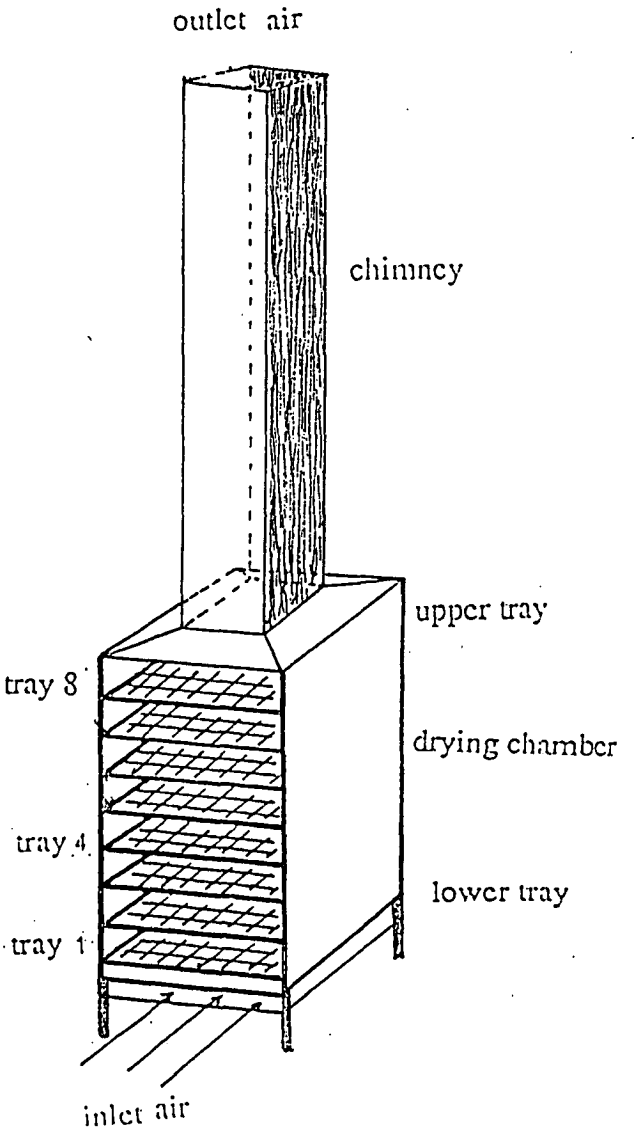

Figure E.3 Drying chamber and trays

APPENDIX F

Materials and construction cost of SCD solar fish drier (drier A)

Wood materials	Rp 140,000.00
Labor	Rp 92,000.00
Plastic trays, nails and wire string	Rp 8,000.00
Black and white plastics	Rp 24,000.00
Stapler and others	Rp 15,000.00
Total	Rp 280,250.00
	US$ 150.00*

* US$ 1.00 = Rp 1,865.00 (Nov. 1990)

APPENDIX G

```
Program SOLAR_DRYING_OF_TROPICAL_FISH_IN_INDONESIA
(Input,Output);


Uses Crt;
Label 10,20;
CONST
  alphap =0.95;     rhog =0.20;
  epsp   =0.95;     rhop = 0.005;
  Sig    =5.67E-8;  g    =9.80;
  kk     =0.0752;   thc  =1;
  Cpf    =4.19E3;   latent=2.45E6;


VAR
   date,month,Ny,Line,tins,j1,p,p1: Integer;

   Bln,Frp : Boolean;
   tstart,tend,delta,wt,tin,time,tec,phi,tilt,gm,
    Rb,Ic,Ib,Id,ITb,ITg,ITd,Zb,Zg,Zs,Zx,Ih,H,Ta,RH,

    Tp,Tc,Ts,Ut,UL,Ub,Tci,F1,F2,FR,qu,Q,Tpj,Tv,
   T3,Tf,Eff,epsc,rhoc,tst,hm1,hm2,Rfd,

    D1,D2,D3,D4,D5,h1,h2,h3,h4,h5,v,vg,s,s1,Ac,Ld,
    wd,Ad,w1,w2,w3,Af,Ap,L,Ach,Lch,wch,rch,Yi,
    Y5,T4,T5,T6,Tf0,Tft,A,dia,Kt1,K11,Qn,

   hm,ht,sd,fd,Mo,M0,Mt,Rcal,Rcd,mc,mco,mdt,mde,fco,
  sco,mcf,kn,D0,Mb,Me,Mec: Real;


PROCEDURE Declination;
Var
  X : Real;
Begin
  Line:=Line+1;
  time:=(tin*Line)+tstart;
  wt := ((15*(time-6))-90)*Pi/180;
  If time<12.0 then gm:=-pi/2 else
  If time=12.0 then gm:=0 else
  If time>12.0 then gm:=pi/2;
  If Month=1 then Ny:=Date;          If Month=2 then Ny:=Date+31;
  If Month=3 then Ny:=Date+59;    If Month=4 then Ny:=Date+90;
  If Month=5 then Ny:=Date+120;  If Month=6 then Ny:=Date+151;
  If Month=7 then Ny:=Date+181;  If Month=8 then Ny:=Date+212;
  If Month=9 then Ny:=Date+243;  If Month=10 then Ny:=Date+273;
  If Month=11 then Ny:=Date+304;If Month=12 then Ny:=Date+334;
  X := (284+Ny)*360/365;
  delta := 23.45*Sin(X*Pi/180)*Pi/180;
End;
```

```
FUNCTION Z(delta,wt,phi,tilt,gm:real):real ;
Var
 Z1:real;
Begin
  Z1:=Sin(delta)*Sin(phi*pi/180)*Cos(tilt*Pi/180);
  Z1:=Z1-(Sin(delta)*Cos(phi*pi/180)*Sin(tilt*Pi/180)*Cos(gm));
  Z1:=Z1+(Cos(delta)*Cos(phi*pi/180)*Cos(tilt*pi/180)*Cos(wt));
  Z1:=Z1+(Cos(delta)*Sin(phi*pi/180)*Sin(tilt*pi/180)*Cos(gm)*Cos(wt));
  Z:=Z1+(Cos(delta)*Sin(tilt*pi/180)*Sin(gm)*Sin(wt));
End;


FUNCTION Iht(t:real):Real;{t:time}
Begin
   If (t>=8.4) then
      Iht:= -1.0661e4 +(2384.3*t) - (151.33*t*t) + (2.8231*t*t*t)
   else Iht:=0;
End;



PROCEDURE TempRH;
Begin
   If time<=14 then Ta := (1.36*time) + 17.06 else
                        Ta := (-1.34*time) + 54.89;
      begin
        If time<=13 then RH := 127.8 - (6.6*time) else
                    RH := 13.4  + (2.2*time);
      end;
   Ts :=0.0552*(273+Ta)*Sqrt(273+Ta);
End;


PROCEDURE Global_Beam_Diffuse_Radiation;
Const Gsc = 1340; {Solar constant,W/sq.m}
Var
  a1,a2,kr,altitude,Tb,Icb,Td,Icd,Z2,Io,Ix :Real;
Begin
  altitude:=0.0045;
  Io:=0.0036*tin*Gsc*(1+(0.033*Cos(pi*360*Ny/365/180)));
  Io:=Io*Z(delta,wt,phi,0,gm);Z2:=Z(delta,wt,phi,0,gm);
  a1:=0.4237 - (0.00821*Sqr(6-altitude));
  a2:=0.5055 + (0.00595*Sqr(6.5-altitude));
  kr:=0.2711 + (0.01858*Sqr(2.5-altitude));
  Tb:=(0.95*a1) + (0.98*a2*exp(-1.02*kr/Z2));Icb:=Io*Tb;
  Td:=0.271 - (0.2939*Tb);Icd:=Io*Td;
  Ic:=Icb+Icd;Ih := 0.0036*tin*Iht(time)*hm2/hm1;
     begin
       Ix:=Ih/Ic;
       If (Ix>0) AND (Ix<0.48) then Id:=(1-(0.1*Ix))*Ih else
       If (Ix>=0.48) AND (Ix<1.10)
       then Id:=(1.11+(0.0396*Ix)-(0.789*sqr(Ix)))*Ih else
       If Ix>1.10 then Id:=0.2*Ih;
     end;
   Ib:=Ih-Id;
End;
```

```
FUNCTION Tb(Zx:Real):Real;
Const rf  = 1.515;
Var
  Zy,rp,rr,Tr:Real;
Begin
  Zy:=Sin(Zx)/rf;
  Zy:=Arctan(Zy*Sqrt(1/(1-sqr(Zy))));
  rp:=Sqr(Sin(Zx-Zy)/Sin(Zx+Zy));
  rr:=Sqr(Sin(Zx-Zy)*Cos(Zx+Zy)/(Cos(Zx-Zy)*Sin(Zx+Zy)));
  Tr:=0.5*(((1-rp)/(1+rp))+((1-rr)/(1+rr)))*exp(-kk*thc/Cos(Zy));
  Tb:=1.01*alphap*Tr;
End;


FUNCTION Zn(x:real):Real;
Begin
  Zn:=(90-(0.5788*x)+(0.002693*sqr(x)))*Pi/180;
End;


FUNCTION Zm(x:real):Real;
Begin
  Zm:=(59.68-(0.1388*x)+(0.001497*sqr(x)))*Pi/180;
End;


FUNCTION Zp(x:real):Real;
Begin
  Zp:=Arctan(Sqrt(1-sqr(x))/x);
End;


PROCEDURE Solar_Radiation_on_an_Inclined_Surface;
Var Z3 :Real;
Begin
  Rb:=Z(delta,wt,phi,tilt,gm)/Z(delta,wt,phi,0,gm);
  Z3:=Z(delta,wt,phi,tilt,gm);Zb:=Zp(Z3);
  Zg:=Zn(tilt);Zs:=Zm(tilt);
  ITb :=Tb(Zb)*Rb*Ib;
  ITg :=0.5*Tb(Zg)*(Ib+Id)*rhog*(1-Cos(tilt*Pi/180));
  ITd :=0.5*Tb(Zs)*Id*(1+Cos(tilt*Pi/180));
  H   :=(ITb+ITg+ITd)/tin/0.0036;{MJ/sq.m}
End;


FUNCTION Hss(tin:Real):Real;
Var Rbc,k1,k2,k3,Hsa:Real;
Begin
  Rbc:=Z(delta,wt,phi,pi/2,gm)/Z(delta,wt,phi,0,gm);
  k3:=Z(delta,wt,phi,pi/2,gm);
  k3:=Zp(k3);k1:=Zn(pi/2);
  k2:=Zm(pi/2);
  Hsa :=(Tb(k3)*Rbc*Ib)+(0.5*((Tb(k2)*Id)+(Tb(k1)*(Ib+Id)*rhog)));
  Hss :=Hsa/tin/0.0036;
End;
```

```
FUNCTION Ysat(Temp:real):Real;
Begin
  Ysat:=0.001*exp((0.063*Temp)+1.41);
End;


FUNCTION mu(Temp:real):Real;
Begin
  mu:=(1.720 + (0.0046*Temp))*1E-5;
  {mu=dinamic viscosity of air, Pas.s or kg/m.s}
End;


FUNCTION kd(Temp:real):Real;
Begin
  kd:=(1.8343 + (0.014614*Temp))*1E-5;
  {kd:thermal diffusivity of air at atmospheric pressure,sq.m/s}
End;


FUNCTION kv(Temp:real):Real;
Begin
  kv:=(1.3179 + (0.0096363*Temp))*1E-5;
  {kv=mu/D, kinematic viscosity, sq.m/s}
End;


FUNCTION k(Temp:real):Real;
Begin
  k:=0.02399 + ((0.77857E-4)*Temp);
  {k= thermal conductivity of air, W/m.K}
End;


FUNCTION Dx(Temp,humidity:real):Real;
Const
 Ma =28.98;  Mv =18.02;
 P  =102.76E3; R  =8.31E3;
Var
 Dx1 :Real;
Begin
 Dx1:=((1/Ma)+(humidity/Mv))*R*Temp/P;
 Dx :=1/Dx1;
End;


FUNCTION Cp(c,humidity:real):Real;
Const
  Cpa=1007;{J/kg.C, specific heat of air}
  Cpv=1884;{J/kg.C, specific heat of water vapor}
Begin
  Cp:= (c*Cpa) + (Cpv*humidity);
End;
```

```
FUNCTION hp(Tx1,Tx2:real):Real;
Var
  Ra,Nu1,Nu2,Nu3,Nu,Tav :Real;
Begin
  Tav:=(Tx1+Tx2)/2;
  Ra:=g*(Tx1-Tx2)*s*s*s/(kd(Tav)*kv(Tav))/(273+Tav);
  Nu1:=(1-(1708/(Ra*Cos((tilt*Pi/180)))));
  Nu2:=exp(1.6*ln(Sin(1.8*tilt*Pi/180)));
  Nu2:=1-(Nu2/(Ra*Cos(tilt*Pi/180)));
  Nu3:=(exp((1/3)*ln(Ra*Cos((tilt*Pi/180)))/5830))-1;
  If ((Nu1<=0) AND (Nu3<=0)) then Nu:=1.0 else
  If ((Nu1<=0) AND (Nu3>=0)) then Nu:=1.0 + Nu3 else
  If ((Nu1>=0) AND (Nu3<=0)) then Nu:=1.0 + (1.44*Nu1*Nu2) else
  If ((Nu1>=0) AND (Nu3>=0)) then Nu:=1.0 + (1.44*Nu1*Nu2) + Nu3;
  hp:=Nu*k(Tav)/s;
End;


PROCEDURE TempOfCover;{The first iteration}
Var
  Tsk,Tpk,Tck,hrpc,hrcs,hcom,hps,hpc,tauc,taua,
  PR,Cr,Lc,Re,hw :Real;
Begin
  Ub:=1;{assumed}PR:=kv(Ta)/kd(Ta);
  Cr:=2*sqrt(sqr((w1-w2)/2)+sqr(L));
  Cr:=Cr+w1+w2;Lc:=4*Ac/Cr;Re:=v*Lc/kv(Ta);
  hw:=0.86*(k(Ta)/Lc)*sqrt(Re)*exp((1/3)*ln(PR));
  tauc:=Tb(Zb)/(1.01*alphap);taua:=exp(-kk*thc/Cos(Zb));
  epsc:=1-taua;rhoc:=1-tauc-epsc;Tsk:=Sqr(sqr(Ts));
  Tpk:=Sqr(sqr(273+Tp));Tck:=Sqr(sqr(273+Tc));hpc:=hp(Tp,Tc);
  hrpc:=(epsc*epsp*sig*(Tpk-Tck))/((1-(rhoc*rhop))*(Tp-Tc));
  hrcs:=(epsc*sig*(Tck-Tsk))/(273+Tc-Ts);
  hcom:=((hpc+hrpc)*(hw+hrcs))/(hw+hrcs+hpc+hrpc);
  hps :=((tauc*epsp*sig)*(Tpk-Tsk))/((1-(rhoc*rhop))*(Tp-Ta));
  Ut :=hps+hcom;Tci :=Tp-((Ut*(Tp-Ta))/(hpc+hrpc+hps));UL :=Ub+Ut;
End;


PROCEDURE Temperature_Of_Plate;{The second iteration}
Var
  T2,Pe,hr,hpc,h1pc,h2pc:Real;
Begin
  Yi:=RH*Ysat(Ta)/100;
  T2:=Ta;hpc:=hp(Tp,Tf);Tv :=(Tp+Tf)/2;
  h1pc:=hpc*(1+(Ut/Ub));h2pc:=hpc*(1+(Ub/Ut));
  hr :=(epsc*epsp*sig*(273+Tv)*sqr(273+Tv))/(1-(rhoc*rhop));
  F1 :=(hr*h1pc)+((Ut+hr+h1pc)*h2pc);
  F1 :=F1/(((Ut+hr+h1pc)*(Ub+hr+h2pc))-sqr(hr));
  Pe :=Ac*UL*F1/(Q*Cp(1,Yi));If Pe>10 then Pe:=1;
  F2 :=(1-exp(-Pe))/Pe;FR :=F1*F2;
  qu :=Ac*FR*(H-(UL*(T2-Ta)));
  Tpj :=Ta+(qu*(1-FR)/(Ac*UL*FR));
  Tf :=Ta+(qu*(1-F2)/(Ac*UL*FR));
  T3 :=T2+(qu/(Q*Cp(1,Yi)));eff :=qu/(Ac*H);
End;
```

```
PROCEDURE Temperature_and_Humudity_Of_Outlet_Air_from_a_Drier;
Const
  C1   =0.88;  C2   =0.55;
  C3   =0.39;  C4   =0.22;
  C5   =0.43;  QL   =0.00;{assumed}
Var
   K6,K7,K8,K9,K10,K1,K2,K3,K4,Ysf :Real;
Begin

  D1:=Dx(Ta+273,Yi);D2:=Dx(Tv+273,Yi);
  D3:=Dx(T3+273,Yi);K6:=1/(2*sqr(Af*C1)*D1);
  K8:=1/(2*sqr(Ap*C3)*D3);vg:=Q/(D4*Ad);
  If vg<=0.6 then begin ht:=10.0;hm:=0.005;end else
             begin ht:=6.0*(1+exp(0.8*ln(vg)));
                 hm:=2.0*0.003*(1+exp(0.8*ln(vg)));
             end;
  Ysf:=Ysat(Tf0);K1:=(2*Q/hm/2/A)-1;
  K2:=K1+2;Y5:=((2*Ysf)+(K1*Yi))/K2;
  K3:=ht*2*A/Q;K4:=(Y5-Yi)*Cp(0,1);
  T4:=(((Cp(1,Yi))-(K3/2))*T3) + ((K3+K4)*Tf0) - (QL/Q);
  T4:=T4/(Cp(1,Y5)+(K3/2));T5:=(T3+T4)/2;
  D4:=Dx(T5+273,Y5);K9:=1/(4*sqr(Ad*C4)*D4);
  K10:=1/(2*sqr(Ach*C5)*D4);Kt1:=K6+K8+K9+K10;
End;


PROCEDURE Chimney;
Const
  alphch =0.90;  epch =0.95;  C6 =0.5;
Var
  Acch : Real;
Begin
  Acch:=(Lch+wch)*h5;
  T6 :=T4+(0.5*0.25*Hss(tin)*Acch/Q/Cp(1,Y5));
  D5:=Dx(T6+273,Y5);K11:=1/(2*sqr(Ach*C6)*D5);
End;


PROCEDURE Flow_Rate;{The third iteration}
Begin
  Qn:=((D1*h1)-(D2*h2)-(D3*h3)-(0.5*D4*h4)-(D5*h5))*g;
  Qn:=Sqrt(Qn/(Kt1+K11));
  Rcd:=3600*2*A*hm*(Ysat(Tf0)-((Yi+Y5)/2));
End;


FUNCTION Aw(ss,md:real):Real;
Var
  Awo,Awn : Real;
Begin
  If (1/md<2.5) then Awo:=0.99 else
  If (1/md>=2.5) AND (1/md<10) then Awo:=1.160-(0.066/md) else
  If (1/md>=10) then Awo:=5*md;If (ss<0.075) then Awn:=0.99 else
  If (ss>0.075) AND (ss<=0.36) then Awn:=1.007-(0.684*ss) else
  If (ss>0.36) then Awn:=0.75;Aw:=Awn*Awo;
End;
```

```
FUNCTION md(AW,Temp:Real):Real;
Var
  sx,ma,mdi,aa,bb,cc,mx : Real;
Begin
  If Aw>=0.5 then ma:=0.066/(1.160-Aw) else
  If Aw>0 then ma:=Aw/5;
  sx:=sd/ma;
  If sx<=0.075 then mdi:=ma else
  begin
    If Aw>0.5 then
      begin
        aa:=1.1681-Aw;bb:=0.7934*sd+0.0665;
        cc:=0.0451*sd;
        mx:=(bb+sqrt(sqr(bb)-4*aa*cc))/2/aa;
      end else
      mx:=(Aw+3.42*sd)/5.035;
      If sx<=0.36 then
        begin
          If mx<=0.4 then mdi:=mx else
                    mdi:=0.0684*sd/(1.007-Aw);
        end else
        begin
          If Aw<=0.375 then mdi:=Aw/3.75 else
          begin
            If Aw<=0.75 then mdi:=0.066/(1.160-1.33*Aw)
                  else mdi:=0.684*sd/(1.007-Aw);
          end;
        end;
  end;
 md:=mdi*exp(0.8*ln(298/(273+Temp)));
End;


PROCEDURE End_Constant_Rate;
VAR
  i : Integer;
  Zn,Zm,Total,mdo,Ce,Co,rds,D01:Real;
Begin
  Zn:=100;i:=0;rds:=dia/2;D01:=D0*exp(-3620/(Tf0+273));
  D01:=D01/(1+(kn*D01*fco));Zm:=-9.8696*D01*tin*3600/sqr(rds);
  Total:=0;
  While abs(Zn)>0.00001 DO
    begin
      i:=i+1;
      Zn:=exp(sqr(i)*Zm)/sqr(i);
      Total:=Total+Zn;
    end;
    mde:=md(RH/100,Ta);mdo:=mc/(1-mc-sco-fco);
    Ce:=1000*mde/(1+mde+sd+fd);Co:=1000*mdo/(1+mdo+sd+fd);
    Rcal:=A*D01*(Co-Ce)/rds;
    Rcal:=Rcal*3600/((D01*tin*3600/sqr(rds))+0.33333-(0.20264*Total));
    Me:=Mb*(1+mde+sd+fd);
End;
```

```
Procedure Check;
Begin
    If (Rcal<=Rcd) OR (Me>=M0)
    then begin
          If p<1 then
          begin
           Mec:=Mt;Frp:=True;
           tec:=time;p:=p+1;
          end;
        end else Frp:=False;
End;


PROCEDURE Constant_Rate;
Begin
  Mt:=M0-(Rcd*tin);
  Tft:=Tf0+(tin*((3600*ht*2*A*(T5-Tf0))-(Rcd*latent))/M0/Cpf);
  mdt:=(Mt/Mb)-1-sd-fd;mc:=mdt/(1+mdt+sd+fd);
  Tf0:=Tft;M0:=Mt;
End;



PROCEDURE Falling_Rate;
Var
  Dt,Tau: Real;
Begin
  Dt:=D0*exp(-3620/(273+Tf0));Dt:=Dt/(1+(kn*Dt*fco));
  Tau:=0.122*sqr(dia/2)/Dt/100;
  If(tec>time) then begin tec:=tst;mec:=Mt;end;
  Rfd:=3600*(Mec-Me)*exp(-(time-tec)*3600/Tau)/Tau;
  Mt:=(Mec-Me)*exp(-(time-tec)*3600/Tau) + Me;
  Tft:=Tf0+(tin*((3600*ht*2*A*(T5-Tf0))-(Rfd*latent))/M0/Cpf);
  M0:=Mt;Tf0:=Tft;mdt:=(Mt/Mb)-1-sd-fd;mc:=mdt/(1+mdt+sd+fd);
End;



PROCEDURE Mass_mc_Aw;
Begin
  Gotoxy(10,1);Write('Mass, m.c and Aw of fish : ');
  Gotoxy(1,3);Write('time');Gotoxy(1,4);Write(' hr ');
  Gotoxy(7,3);Write('Mass');Gotoxy(7,4);Write(' % ');
  Gotoxy(15,3);Write(' mc ');Gotoxy(15,4);Write(' % ');
  Gotoxy(23,3);Write(' md ');Gotoxy(22,4);Write(' % ');
  Gotoxy(31,3);Write(' Aw ');Gotoxy(30,4);Write('No.D');
  Gotoxy(39,3);Write('To1');Gotoxy(47,3);Write('To2');
  Gotoxy(1,j1+4);Write(time:4:1);Gotoxy(7,j1+4);Write(Mt:4:2);
  Gotoxy(15,j1+4);Write(mc*100:4:2);Gotoxy(23,j1+4);Write(mdt:5:2);
  Gotoxy(31,j1+4);Write(Aw(sco/mc,mdt):4:3);
  Gotoxy(39,j1+4);Write(T3:4:1);Gotoxy(47,j1+4);Write(T4:4:1);
End;
```

```
PROCEDURE Read_Input_Data;
Var
  Afish,Nofish,Mf,md1 :Real;
Begin
  Lch :=0.4;  wch :=0.4;Ach :=Lch*wch;
  Month :=12; date :=7;  phi  :=2.13;     tilt :=10;
  Ld  :=1.0;  wd  :=0.8;Ad  :=Ld*wd;
  s   :=0.075; w1  :=2.5;
  w2  :=1.0;  w3  :=0.75*w1;
  L   :=3.0;     s1  :=0.05;
  Af  :=s1*w3; v   :=1.67;
  Ap  :=(Ld-0.05)*0.075;
  Ac  :=L*(w1+w2)/2;
  h2:=L*Sin(tilt*Pi/180);h3:=0.20;{h2+h3=72.0cm}
  h4  :=1.15;h5  :=2.0;
  h1  :=h2+h3+h4+h5;
  Q   :=0.06;
  Nofish:=288;
  Afish :=7.0E-3;{sq.m}
  dia  :=0.04;kn=5.2e11;
  A    :=Nofish*Afish;
  Mo   :=20.5;{Initial mass,kg}
  Mf   :=7.55;{Final mass,kg}
  M0   :=Mo;
  fco  :=11.57/100;
  sco  :=9.99/100;
  mcf  :=27.31/100;
  sd   :=sco/(1-mcf-sco-fco);
  fd   :=fco/(1-mcf-sco-fco);
  D0   :=(10.167-3.3*sd)*1E-5;
  Mb   :=Mf*(1-mcf-sco-fco);
  md1  :=(Mo/Mb)-1-sd-fd;mdt:=md1;
  mco  :=md1/(1+md1+sd+fd);mc:=mco;
  tin  :=0.1;  j1  :=0; tstart:=8.5; p1:=0;
  day  :=1;    FRP :=False;Mt   :=Mo;
End;


PROCEDURE StartingEnding;
Var i : Integer;
  Begin
    Repeat
    i:=0;
    Write('Start = ');Readln(tst);
    Write('End = ');Readln(tend);
    Write('Maximum solar radiation intensity (W/sqm)= ');Readln(hm1);
    Write('Measured solar radiation intensity (W/sqm) = ');Readln(hm2);
    Write('press 1 = ');Readln(i);
    until (i>0) and (i<2);ClrScr;
    mec:=0;
  End;
```

```
BEGIN
  ClrScr;
  Read_Input_Data;
  WHILE mc-mcf>0 DO
  Begin {of mc}
    Tf0:=25;  Tft:=Tf0;     Ta:=30;
    Tp :=40;  Tc :=28;      Tf:=32;
    TempRH;D4:=Dx(273+Ta,Yi);
    Line:=0; time:=0;
    StartingEnding;
    While time<=(tend-tin) DO
    begin {of time<=tend-tin}
      tins:=0;
      While tins<5 DO
      begin {of tins<5}
        If mc-mcf<=0 then goto 10;
        tins:=tins+1;
        Declination;
        Global_Beam_Diffuse_Radiation;
        Solar_Radiation_on_an_Inclined_Surface;
        TempRH
        If time>=tst then
        begin
        Repeat
          Repeat
            Repeat
              TempOfCover;
              begin
                If (((Tci-Tc)>0.01) OR ((Tci-Tc)<-0.01)) then
                begin
                  Bln:=False;
                  Tc:=Tci;
                end else
                begin
                  Bln:=True;
                end;
              end;
            Until Bln;
            Temperature_Of_Plate;
            begin
            If (((Tpj-Tp)>0.01) OR ((Tpj-Tp)<-0.01)) then
              begin
                Bln:=False;
                Tp:=Tpj;
              end else
              begin
                Bln:=True;
              end;
            end;
          Until Bln;
          Temperature_and_Humudity_Of_Outlet_Air_from_a_Drier;
```

```
        If h5>0 then Chimney else
        If h5<=0 then begin
                    K11:=0;D5:=0;
                    T6:=0;
                  end;
        Flow_Rate;
        begin
        If (((Qn-Q)>0.01) OR ((Qn-Q)<-0.01)) then
          begin
            Bln:=False;
            Q:=Qn;
          end else
          begin
            Bln:=True;
          end;
        end;
      Until Bln;
      End_Constant_Rate;Check;
      If Frp=False then begin p:=0;Constant_Rate;end else
      If Frp=True then Falling_Rate;
    end;
        If (line=1) OR (tins=5) then
        begin
          10:j1:=j1+1;If j1>=19 then begin
                              j1:=1;
                              ClrScr;
                            end;
                          Mass_mc_Aw;
                          If (Frp=True) and (p1<1) then begin
                          Gotoxy(44,j1+6);p1:=p1+1;
                          Write('FALLING RATE COMMENCES');
                          end;
                          If (mc-mcf<=0) then Goto 20;
        end;
    end;{of tins<5}
  end;{of time<=tend-tin}
  date:=date+1;
End;{of mc>mcf=0.23}
20:
END.
```